Impacts of land use and climate change on carbon and greenhouse gas dynamics of Irish peatland ecosystems

Thesis submitted for the degree of Doctor of Philosophy

March 2023

Ruchita Ingle

The University of Dublin, Trinity College

Department of Botany

School of Natural Sciences

Declaration

I declare that this thesis has not been submitted as an exercise for a degree at this or any other university and it is entirely my own work.

I agree to deposit this thesis in the University's open-access institutional repository or allow the library to do so on my behalf, subject to Irish Copyright Legislation and Trinity College Library conditions of use and acknowledgment.

Signed,

Ruchita Ingle

Abstract

Peatlands are wetlands that are found on every continent except Antarctica, covering around 3% of the global land area and are the largest terrestrial soil organic carbon store. They are estimated to store around 550 gigatons of carbon (C) which is equivalent to twice the amount stored in all of the world's forests. In Ireland, peatlands cover almost one-fifth of the total land area and are recognized as a major C sink that has been depleted but still represents a key climate mitigation tool. Unfortunately, many of Ireland's peatlands have been drained and degraded for peat extraction, or converted to forestry and agriculture. The Irish government has taken steps to protect and restore these peatlands as part of the national climate mitigation strategy. However, it is vital to understand the impacts of drainage along with changing climate on carbon and methane dynamics of these ecosystems and the key drivers of the emissions for effective management. Additionally, long-term monitoring can aid in assessing vulnerability and resilience of these ecosystems to climate change. The primary aim of this PhD research was to develop an interdisciplinary approach to investigate the impact of anthropogenic activities and climate change on the carbon and methane dynamics of a raised bog ecosystem across a drainage gradient by combining innovative experimental and observational techniques.

Chapter 4 outlines the carbon dynamics and the key drivers influencing the uptake and emissions at a near-natural raised bog in Ireland using the Eddy Covariance technique. The measurement period included two drought years with different hydrological conditions (2018 and 2021) followed by humid/wetter normal climatic years (2019 and 2020) which provided insight into the response of such ecosystems to climate change. The reduction in soil moisture below 80% in 2018 was caused by a combination of a lowering water table for consecutive 109 days and higher temperatures compared to the other very

dry year of 2021. The differing hydrological and climatic conditions between years resulted in the study area acting as a net source of carbon of 53.5 g C m^{-2} in 2018 and a net sink of -125.2 g C m^{-2}, -75.7 g C $m^{-2,}$ and -49.8 g C m^{-2} in 2019, 2020 and 2021 respectively. The carbon dynamics in 2018 were primarily driven by ecosystem respiration however, the system went back to being a carbon sink in the following years displaying its resilience to drought events. Overall, this study highlights both the vulnerability and resilience of these ecosystems to climatic variability and emphasizes the need for long-term monitoring networks to enhance our understanding of the impacts of these events.

This PhD research also focuses on using closed chamber measurement techniques (chapter 5) to understand methane dynamics at raised bogs under various management practices which included near-natural bog, under rehabilitation site, and degraded peatland. The average annual methane flux was ranging between 1.44 to 8.89 g C m^{-2} y^{-1} at a near-natural bog, -1.1 to 1.55 g C m^{-2} y^{-1} at an under-rehabilitation site, and 0 to 0.53 g C m^{-2} y^{-1} at the degraded site. Furthermore, this study proposes a framework to upscale these emissions from the chamber to ecosystem scale by testing the applicability of high-resolution multispectral satellite imagery with machine learning algorithms to provide fine-scale vegetation maps. These maps were used to upscale chamber-based methane fluxes at peatland sites across a drainage/management gradient. Our results provide evidence that upscaling is successful, as long as the dominant vegetation communities are appropriately mapped. Results from this study highlight the complex spatial heterogeneity of peatlands and their impact on methane fluxes. This study emphasis the need to include dominant plant species information in methane budget models and upscaling approaches. The framework proposed in this study was able to map all the ecotopes at the Lullymore (under rehabilitation) and Garryduff (degraded) sites with an overall validation accuracy above 95% in 2020 and 2021. However, Clara bog (near-natural) is an extremely challenging and complex site to map due to the heterogeneity of vegetation at the site, however, this framework was able to map all of the ecotopes present with an overall validation accuracy above 83%. This approach could be used to upscale fluxes at other sites and aid in refining site-specific emission factors for these systems.

Chapter 6 highlights the potential of using remote sensing models to estimate Gross Primary Productivity (GPP) at sites where it is not feasible to install EC towers or conduct chamber measurements. GPP represents one of the key components of the peatland carbon cycle, and detailed knowledge of the spatial and temporal extent of GPP under changing management practices and climate variability is imperative to improve our predictions of peatland ecology and biogeochemistry. This research assessed the relationship between remote sensing and ground-based estimates of GPP for a near-natural peatland in Ireland using Eddy Covariance (EC) techniques and high-resolution Sentinel 2A satellite imagery. Hybrid models were developed using multiple linear regression along with six widely used conventional indices and light use efficiency model. Estimates of GPP using NDVI, EVI, and NDWI2 based hybrid models 2 and 4 performed well with a significant correlation over 0.89 between modelled GPP and EC-derived GPP. This study also reports site-specific light use efficiency parameters for both dry and hydrologically normal years based on the light response curves method (LRC). Overall, this research demonstrated the potential of combining EC techniques with satellite-derived models to better understand and monitor key drivers and patterns of GPP for raised bog ecosystems under different climate scenarios and has also provided light use efficiency parameters values for variable climatic conditions which can be used to estimate GPP using LUE models across various scales.

Finally, this thesis emphases the importance of long-term measurements and monitoring at peatland sites across drainage gradients to better understand the impact of land use change and climate variability on carbon and methane dynamics. This information will enhance conservation, rehabilitation, and restoration activities and strategies and, will help to increase the carbon storage potential of these ecosystems. Additionally, this research shows the successful integration of innovative remote sensing and machine learning techniques with field measurements which could aid in refining tier 2 and tier 3 level emission factors for peatland systems in Ireland.

Acknowledgment

Life begins at the end of your comfort zone (by Neale Walsch) – these words have been a constant motivation during my PhD. As this exciting journey comes to an end, I would like to thank those without whom this journey would not have been possible. I am deeply grateful to Dr. Matthew Saunders for his guidance and support throughout my PhD. His influence not only taught me the basic principles of science but also the true virtues of life in general. His mentorship has made me a more sincere, patient, and hardworking individual, and for that, I am truly thankful. I also want to express my gratitude to Dr. John Connolly for his guidance and encouragement.

A special thanks to my colleagues and friends Marine, Erika, Peter, and Aneta for their help with field measurements, especially during the COVID times. I am also grateful to Late Dr. Aigar Niglas and Late Dr. J. Matthew for inspiring me to pursue my dreams. My PhD provided me with an opportunity to meet and work with some wonderful people at TCD including Wahaj Habib, Dr. Saheba Bhatnagar, Dr. Magdalena Matysek, and Dr. Rachael Murphy. They were of immense assistance with remote sensing and Eddy Covariance tower queries. The front and back cover pictures of this thesis are provided by Emily Toner. Thanks a lot for capturing stunning pictures of Clara bog.

I am also thankful to Kathy Casson, Prof. Scott Wells, Dr. Renaat De Sutter, and Prof. Dev Niyogi for encouraging and guiding me in all my endeavors. A special thanks to Dr. Bart Kruijt and Dr. Ronald Hutjes for providing me with time and flexibility to wrap up this PhD dissertation while working at Wageningen.

My heartfelt gratitude also goes out to my friends Uttara, Jigar, Vidya, Ketaki, and all the relatives for always being there for me. My family played an instrumental role in my life, and for that, I am eternally grateful to my parents (Anil Ingle and Sujata Ingle), brother (Aditya Ingle), husband (Dr. Samir Vinchurkar), and our daughter (Yuga) who have provided me with unconditional love, support, and encouragement throughout life. Without them, I would not have been able to complete this thesis. Finally, I would like to thank everyone with whom I have crossed paths during this PhD adventure.

Table of Contents

List of Figures

List of Tables

List of Abbreviations

AF	Active Flush
APAR	Absorbed photosynthetically active radiation
API	Application Programming Interface
ARB	Active raised bog
BOA	Bottom-of-atmosphere
BP	Bare peat
BW	Bog woodland
C	Carbon
Ce	Central
CDD	Consecutive dry days
CEAS	Cavity-Enhanced Absorption Spectroscopy
CH_4	Methane
CLWTD	Consecutive days with low water table depth
CO_2	Carbon dioxide
D	Dormant
DEFRA	Department for Environment, Food, and Rural Affairs
DRB	Degraded raised bog
EC	Eddy Covariance
EGU	European Geosciences Union
EO	Earth Observation
EPA	Environmental Protection Agency
ESA	European Space Agency
EU	European Union
EUMETSAT	European Organisation for the Exploitation of Meteorological Satellites
EVI	Enhanced vegetation index
GC	Gas chromatography
GD	Garryduff

GEE	Google earth engine
GHG	Greenhouse gas
GNDVI	Green Normalized Difference Vegetation Index
GPP	Gross primary productivity
GWP	Global Warming Potential
H_2O	Water
IE	Ireland
IF	Inactive flush
IPCC	Intergovernmental Panel on Climate Change
J-O	July-October
LAI	Leaf area index
LM	Lullymore
LRC	Light response curve
LST	Land surface temperature
LSWI	Land surface water index
LUE	Light use efficiency
LWTD	Low water table depth
M	Marginal
MCARI	Modified chlorophyll absorption in reflectance index
M-J	March-June
MODIS	Moderate Resolution Imaging Spectro-radiometer
MSI	Multispectral Instrument
NA	Not applicable
NASA	National Aeronautics and Space Administration
NDVI	Normalized difference vegetation index
NDWI	Normalized Difference Water Index
NEE	Net Ecosystem CO_2 Exchange
NHA	National Heritage Areas
NIR	Near-infrared

NPWS	National Parks and Wildlife Service
NR	Net radiation
OA	Overall validation accuracy
OF	Optical feedback
OW	Open water
PA	Producers accuracy
PAR	Photosynthetically active radiation
PCAS	Peatland Climate Action Scheme
PRI	Photo-chemical Reflectance Index
PVC	Polyvinyl chloride
Reco	Ecosystem respiration
REP2	Red edge position
RF	Random forest
RGB	Red, green and blue
S	Shrub
S1	Sentinel-1
S2	Sentinel-2
SAC	Special area of conservation
SC	Subcentral
SDG	Sustainable development goal
SM	Submarginal
SMILE	Statistical Machine Intelligence and Learning Engine
SNAP	Sentinel Application Platform
SOC	Soil organic carbon
SOM	Soil moisture
UA	User accuracy
UAV	Unmanned Aerial Vehicle
UN	United National
UNFCCC	United Nations Framework Convention on Climate Change

USGS	United States Geological Survey
V	Vegetation
VI	Vegetation index
VPD	Vapor pressure deficit
VWC	Volumetric Water Content
WTD	Water table depth

Chapter 1: Introduction

1.1 Peatlands

Peatlands are an integral part of the global carbon (C) cycle as they act as a significant store of soil organic carbon (Gorham, 1991). These ecosystems only cover 3% of the global land area and are estimated to store around 30% of global soil organic carbon (Blodau, 2002; Gorham, 1991; Scharlemann et al., 2014). Worldwide peatlands are under threat from extensive drainage due to anthropogenic activities such as peat harvesting, agriculture, and forestry releasing around 2-3 Gt CO_2 per year (Parish et al., 2008). A recent expert assessment by Loisel et al. (2021) implies that in the future (2020 through 2100) the global peatlands may switch from being a C sink to a C source. Furthermore, climate change is acting as a catalyst for anthropogenic activities by contributing to the C emissions (Bu et al., 2011; Wilson et al., 2013). The carbon dynamics of peatlands are governed by the hydrological conditions, predominantly the water table depth (WTD) closer to the peat surface is one of the crucial drivers to maintaining the carbon sink function of these systems (Evans et al. 2021). Several studies (Aslan-Sungur et al., 2016; Baldocchi et al., 2018; Marcisz et al., 2020) highlight the importance to enhance our understanding of the impacts of climate change on the carbon and greenhouse gases (GHG) of these sensitive ecosystems. This research refers to interannual variation in climate characterized by elevated summer temperatures and precipitation deficits which can alter the hydrological condition of these systems influencing the C and GHG exchange as drought throughout the thesis. Peatlands are an important source of atmospheric CH_4 and contribute around 20-40% of the total global CH_4 emissions (Zhang et al., 2020).

Quantification of these emissions is crucial to better understand the impacts of these systems on the climatic feedback loop and to devise suitable mitigation strategies with a focus on the rehabilitation of these systems and their return to a net cooling state.

Around 50% of peatlands in Europe are under degraded conditions to an extent that there is no substantial active peat formation occurring (Tanneberger et al., 2017). Peatlands cover around 20% of the land area in Ireland and over 95% of these have been degraded by draining for peat extraction, agriculture, and forestry (Connolly & Holden, 2009; Fluet-Chouinard et al., 2023; Minasny et al., 2019). Proper management of degraded peatlands and conservation of near-natural peatlands is vital to halt their contribution to the atmospheric CO_2 and reduce CH_4 release into the atmosphere. Emission reduction from degraded peatlands followed by regaining the C store function of these ecosystems conservation, rehabilitation, and restoration is increasingly recognized as an important strategy to tackle climate change (Evans et al., 2016; Leifeld & Menichetti, 2018; Renou-Wilson, 2018). However, with the increase in global initiatives for effective peatland management, there is a necessity to understand how drainage and rehabilitation alter these ecosystems and their C and greenhouse gas (GHG) balances (Baird et al., 2019; Dooling, 2014). Rewetting of peatlands is becoming very popular as an effective starting point for rehabilitation of degraded peatlands by reducing their contribution to atmospheric CO_2 however the impact of rewetting on CH_4 dynamics is poorly understood. There is a need to study CH_4 dynamics across various stages of peatland which includes degraded, under rehabilitation, and near-natural peatlands.

This PhD focuses on raised bog ecosystems which are unique ecosystems with the potential to store more carbon than blanket bogs, fens, and turloughs. The main aim of this research is to assess the impact of climate change and management practices on C and

GHG dynamics of these ecosystems and investigate the key drivers of the emissions. Additionally, this research integrated field measurements with remote sensing techniques to understand the spatio-temporal extent of the emissions and ways to upscale field measurements.

1.2 Project information

This research was funded by the Trinity College Dublin, Provost's PhD Scholarship awards, and the Environmental Protection Agency of Ireland 2014-2020 programme of research as part of the SmartBog project (project ref: 2018-CCRP-LS.2).

1.3 Thesis objectives

The primary aim of this PhD project is to develop an interdisciplinary approach to assess the impact of climatic variability and anthropogenic activities on C/GHG fluxes and upscale emissions at the ecosystem scale for raised bog ecosystems.

Objective 1:

Quantify the carbon fluxes of a near-natural bog during drought and normal climatic years and investigate the key environmental and ecological drivers of the emissions.

Rationale: For effective management and policy recommendations, it is vital to understand the carbon dynamics of a near-natural raised bog as it represents a baseline scenario to evaluate the impact of rehabilitation across raised bogs. Additionally, long-term studies of ecosystem carbon dioxide (CO_2) exchange improve our understanding of the links between climate and the C cycle. We should continue to develop such an understanding of all major terrestrial ecosystems to resolve current uncertainties in C cycling and the global C budget. In recent times, there are numerous studies available that assess the C/GHG dynamics of peatlands however very limited long-term studies are available for raised bogs and little is known about the vulnerability and resilience of raised bogs to climatic events. Furthermore, most studies focus on the growing season dynamics due to logistical issues which can increase uncertainties in the estimation of annual carbon budgets at the site level. These knowledge gaps were addressed as a part of this objective with continuous long-term measurements of net ecosystem carbon exchange. This research measured CO_2 fluxes using the eddy covariance (EC) technique at a near-natural bog over four years. The study duration comprised two drought and two humid/wetter years allowing for an analysis of the impact of these short climatic events on C dynamics. Along with CO_2 measurements, various meteorological and environmental parameters were also measured which provided insights into the key drivers of CO_2 uptake and release. The equipment used in this research and the methodology used are briefly explained in Chapter 3. This objective is addressed in detail in a manuscript format in Chapter 4 of this thesis.

Objective 2:

Develop a methodology to upscale methane fluxes by integrating chamber measurements with remote sensing data and machine learning techniques.

Rationale: Upscaling is a key focus in ecology, as many studies are conducted at the field or farm scale, but the information required by stakeholders and policymakers is often needed at an ecosystem, regional or national scale. Remote sensing has the potential to act as a link between the various scales and can also act as a useful monitoring tool for large areas over longer timescales. This PhD developed a methodology using high-resolution PlanetScope imagery (3 m) with a Random Forest algorithm to upscale chamber methane fluxes. This approach was successfully implemented at raised bog sites across drainage gradient. The sites were selected in such a way that they covered a broad spectrum of the various stages of bog condition and management practices which included near natural, a former industrial extraction site, and an under-rehabilitation site. The satellite data and methodology used in this research are explained in Chapter 3 and this objective is addressed in detail in a manuscript submitted to Nature scientific reports which is currently under review and can be found in Chapter 5.

Objective 3:

To develop hybrid models for Gross Primary Productivity (GPP) estimation using satellite data and Light Use Efficiency approach for raised bog ecosystems. Additionally, site-specific light use efficiency parameters will be provided for dry and wet years.

Rationale: Satellite data and remote sensing techniques and associated models are gaining a lot of attention as a means to estimate carbon fluxes, particularly where the site of interest is inaccessible for direct measurements and where they are of benefit for inclusion in National carbon accounting inventories. However, the use of spectral indices which were developed for a homogeneous system such as grassland, cropland, and forestry can bring in a lot of uncertainty in GPP estimation as raised bogs are heterogeneous ecosystems. Moreover, the spectral reflectance of raised bogs is different than other ecosystems and the presence of hummock and hollows structure makes it even more challenging to use a single index for GPP estimation. This study proposes hybrid models which are a combination of spectral indices extracted from Sentinel-2 satellite data and can be used to estimate GPP using a light-use efficiency model. These estimates were then validated against EC-derived GPP data collected at a near-natural raised bog (Chapter 4). While exploring literature on Light Use efficiency models, this research found that very limited information is available on light use efficiency parameters (LUE) for dry and wet years at the site scale for raised bog ecosystems. To address this knowledge gap, this research provides LUE parameter values derived from field measurements at a near-natural raised bog in Ireland. The details of the methodology and data used in this study are explained in Chapter 3 and the objectives are addressed in detail in a manuscript that is published in a special issue on carbon stocks and remote sensing in MDPI and can be found in Chapter 6.

1.4 Thesis organization

This thesis consists of seven chapters. Chapter 1 provides an overview of carbon and methane emissions from peatlands along with the thesis objectives and organization. Chapter 2 summarizes the background knowledge on carbon and methane emissions with a focus on the current extent and status of raised bogs in Ireland. It also underlines the initiatives and policies implemented by the Irish Government to reduce the C emission from degraded peatlands and to enhance the C potential of these ecosystems through conservation and rehabilitation. Chapter 3 describes the methodological approaches used in the research chapters (4, 5, and 6), and explains their respective data and experimental setups. Chapter 4 explores the application of the EC technique in quantifying CO_2 emissions from a near-natural raised bog during drought and normal climatic years. Chapter 5 investigates how to upscale chamber-based methane measurements from sites across a drainage gradient with the help of high-resolution satellite data and machine learning algorithms. Chapter 6 evaluates how to estimate GPP using satellite data and the light-use efficiency model. It also highlights the need for raised bogs ecosystem scale indices and has developed new hybrid models that can be used exclusively to estimate GPP from raised bogs. Additionally, light use efficiency parameters for drought and humid/wetter years were provided for a near-natural raised bog. Chapter 7 synthesizes and discusses the key findings outlined in Chapters 4, 5, and 6 and also illustrates the key knowledge gaps and the areas of research which require further exploration. This chapter also outlines the applicability of the work presented in this thesis to enhance the quantification and upscaling of carbon and methane emissions in space and time from raised bogs.

1.5 List of publications and presentations

1. Ingle Ruchita, Bhatnagar Saheba, Ghosh Bidisha, Gill Laurence, Regan Shane, Connolly John, & Saunders Matthew; Development of hybrid models to estimate gross primary productivity at a near-natural peatland using Sentinel 2 data and light use efficiency model. MDPI Biogeosciences and Remote sensing

   https://doi.org/10.3390/rs15061673

2. Ruchita Ingle, Wahaj Habib, John Connolly, Mark McCorry, Stephen Barry & Matthew Saunders; Upscaling methane fluxes from peatlands across a drainage gradient in Ireland using PlanetScope imagery and machine learning tools, Nature Scientific reports-Peatlands conservation and restoration

   https://www.nature.com/articles/s41598-023-38470-6

3. Ingle Ruchita, Regan Shane, Cox Peter, Gill Laurence, and Saunders Matthew; Multiyear carbon fluxes were driven by ecosystem respiration at a near-natural peatland during exceptional climatic conditions (Submitted: Global Change Biology).

4. Wahaj Habib, Ruchita Ingle, Matthew Saunders and John Connolly; Status and condition of raised bogs in Ireland – A national-scale assessment using Sentinel-2 data and Google Earth Engine (Accepted: Nature Scientific reports-Peatlands conservation and restoration).

5. Nwamaka Okafor, Ingle Ruchita, Saunders Matthew and Declan Delaney; SmartBog: IoT-based in-situ Monitoring and Evaluation Testbed (In preparation).
6. Ingle Ruchita, Regan Shane, Cox Peter, Gill Laurence, and Saunders Matthew; Annual carbon budget at a near-natural raised bog in Ireland (In preparation).
7. Ingle Ruchita and Saunders Matthew, 2022, Carbon and Greenhouse gas dynamics at an industrial cutaway peatland. Presented at the EGU General Assembly Conference 2022 (Oral presentation) (https://meetingorganizer.copernicus.org/EGU21/EGU21-13199.html)
8. Ingle Ruchita and Matthew Saunders, 2021, Estimation of Gross Primary Productivity of a raised bog ecosystem using satellite models and eddy covariance techniques under exceptional climatic conditions. Presented at the EGU General Assembly Conference 2021 (Oral presentation) (https://meetingorganizer.copernicus.org/EGU21/EGU21-13199.html)
9. Ingle Ruchita and Matthew Saunders, 2021, Assessing the impact of exceptional climatic conditions on the net ecosystem carbon balance at Clara Bog. Presented at the 31st ENVIRON conference (Oral presentation).
10. Ingle Ruchita, John Connolly, Matthew Saunders, 2019, Impacts of climatic variability on carbon dynamics of Clara bog using Eddy Covariance and Satellite data. EUGEO Conference (Oral presentation).

Chapter 2: Literature review

2.1 Peatland as Carbon Store

2.1.1 Background

Peatlands are the largest natural terrestrial carbon store holding between 113 and 612 Pg (Peta gram=1015 g, or equivalent to Gigatonne) of C on 3% of the global land area (Gorham, 1991; Limpens et al., 2008; Thom et al., 2018). In their natural state, peatland functions as a long-term carbon sink with the rate of plant production generally exceeding the rate of organic matter decomposition (Frolking et al., 2011). Peatlands are not only carbon-dense landscapes but they also play important roles in the provision of water resources and represent an important component of global biodiversity (Biancalani & Avagyan, 2014; Bullock et al., 2012). Even though natural peatlands are large carbon stores, they can still emit a considerable amount of methane (CH_4) and carbon dioxide (CO_2) into the atmosphere (Renou-Wilson et al., 2019; Vitt, 2008; Warmenbol & Smith, 2018). However, the amount of carbon sequestered by these ecosystems through rehabilitation outweighs the CO_2 and CH_4 emissions when we look at longer timescales such as decades (Bain et al., 2011).

The recent Global Peatlands Initiative assessment report (UNEP, 2022), highlighted the distribution of global peatlands (Figure 2.1) with the largest areas in Asia (33%) followed by North America (32%), Latin America, and the Caribbean (13%), Europe (12%), Africa (8%) and, Oceania and Sub-Antarctic Islands (2%). However, natural peatlands are being destroyed at a rate of 4,000 km^2/year globally (Parish et al. 2008).

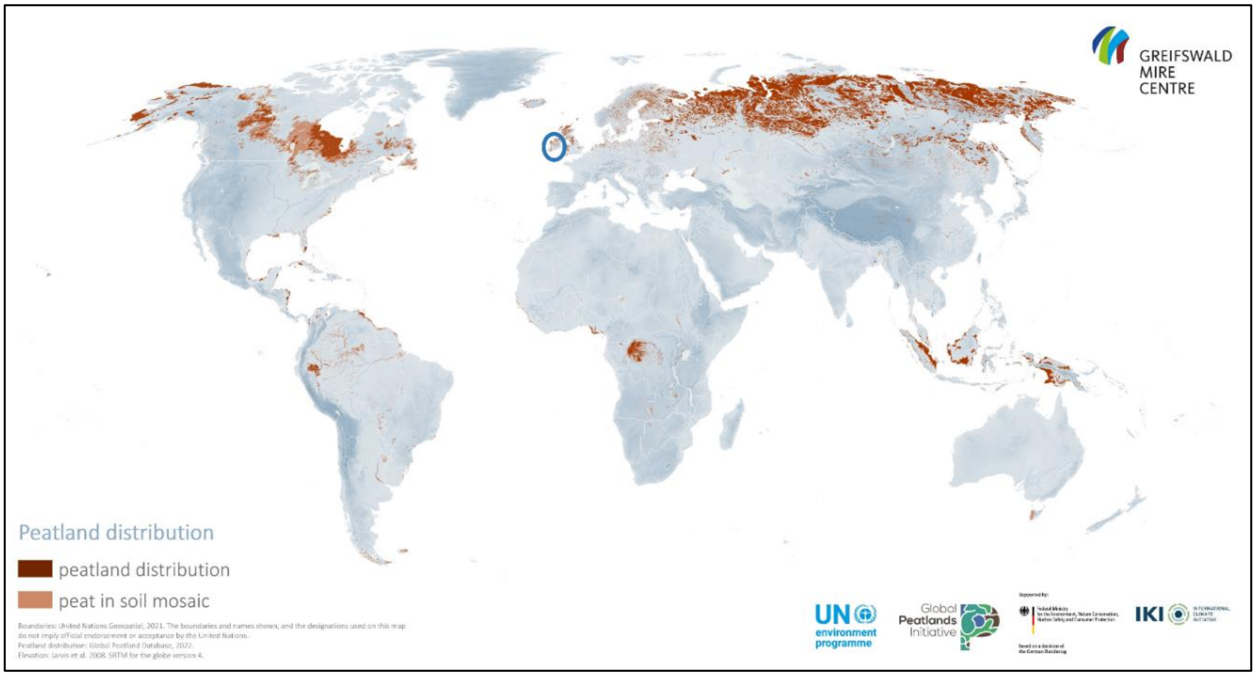

Figure 2. 1 World map showing the distribution of peatlands across the globe (UNEP, 2022)

Europe has over 59 million hectares of peatlands with a higher density in the northern lowlands, highlands, and coastal areas (Figure 2.2 inset). The largest peatland systems in Europe are in northwest Russia and the smallest peatlands are in the highlands and the steppe zone (UNEP, 2022).

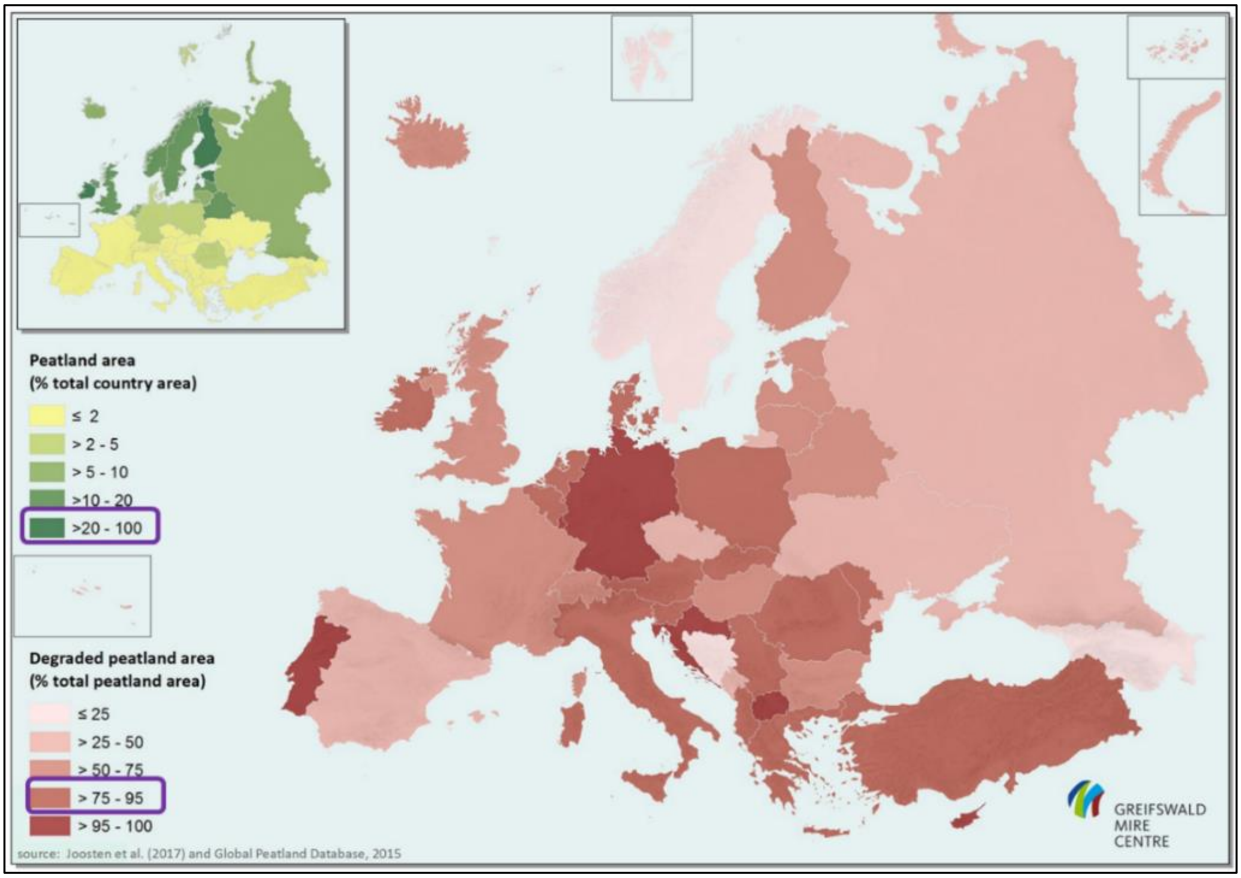

Figure 2. 2 Europe map showing peatland area (%) and degraded peatland area(%) (Joosten et al., 2017)

Almost 50% of the European peatland area is degraded(Figure 2.2), making Europe the second largest greenhouse gas emitter from drained peatlands of around 600 Mt CO_2 equivalent per year (UNEP, 2022). Drainage for agriculture is one of the main reasons for peatland degradation in Europe (UNEP, 2022) and western Europe has already lost over 90% of its natural peatland area over the last 300 years (Fluet-Chouinard et al., 2023; Joosten & Clarke, 2002). The development of sustainable management plans for both near-natural and degraded bogs through rehabilitation, restoration, and conservation programs is of prime importance to reduce/halt GHG emissions and revive the carbon sequestration capacity of these ecosystems (Kiely et al., 2018; NPWS, 2014; Oertel et al., 2016). For effective management and mitigation strategies, it is vital to understand the impact of climatic change and associated variability on the carbon and GHG dynamics of peatlands and the major drivers of the emissions (Kiely et al., 2018). Current estimates of global peatland cover contain large uncertainties as the capacities of peatlands to store soil carbon and to provide water and other ecosystem services are poorly constrained (Jurasinski et al., 2020; Limpens et al., 2008).

2.1.2 Carbon and methane dynamics in peatlands

Peatlands in their natural state can act as a long-term carbon store by accumulating more carbon dioxide than they emit and releasing considerable amounts of methane as a by-product of the anaerobic decomposition of organic material as shown in Figure (2.3a). Drainage of peatlands and lowering of the water table upset the C accumulation process by exposing the anoxic peat layer to the atmosphere, which leads to a vast increase in the rate of CO_2 being released into the atmosphere as illustrated in Figure (2.3b).

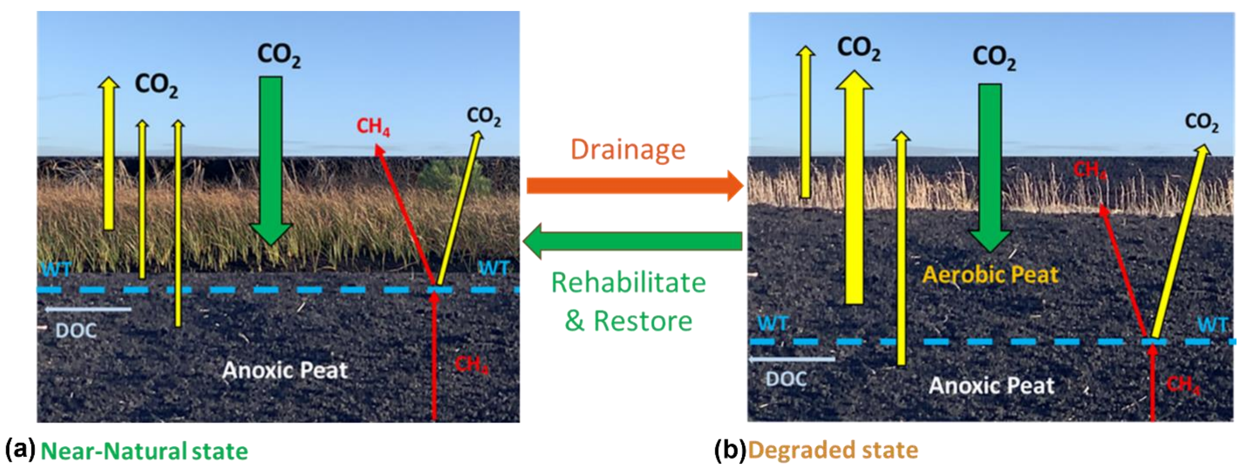

Figure 2. 3 Carbon dynamics in an intact peatland: (a) high water table (b) low water table

The management of peatlands is sensitive to anthropogenic perturbations as the net annual C and GHG budget varies spatially and temporally (Petrescu et al., 2015; Renou-Wilson et al., 2019b; Renou-Wilson & Wilson, 2018). The global warming potential (GWP) of bogs at various stages of degradation and rehabilitation in comparison to near-natural systems has been shown by Bain et al., (2011) in Figure 2.4. The emissions savings that can be achieved through peatland rehabilitation are significant as when re-wetted the emissions of CO_2 can be significantly reduced. As the vegetation starts to recolonize over time, these systems the peatland can revert to having a net cooling effect on the atmosphere.

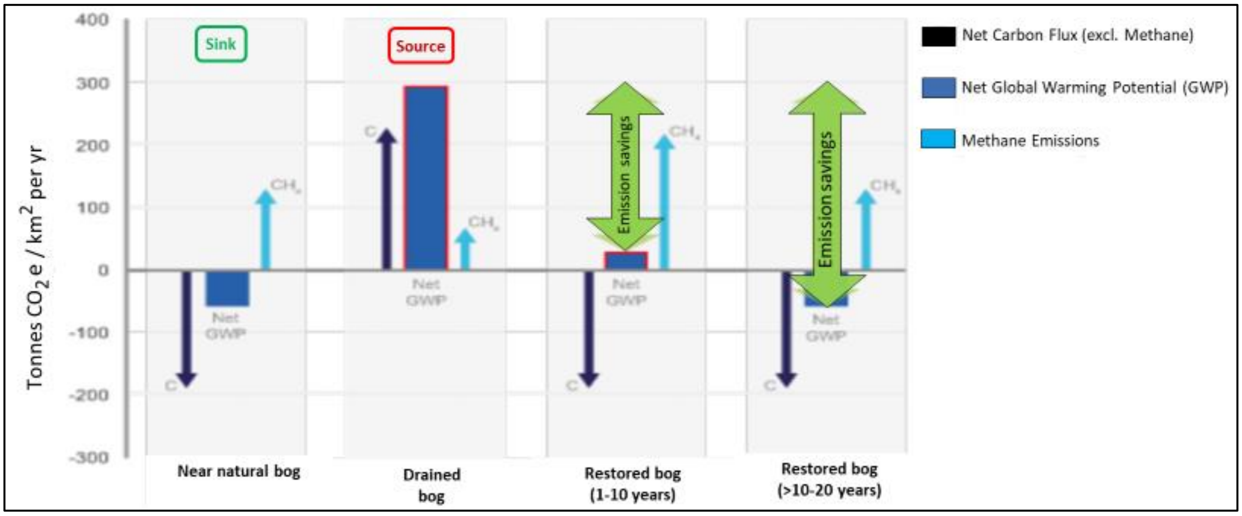

Figure 2. 4 Global Warming Potential (GWP) of UK peat bogs under natural, drained, and rewetted state (Bain et al., 2011)

Another aspect of rehabilitation and restoration is to manage methane emissions from Peatlands (Günther et al., 2020). The methane dynamics of peatlands are complex and poorly understood, but the production, uptake, and emission of methane are mostly governed by the hydrological conditions of the peatland. Methane production by anaerobic microbial respiration of organic matter in peatlands occurs predominantly inside the saturated soils and in the water bodies (Lai, 2009). Variations in precipitation, temperature, and water table levels can alter the uptake/release of methane (Abdalla et al., 2016). Climatic events driven by higher temperatures and lower water tables can lead to increased production of methane, while higher precipitation and higher water tables can lead to increased consumption. The management of methane emissions from peatlands is critical during the restoration phase for mitigating climate change.

2.1.3 Peatland in the Irish context

Peatlands in Ireland cover around 21% of the national land area and are estimated to store between 53% to 75% of the total soil C stock (1064 –1503 Gt of C) (Renou-Wilson et al., 2019; Tomlinson, 2005; Wilson & Müller, 2013). Irish peatlands consist of Fens, Blanket bogs, and Raised bogs, and around 95% of these ecosystems are degraded since 18th century as shown in Figure 2.5 (Fluet-Chouinard et al., 2023).

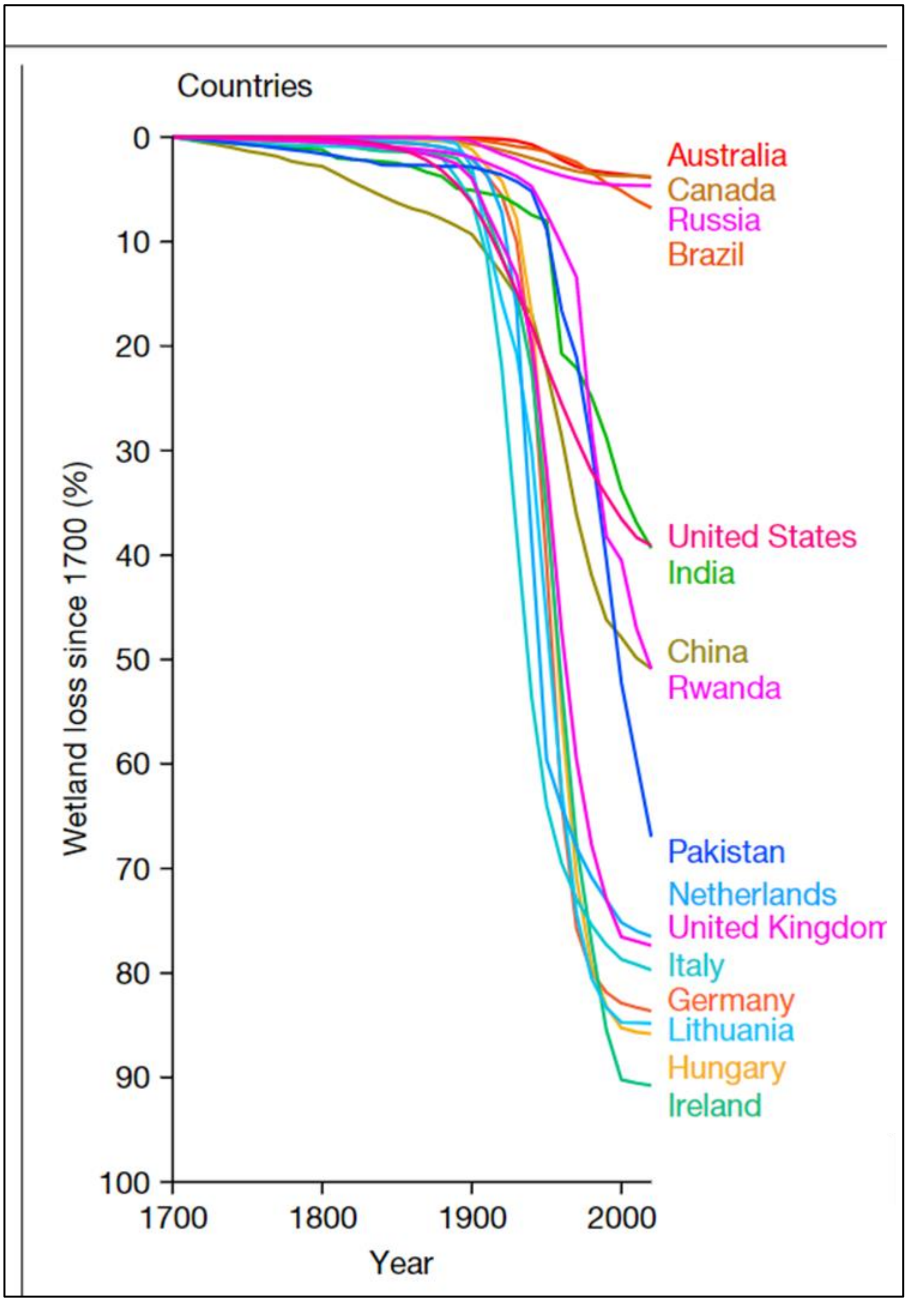

Figure 2. 5 Global heterogeneous wetland loss since 1700 (Fluet-Chouinard et al., 2023)

Fens and bogs mostly differ based on their source of water, the majority of bogs are fed by precipitation (ombrotrophic) while fens are nourished by both precipitation and groundwater (NPWS, 2014; Renou-Wilson, 2018). Raised and blanket bogs are distinguished by their topography, age, and climatic conditions (Fossitt, 2000; Hammond, 1981; Tomlinson, 2005). However, most of the Irish peatlands have been drained and are impacted by peat cutting (industrial and turbary), land-use change (conversion to grassland or afforestation), grazing, or fire to one extent or another. As per the Irish Peatland Conservation Council (IPCC) peatland site database (Table 2.1), it was estimated that only 10% of the original raised bog, 23% of fen, and 28% of the original blanket bog are deemed suitable for conservation.

Table 2. 1 Peatland type, original area, and its area of conversation importance (IPCC, 2009)

Peatland Type	Republic of Ireland Original area (ha)	Area of Conservation Importance (ha)	Proportion of original area remaining (%)	Number of sites
Fen	92,508	20,912	23	375
Raised Bog	308,742	31,756	10	196
Blanket Bog	774,367	216,599	28	194
Total	1,175,617	269,267	23	736

Intact or near-natural raised bogs cover a small area but can store more carbon than blanket bogs and fens and as such are of significant importance for global carbon budgeting (Renou et al., 2006; Tomlinson, 2005). Figure 2.6 shows the extent of raised and blanket bogs in Ireland with study locations of the research undertaken in this thesis in green circles.

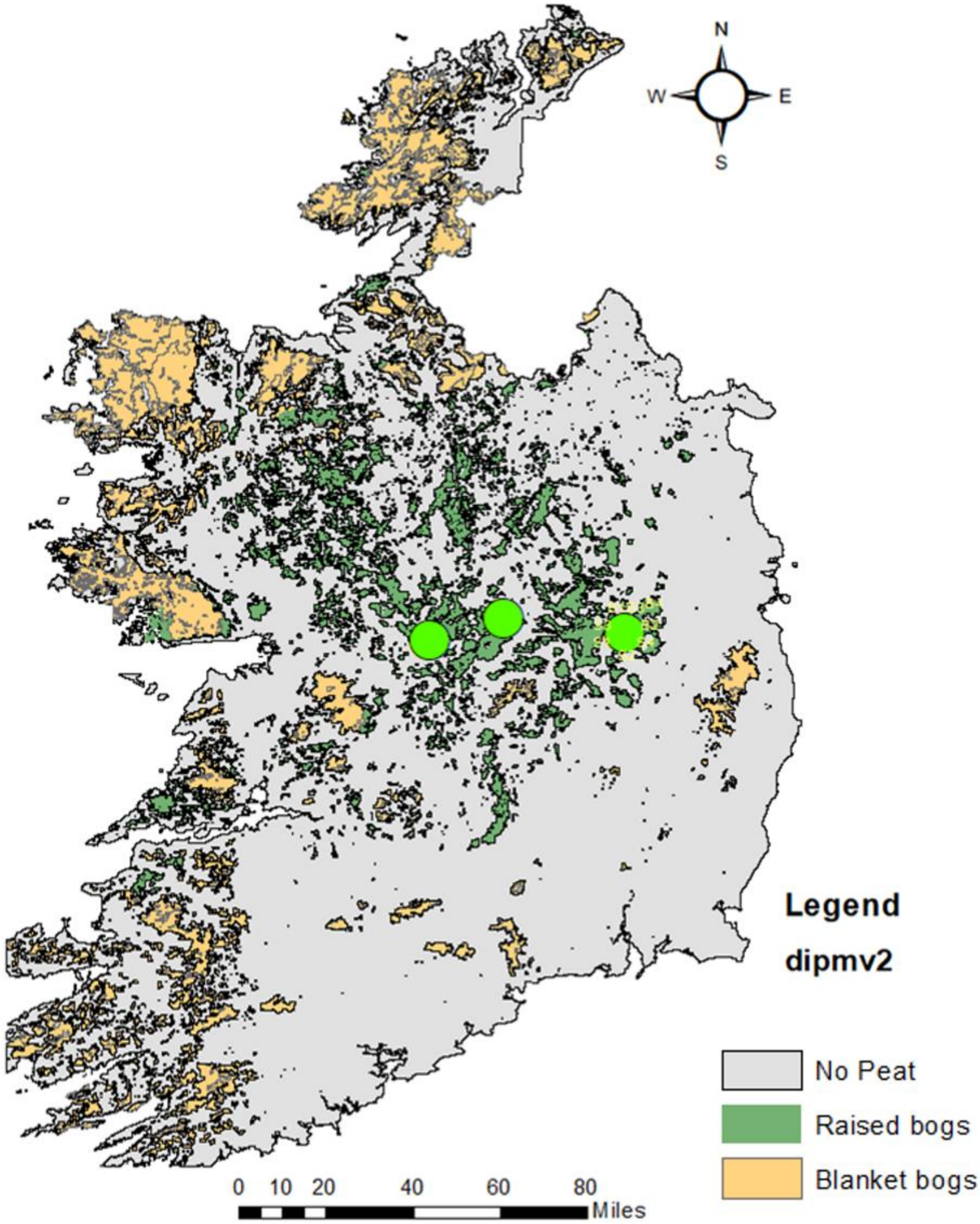

Figure 2. 6 Map of Ireland showing the distribution of raised and blanket bogs (Connolly et al. 2009). Green circles indicate the approximate location of the study sites in this thesis.

Each peatland is unique in its geographical location, peat composition, hydrology, topography, age, type, and degree of natural disturbances and land use change. If peatlands are to be used for mitigation of climate change and to offset emissions from other sectors, then an improved understanding of peatland C/GHG dynamics is vital. It is necessary to better understand the fluxes of C and GHG in and out of each peatland system, related both to climatic variability and management practices. Then the contribution of these ecosystems to atmospheric cooling or warming can be determined. Ireland is required to submit an inventory of GHG emissions to the European Commission and the United Nations Framework Convention on Climate Change (UNFCCC) each year. This requires accurate knowledge of ecosystem emissions, including peatlands which are important sources or sinks of C and CH_4. Knowledge of C fluxes could also be valuable for designing a protocol on effective management practices which can further inform the policy framework.

2.1.4 Policy framework

Several recent policy developments directly contribute to the conservation and sustainable management of peatlands in Ireland. The European Union Climate and Energy legislation for 2021-2030 proposes that Ireland reduce its GHG emissions by 30% by 2030, relative to a 2005 baseline and 5.6% of this can be achieved via offsetting emissions by sequestering C into vegetation and soils (Lanigan et al., 2018). The National Parks and Wildlife Service (NPWS) published an updated national peatland strategy in 2017 (Mackin et al., 2017) that includes a restoration framework designed to address the requirements of the EU Habitats Directive and EU Biodiversity Strategy, and the Water Framework Directive which is designed to protect the wetland and water systems that support groundwater dependent ecosystems. Through this process, the NPWS has designated peatland areas as Special Areas of Conservation (SAC) or National Heritage Areas(NHA) (NPWS, 2014) as a part of the EU-Life environmental program and is actively rehabilitating degraded peatlands and encouraging public support for these initiatives through the raised bog community engagement scheme. The current designated raised bog network consists of 53 raised bog SACs and 75 raised bog NHAs covering an area of 17,995 ha (Fernandez et al., 2014; Mackin et al., 2017; NPWS, 2014). It is considered necessary to protect SACs under the EU Habitats Directive as they contain habitats and species that are rare and threatened on a European scale. SACs are also referred to as Natura 2000 sites or European sites in legislative terms. The conservation of wetland and peatland ecosystems also has direct relevance to some of the United Nations Sustainable Development Goals(SDGs) (Wilson et al., 2015). The role of peatlands in climate mitigation is of greater importance to the national Climate Change Bill and international climate policy, as an example to report emissions under the Kyoto protocol addressing the 1.5°C temperature target. Policymakers are now recognizing the value of peatlands as carbon stores and peatland restoration is becoming accepted as a way of reducing national carbon emissions(Hiraishi et al., 2014; Thom et al., 2018; Warmenbol & Smith, 2018). The EU 2030 climate and energy framework emphasizes that forests, agricultural land, and wetlands, will play a central role in realizing the Paris Agreement. Under this framework, from 2021, all EU member states need to report on the emissions and removals of greenhouse gases from wetlands(Hiraishi et al., 2014; Warmenbol & Smith, 2018). Other global initiatives on peatlands include the UN Framework Convention on Climate Change (UNFCCC), the International Union for the Conservation of Nature (IUCN), and the establishment of the Global Peatlands Initiative (GPI). The government of Ireland and a former commercial peat extraction company (Bord na Móna) has also set an ambitious target of regenerating 33,000 hectares of Peatlands over five years as a part of the Peatland Climate Action Scheme (PCAS) funded by the government of Ireland.

2.2 Measurements of carbon and methane dynamics

2.2.1 Background

Measurements of C and GHG fluxes are essential to understand site scale emissions and carbon budget which are crucial for effective management and Tier-2 emission factors recommendations. The most commonly used techniques to measure land-atmosphere carbon and GHG emission from soils and ecosystems are chambers and micro-meteorological techniques (Nugent et al., 2018; Oertel et al., 2016; Rowson et al., 2013).

2.2.2 Eddy covariance method

Eddy Covariance (EC) is one of the most widely used micro-meteorological techniques to measure the turbulent flux between the vegetation canopy and atmosphere by assessing the covariance between changes in vertical wind velocity and the mixing ratio of the gas scalar of interest (Baldocchi, 2003; Burba & Anderson, 2008; Rowson et al., 2013).

This technique has been used over the past two decades to measure the turbulent exchange of CO_2, H_2O, energy, and other GHGs from a variety of ecosystem types (Baldocchi, 2003; Dondini et al., 2016; Morin et al., 2017; Paço et al., 2006; Poyda et al., 2017; Wang et al., 2010) Two fast-response instruments are necessary for EC measurements: a 3D sonic anemometer and a gas analyzer, both operating at high frequency (~10Hz) to cover the full range of the turbulent motion of gas concentrations, for example, CO_2, CH_4, H_2O, and N_2O (Kiely et al., 2018). The EC technique provides higher temporal resolution of measurement fluxes when compared to chamber measurement (Eugster, 2012). The EC method can measure continuously without disturbing the environment and can cover a larger area (250–3000m radius around flux towers) by capturing seasonal and inter-annual variability (Baldocchi, 2003). The disadvantage of the EC method is that this method requires a flat and homogeneous area (Myklebust et al., 2008; Poyda et al., 2017). Several studies (Chaichana et al., 2018; Poyda et al., 2017; Webster et al., 2018) compared GHG fluxes measured using the closed chamber technique and EC methods and demonstrated that the closed chamber fluxes were larger than those from the EC method (Myklebust et al., 2008; Poyda et al., 2017).

However, the EC footprint is often heterogeneous due to changing wind speed and direction, vegetation height, various land use patterns, and different management activities (Barba et al., 2018). It is therefore important to consider the ecosystem heterogeneity while selecting a measurement site. In practice, however, sites are often located in remote and spatial heterogeneous regions and are thus may be susceptible to various measurement errors (Baldocchi, 2003, 2014, 2018). Footprint models can act as a guiding tool while selecting a site and the exact location for a tower to ensure optimum data capture and can be used as a post-processing quality control tool for identifying and removing flux measurements influenced by heterogeneities in the footprint (Järvi et al., 2018; Moffat et al., 2007; Novick et al., 2013). Understanding the spatial representativeness of site measurements is required for landscape-scale integration and interpretation of carbon flux measurements. While an individual site might be considered representative of the ecosystem where its located, it would be difficult to translate the information to another location which might differ with vegetation composition, climate, and stages of disturbance (Barba et al., 2018; Chen et al., 2009).

Over the past number of years, a community of practice has evolved in the EC flux community and has led to the development of a globally coordinated network of sites (FLUXNET) of individual sites that measure the exchange of carbon dioxide, water vapor, and energy between the biosphere and the atmosphere (Baldocchi, 2003). FLUXNET consists of over 750 sites worldwide that are independently operated by regional networks. Upscaling of fluxes to regional and global scales requires an understanding and quantification of the spatial representativeness of the global network of flux sites. At the European level, the Integrated Carbon Observation System (ICOS) provides standardized and open data from more than 130 measurement stations across 12 European countries. These stations measure greenhouse gas concentrations in the atmosphere and carbon fluxes between the atmosphere, and the land surface. These types of networks provide qualitative and quantitative flux data at a global scale which can be useful for upscaling from ecosystem to regional and global scales. It can also form the basis for the validation of soil-vegetation transfer models and biogeochemical cycling models (Rebmann et al., 2018).

2.2.3 Chamber measurements

The chamber technique measures gas fluxes by capturing an increase in gas concentrations inside a closed chamber over a specified duration depending on the type of analytical techniques used (GC or in-line analyzer) and the gas species of interest. This method is easily applied to various ecosystems and can capture the spatial variability of a site and assess low levels of fluxes (Baird et al., 2019; Laine et al., 2006; Rowson et al., 2013).

Chamber measurements can be either dynamic or static. The air within a dynamic chamber's headspace is exchanged at a high rate (>1-2 times the volume of the chamber per minute). Static chambers are cheaper and can be easily deployed in multiple numbers over a given land area (Jensen et al., 1996; Windham-Myers et al., 2018). In absence of an inlet gas, static chambers can detect lower flux measurements as compared to dynamic chambers (Davidson et al., 2002; Pirk et al., 2016). Static chambers are not advisable at locations where emissions are expected to be high as the flux reduction induced by a concentration gradient build-up will be significant unless they are measured over a very short period (Veber et al., 2018). Dynamic chambers are suitable for such locations due to the inflow and outflow of sweep gas. The chamber technique is not a continuous measurement like the EC measurements except for the auto chamber set-up which is quasi-continuous and the area the chamber covers is smaller as compared to the EC flux footprint (Baird et al., 2019; Pumpanen et al., 2004). These measurements are useful to get insight into the site-specific heterogeneity and can be beneficial along with the EC tower measurement for upscaling across various scales (Baird et al., 2019; Morin et al., 2017; Rowson et al., 2013). Raised bogs are often comprised of heterogeneous vegetation areas known as ecotopes which exhibit significant variability in flux rates (Crushell, 2008; Vitt, 2008). Understanding how fluxes vary between and among ecotopes is important when considering the uncertainties associated while deriving a total carbon/GHG budget for these ecosystems (Lee et al., 2017). In most cases, manual chamber data are gathered based on a sampling schedule, typically on a monthly, fortnightly, or biweekly basis (Webster et al., 2018). The high-magnitude flux events/peaks (hot-moments) and diurnal dynamics are rarely captured by chamber techniques due to their lower temporal resolution (Barba et al., 2018; Morin et al., 2017). In many studies, chamber fluxes have been up-scaled to the site level (Chaichana et al., 2018; Jensen et al., 1996; Kiely et al., 2018; Rowson et al., 2013; Veber et al., 2018). However, point measurements cannot effectively sample the full spatial variation and at the same time, they cannot capture the full intra and inter-daily variations that occur within a site (Chaichana et al., 2018; Myklebust et al., 2008; Poyda et al., 2017). As a result, several studies have shown limitations of using point measurements to represent site scale flux estimations (Desai et al., 2015; Wagle et al., 2015; Xiao et al., 2011; Yuan et al., 2015). However, it is useful to understand local C/GHG dynamics in the dominant vegetation communities. It is recommended to combine chamber measurements with the EC site-level observations wherever possible as it can mitigate the limitation associated with using either method on its own (Barba et al., 2018; Forbrich et al., 2011).

2.2.4 Remote sensing

Remote sensing and satellite data are gaining a lot of attention in the field of peatlands as they are being extensively used to understand the extent and status of peatlands globally (UNEP, 2022). Several studies highlighted the use of high-resolution satellite data to survey ecological and hydrological characteristics of peatlands such as water levels, vegetation cover, and soil types (Lees et al., 2018). One of the most important applications of remote sensing to peatlands is monitoring the effects of climate change and change detection over time. Peatlands are highly sensitive to changing environmental conditions, and their health can be monitored over time by making use of remote sensing data (Czapiewski & Szumińska, 2022; Harris & Bryant, 2009; Rastogi et al., 2018). This data can be used to determine the extent of changes in water levels, vegetation cover, and soil composition. By monitoring changes in these parameters, researchers can determine the extent to which climate change is affecting the local environment (Cole et al., 2014; Lees et al., 2018). Remote sensing can also be used to identify areas where peatland restoration might be needed and also to identify hotspots of emissions. Reliable and long-term monitoring is a crucial part of any rehabilitation and restoration strategy. To determine the success of restoration progress, monitoring needs to be continued over several years or even decades to assess the full implications of the management scheme (Lees et al., 2020). The selected monitoring method needs to be cross-validated with the ground measurements.

Remote sensing techniques are also emerging as a new approach to both the estimate and upscale C/GHG dynamics of many ecosystems including peatlands, especially for remote sites (Chen et al., 2009; Hilker et al., 2008; Lees et al., 2018). More recent methodologies have included the use of vegetation communities as a proxy for carbon fluxes (Bhatnagar et al., 2018; Couwenberg et al., 2011), but this also requires detailed knowledge of the vegetation species coverage of a site, which can be heterogenous and challenging to identify from the satellite data across peatland areas. Many peatland ecosystems are located in remote areas making it challenging and difficult to access for measurements and detailed vegetation surveys (Schubert et al., 2008). The vegetation communities at peatlands are often changing due to the variability in hydrology which also makes it difficult to assess composition and track change. The satellite data with high spatial and temporal resolution can be used as a potential cost-effective tool for large-scale monitoring with limited site access/visits (Minasny et al., 2019). The details on the spatial and temporal resolution of different satellite data are provided in Table 2.3. Remote sensing has been successfully used to estimate water content, vegetation composition, and extent and rates of photosynthesis across peatland landscapes (Gatis et al., 2019; Kross et al., 2016; Minasny et al., 2019). There are several models which can be used to estimate photosynthesis from remote sensing data with the limitation that they were developed for ecosystems other than peatlands (Gatis et al., 2019; Gilabert et al., 2017). Vegetation Indices are simple and effective algorithms for the quantitative and qualitative evaluations of vegetation cover, vigor, and growth dynamics (Joiner et al., 2018; Lees et al., 2018; Xiao et al., 2019), which often use remotely sensed data as inputs.

Satellites such as MODIS and Sentinel have been used in many studies of terrestrial carbon fluxes over various ecosystems (Connolly & Holden, 2017; Peng et al., 2018; Vanikiotis et al., 2018). Many of the satellite datasets are now freely available covering large areas at a frequency between one to sixteen days (Connolly & Holden, 2011; Minasny et al., 2019; Peng et al., 2018; Ruiz, 2019). Table 2.2 summarises the satellite dataset with resolution and duration.

Table 2. 2 Most commonly used satellite datasets for carbon flux estimation

Satellite	**Spatial resolution**	**Temporal resolutio n (days)**	**Operated by**	**Operational since**	**Remark**
Landsat 7	30m	16	USGS/NASA	1999	Band 8 at 15m resolution
Landsat 8	30m	16	USGS/NASA	2013	Band 8 at 15m resolution
Terra and Aqua (MODIS)	250m, 500m, 1km	1-2	NASA	1999 (Terra); 2002 (Aqua)	
Worldview-1	0.5m	2	DigitalGlobe	2007	Commercial
Worldview-2	0.3m - 2m	1	DigitalGlobe	2009	Commercial
Worldview-3	0.3m – 3.7m	1	DigitalGlobe	2014	Commercial
Sentinel-2	10m, 20m, 60m	5	ESA	2017	Vi and IR band at 10m resolution
Sentinel-3A	300m – 1km	1-4	EUMETSAT	2016	
PanetScope	3 m -4.7 m	1	ESA	2020	Planetlab

The integration of field measurements and satellite datasets would be extremely helpful in upscaling carbon and GHG fluxes at various levels which will lead to effective management and monitoring of peatland ecosystems (Chen et al., 2009; Hilker et al., 2008; Lees et al., 2018; Wu et al., 2011). Figure 2.7 summarises the various spatial scales at which carbon flux estimation can be extended. It provides a guideline for upscaling from point scale (chamber measurement), ecosystem scale (EC tower) followed by regional (aerial and satellite imagery), and national scale (Satellite imagery).

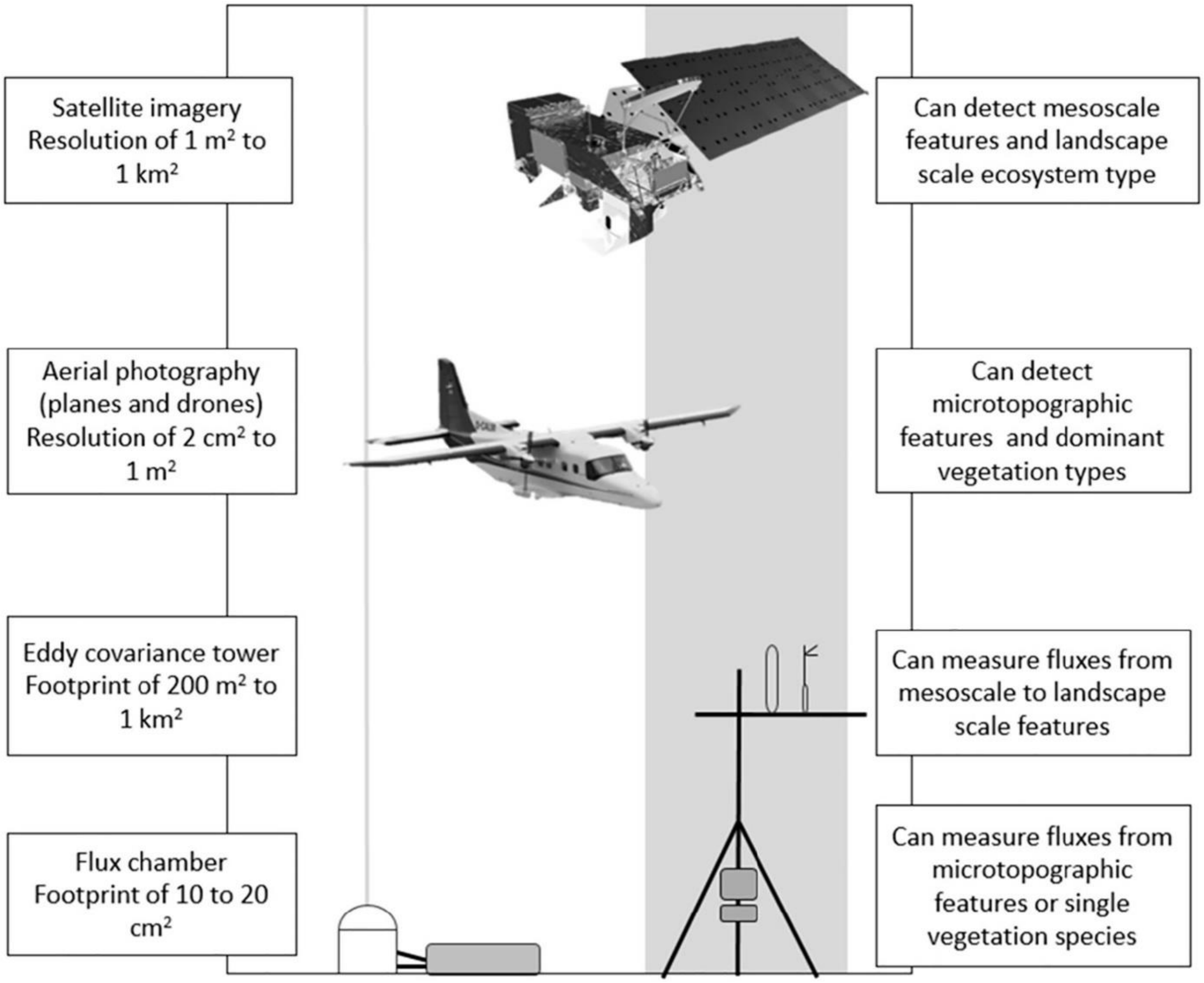

Figure 2. 7 Spatial scales of carbon flux measurements (Lees et al., 2018)

Chapter 3: Materials and Methods

3.1 Study Sites

Peatlands sites were selected to show various stages of degradation starting with a near-natural raised bog with no to minimal impact of drainage followed by former industrial peat extraction (cutaway) site which is being rehabilitated over a decade. This study also focuses on a former industrial peat extraction site where peat extraction ceased recently and the location of all the sites were shown in Figure 3.1. The C flux was measured using the EC technique (Chapter 4) at the near-natural bog (Clara bog) and CH_4 flux (Chapter 5) using closed chambers at the near-natural raised bog, cutaway sites: under rehabilitation (Lullymore), and degraded (Garryduff) as illustrated in Figure 3.1(a-c). A novel approach is explored to estimate GPP at Clara bog using a remote sensing approach and Light Use Efficiency model (Chapter 6).

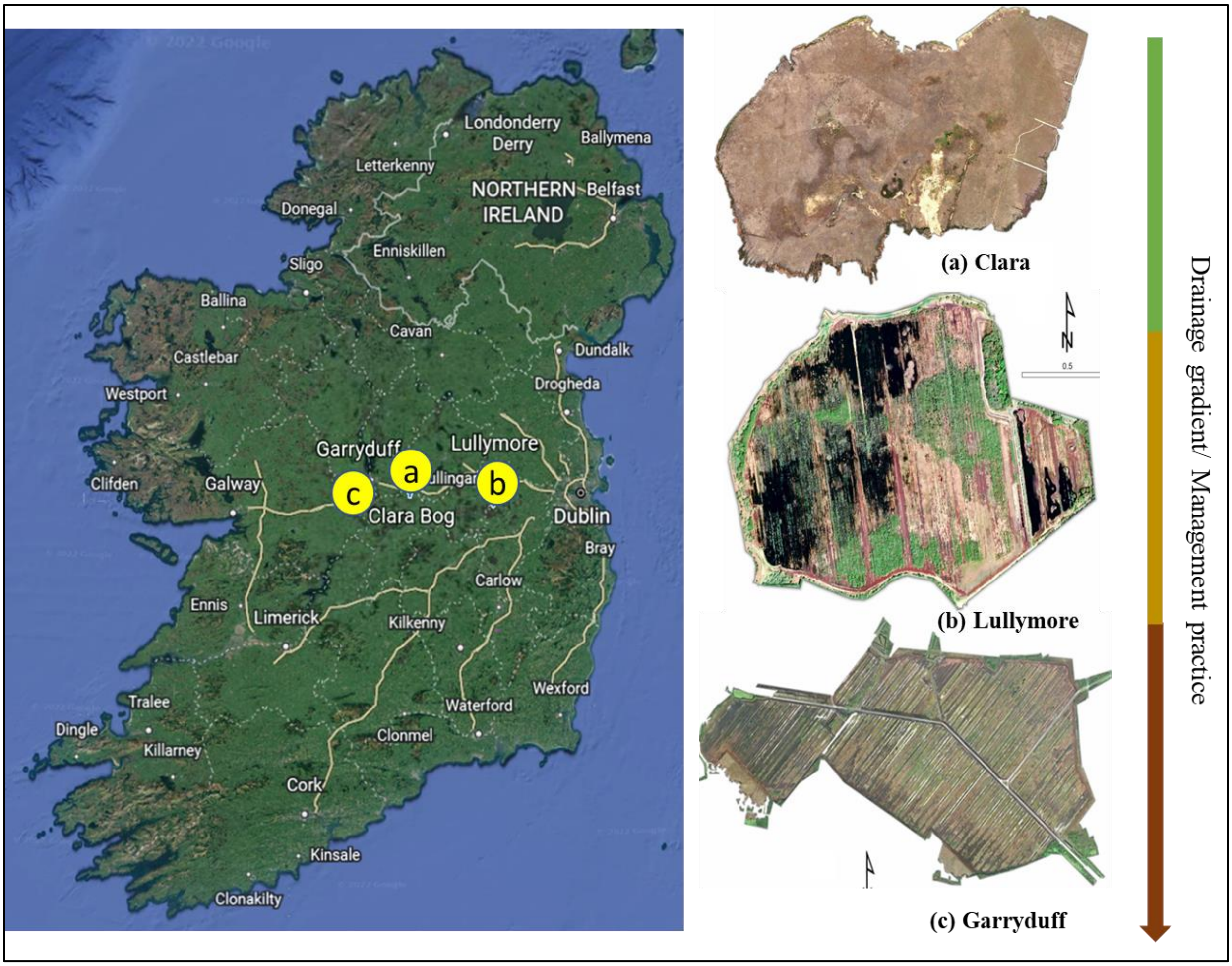

Figure 3. 1 A map of Ireland showing the study sites; (a) Clara bog (near-natural) (b) Lullymore (rehabilitation through re-wetting) (c) Garryduff (Industrial extraction)

3.1.1 Clara Bog

Clara bog is an ombrotrophic raised bog located in County Offaly in the midlands of Ireland (53°19 N, 7°36 W). It is one of the largest remaining relatively intact raised bogs in Western Europe (Crushell et al., 2008). The site covers an area of approximately 440 ha and has been designated as a special area of conservation (SAC) under the European Union Habitats Directive (Council of the European Communities, 1992). It has an Atlantic temperate climate with an average annual rainfall of 883 mm and an average annual temperature of 9.6°C (Hammond, 1981; Schaff & Streefkerk, 2011). The site is bisected by a road into two halves Clara East (206 ha) and Clara West (234 ha), and this study focuses on the western part of the bog which will be addressed as Clara bog in this thesis and is shown in Figure 3.1a and Figure 3.2. Despite being described as a near-natural bog, the site is significantly influenced by the underlying hydrology and has been subjected to continued subsidence of 4–6 mm/year over a decade which is attributed to drainage of the regional groundwater table surrounding the bog and the hydrogeological complexity of the bog itself (Regan et al., 2020). This has resulted in a change in the ecological composition of the bog by gradually losing nearly 40% of the active raised bog (ARB) area since 1991 (Regan et al., 2019).

While there is considerable variation in the distribution and diversity of vegetation on raised bogs, the vegetation succession can be grouped into an "ecotope" classification and mapping scheme (van der Schaaf, 2002). Ecotopes are vegetation communities with similar characteristics in water table depth, fluctuation in the water table, and hydrochemistry (Schaff and Streefkerk, 2011). The ecotopes can be used to classify the ecological quality of habitat areas and also represent a hydro-sequence from dry to permanently saturated zones. Several ecotopes have been classified for raised bogs and a full description is available in Schouten (van der Schaaf, 2002). The differentiation in the ecotope is driven by the hydrological characteristics of the site and is broadly based on the percentage of *Sphagnum* spp. cover and the presence of micro-topographical features and the ecotopes used in this study are summarised in Table 3.1.

Table 3. 1 Vegetation communities associated with the major ecotopes at Clara Bog (Regan et al. 2020)

Ecotope	Abiotic characteristics	Biotic characteristics
Marginal	No hummocks and hollows	Few or no peat-forming plant communities
	Acrotelm is usually absent or poorly developed (< 0.05 m)	Vegetation dominated by *Calluna vulgaris* and *Trichophorum cespitosum*
Sub-marginal	Some differentiation between hummocks and hollows	Hollows dominated by *Narthecium ossifragum* and *Sphagnum tenellum*
	Hollows inundated during a small fraction of the year	
	Acrotelm absent or thin (< 0.05 m)	
Sub-central	A micro-topography of hummocks, hollows, and lawns, but no pools	Lawns dominated by *Sphagnum magellanicum*
	Lawns are dominant	
	Acrotelm depth variable from 0.10 m to locally well-developed 0.40m	
Central	A micro-topography of hummocks, hollows, and pools	Pools, and hollows dominated by *Sphagnum cuspidatum*
	Acrotelm is moderately to well developed	
	Depth of up to 0.5 m	
Active flush/soak	Wet to extremely wet conditions	*Sphagnum cuspidatum* and *Sphagnum recurvum* lawns with *Carex rostrata*
	In the wettest parts, lawns; in some parts pools and hollows and large, flat hummocks	*Myrica gale* and *Betula pubescens* scrub/woodland with *Sphagnum palustre* in drier places
	Acrotelm well developed > 0.4 m	*Molinia caerulea tussocks* in some areas

The Ce and SC ecotopes represent areas of ARB while the sub-marginal ecotopes constitute degraded raised bog (DRB). The marginal ecotopes are considered damaged and incapable of regenerating to ARB or DRB (Regan et al., 2020). Figure 3.2 shows the Clara bog (West) study site where the measurements were conducted including the location of the chamber collars in each ecotope and the EC tower. The EC tower is located close to the centre of Clara west and predominantly covers the subcentral and submarginal ecotopes which cover approximately 77% of the bog area.

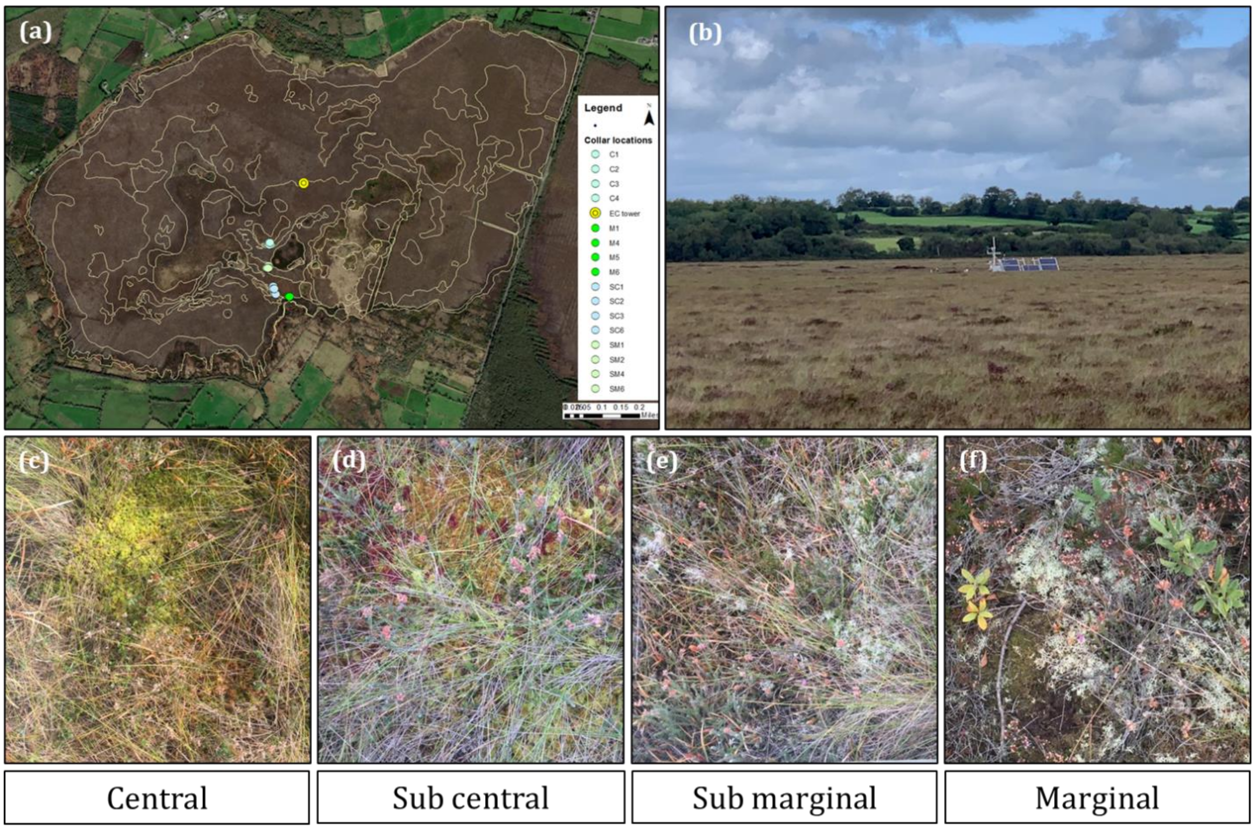

Figure 3. 2 (a) Clara west showing chamber collar and EC tower location (b) Picture showing Clara tower with vegetation; Ecotopes showing vegetation at (c) Central (d) Sub central (e) Submarginal (f) Marginal ecotope

3.1.2 Lullymore

Lullymore peatland (N53°16’ 9.808”, W 6° 57’ 52.808”) is located in County Kildare and it was previously used for industrial milled peat production (Figure 3.1b and 3.3). This site underwent rehabilitation through drain-blocking and rehabilitation on a phased basis over 15 years. The majority of this site has been zoned for biodiversity and developed as a wetland. One of the key highlights is colonization by Saw Sedge (*Gahnia aspera*) which is an indicator of rich fen development and enhances the potential biodiversity value of the site. Some bare peat-dominated fields are scattered throughout the area with typical pioneer cutaway habitats with birch scrub and poor fen habitats between the bare peat fields.

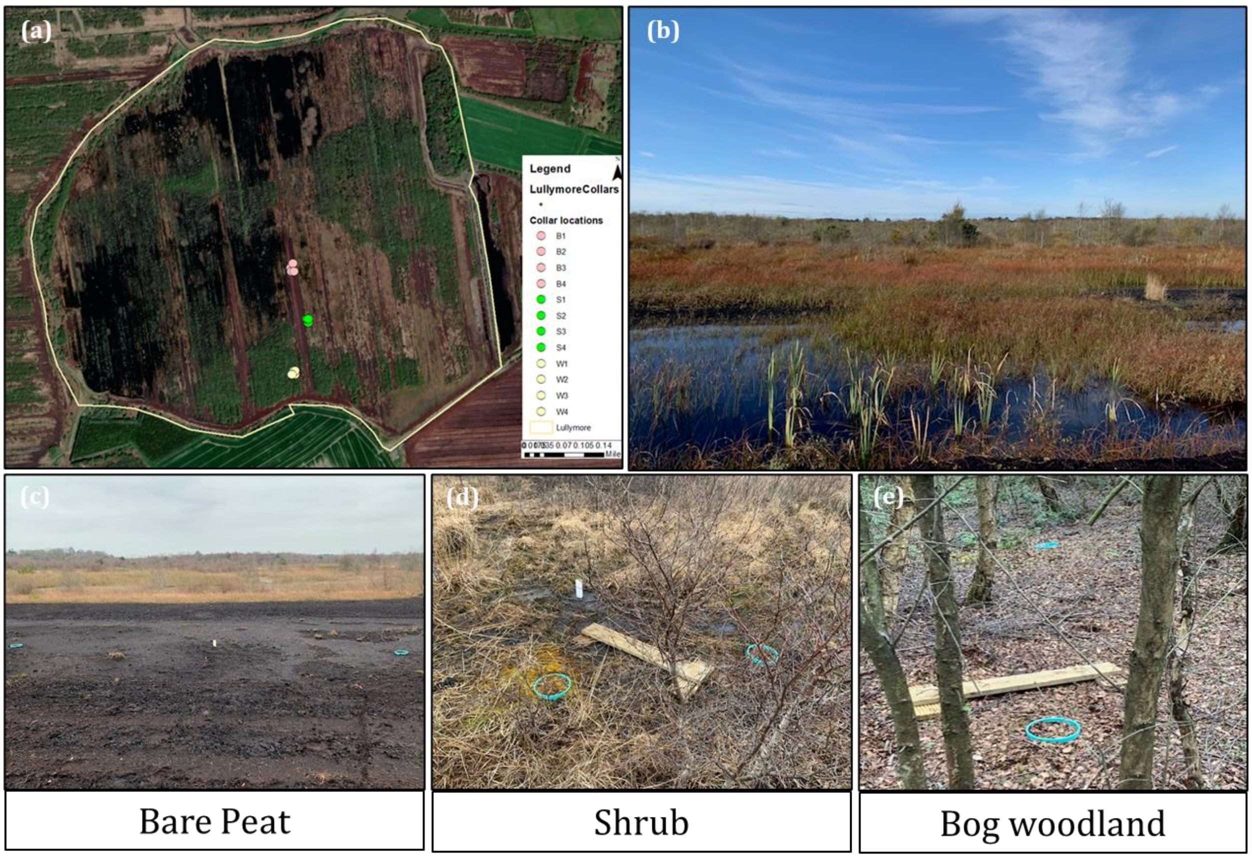

Figure 3. 3 (a) Lullymore bog boundary with chamber collar locations (b) Picture showing vegetation at Lullymore site; (c) Bare peat; Dominant vegetation at the site (d) Shrub and (e) Bog woodland

3.1.3 Garryduff

Garryduff is located approximately 1 km south of Shannon bridge in Co. Galway (N 53˚ 15' 6.451", W 8˚ 3' 10.666"). The surrounding landscape is a montage of low-lying agricultural land (pasture) mixed with other raised bogs, many of which have also been managed by

Bord na Móna for peat production with some areas of domestic turbary. Garryduff site has a pumped regime with a water table significantly lower than the surrounding area. The River Shannon and River Suck are immediately adjacent to the northern and eastern sides and parts of the Garryduff site shape the flood plain of these rivers. This site is regularly inundated during winter and occasionally at other times when the water levels on the river are high. The majority of the site is bare peat with pioneer poor fen vegetation and some open water sections (Figure 3.4).

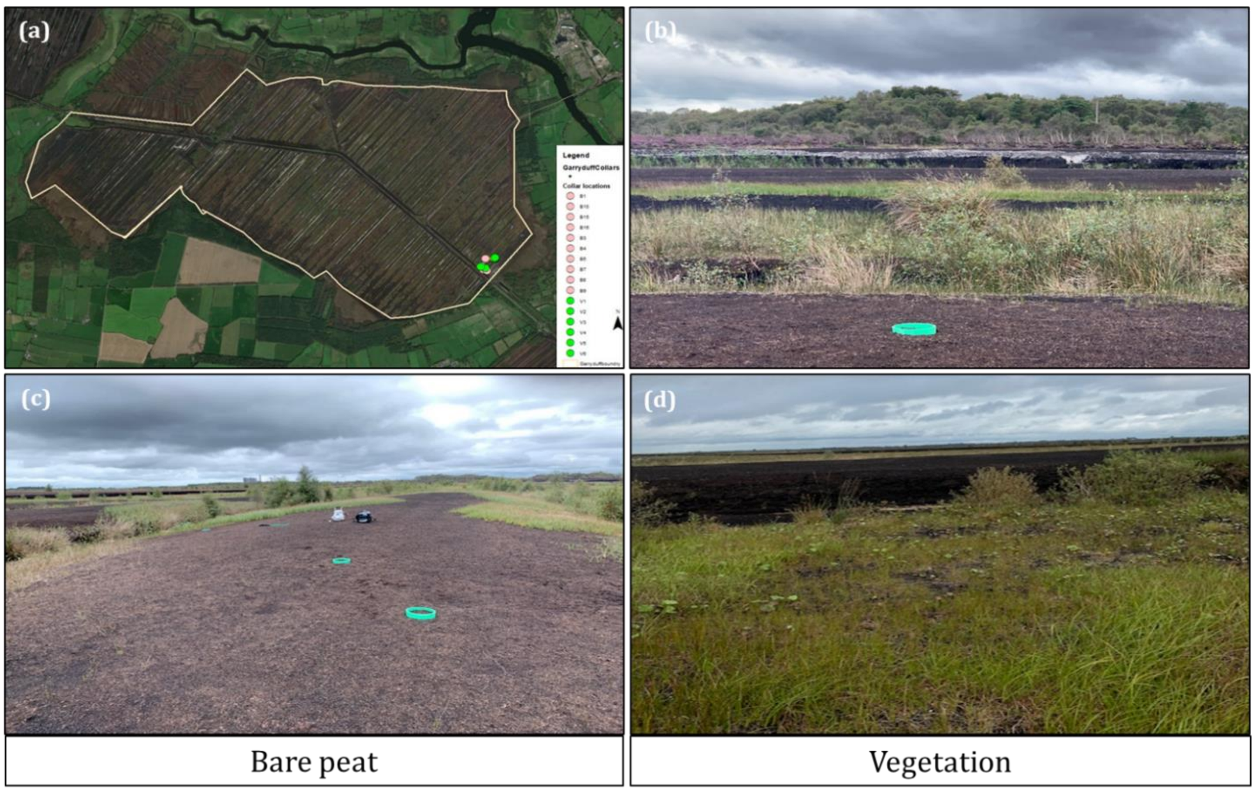

Figure 3. 4 (a) Garryduff bog boundary with chamber collar locations (b) Picture showing vegetation at the site; (c) Bare peat; (d) Natural vegetation at the site

3.2 Net ecosystem exchange of CO_2

Measurements of Net Ecosystem CO_2 Exchange (NEE) were conducted at Clara bog with the EC tower installed at the center of Clara West as shown in Figure 3.2 in 2018. The instrumentation (Figure 3.5) consists of a Sonic Anemometer (Windmaster, Gill

Instruments, Lymington, UK) which measures wind speed and direction in three dimensions, and an embedded closed path infra-red gas analyzer (LI-7200, LI-COR Lincoln, Nebraska, USA) as shown in Figure 3.5. The raw EC data were collected at 10Hz and processed using Eddy Pro version 7.0.6. The EC tower was equipped with a range of ancillary sensors for measuring environmental and meteorological conditions every 30 minutes. These variables included precipitation (Tipping bucket rain gauge, RM Young, Traverse City, Michigan, USA), air temperature and humidity (CS215, Campbell Scientific, Shepshed, England), Volumetric Water Content of the soil (VWC) (CS616 Water Reflectometer, Campbell Scientific, Shepshed, England), soil heat flux (HFP01 Hukseflux, Delft, The Netherlands), soil temperature (105E, Campbell Scientific, Shepshed, England), photosynthetically active radiation (PAR) (Skye Instruments, Llandrindod, Wales) and Net Radiation (NR) (NRLite, Kipp & Zonen, Delft, The Netherlands). The meteorological data were recorded using a Campbell Scientific micro-logger (model-CR3000) (Campbell Scientific, Shepshed, UK) at thirty minutes intervals. Water table height was recorded at hourly intervals using Orpheus Mini vented-pressure level transducers located in phreatic tubes. The EC tower flux footprint predominately covers the subcentral and submarginal ecotopes which constitute more than 77% of the site area. The CO_2 measurements along with auxiliary parameters were conducted from February 2018 to December 2021. The LI-COR 7700 methane sensor shown in Figure 3.5 was installed in July 2022 after this study ended so the measurements and analysis are not included in this thesis.

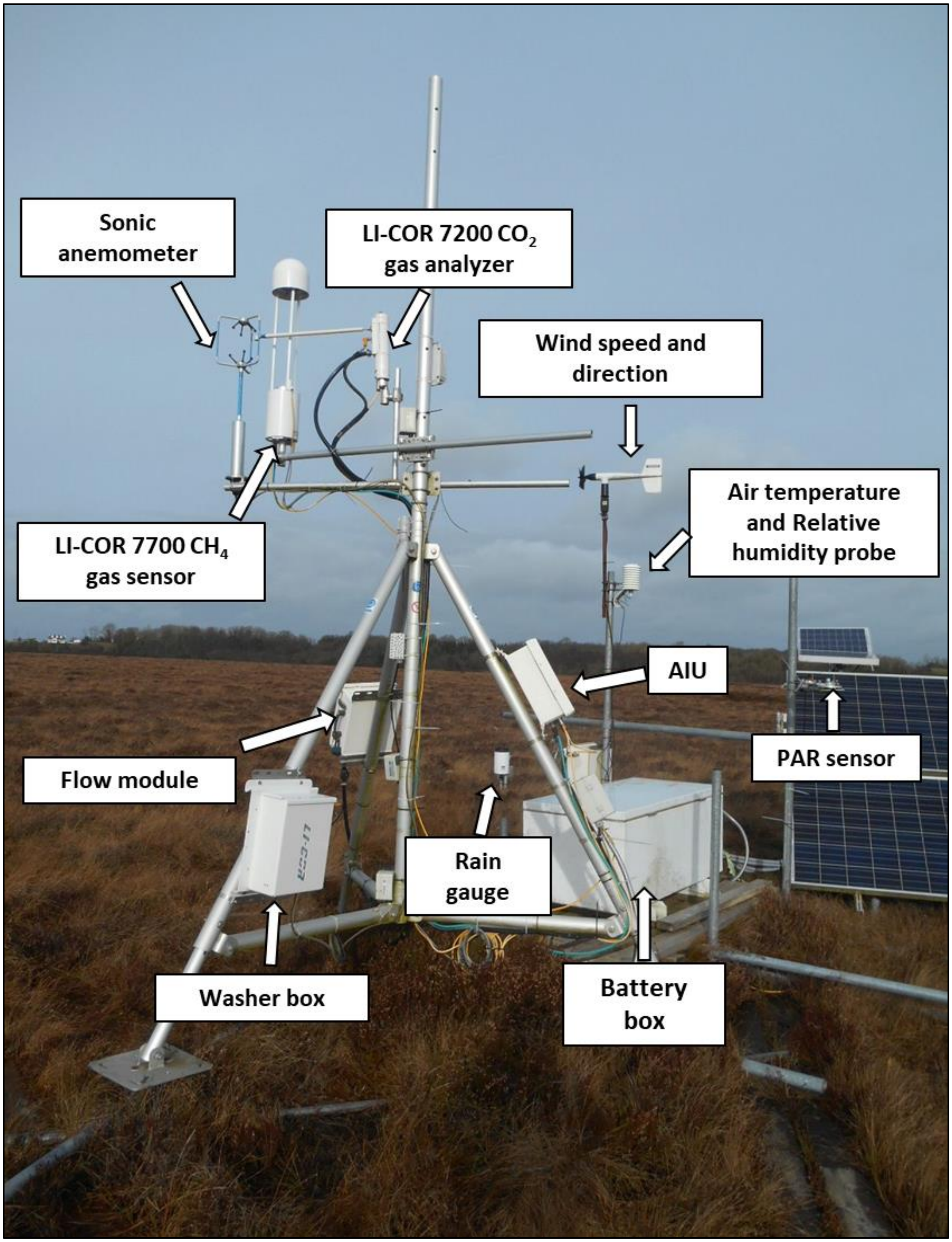

Figure 3. 5 The eddy covariance tower used in this research for measuring the net ecosystem exchange of carbon dioxide (CO_2) along with ancillary environmental and meteorological variables (soil sensors are not shown)

The eddy covariance data processing and quality control procedures (Figure 3.6) included spike removal and double coordinate rotation, while tests on developed turbulence and stationarity were also applied (Mauder, 2011; Reichstein et al. 2005; Foken et al. 2004). The flux data was gap-filled using semi-empirical models parameterized using high-quality flux data (Falge et al. 2001), and fluxes were partitioned through the extrapolation of night-time respiration (Reichstein, et al., 2005; Falge, et al., 2001). Missing meteorological data were gap-filled using the nearby meteorological weather station Horseleap, which is 7.5 km to the north of the EC station. The sensors of the EC tower and meteorological station were powered by 6 solar panels with a total rated power of 1.89 kWp. A simple two-dimensional model by Kljun (2004) was used for flux footprint analysis within the LI-COR TOVI software environment. The data from the EC tower is presented in Chapter 4 which assesses the impact of drought on Clara bog along with key drivers of emissions.

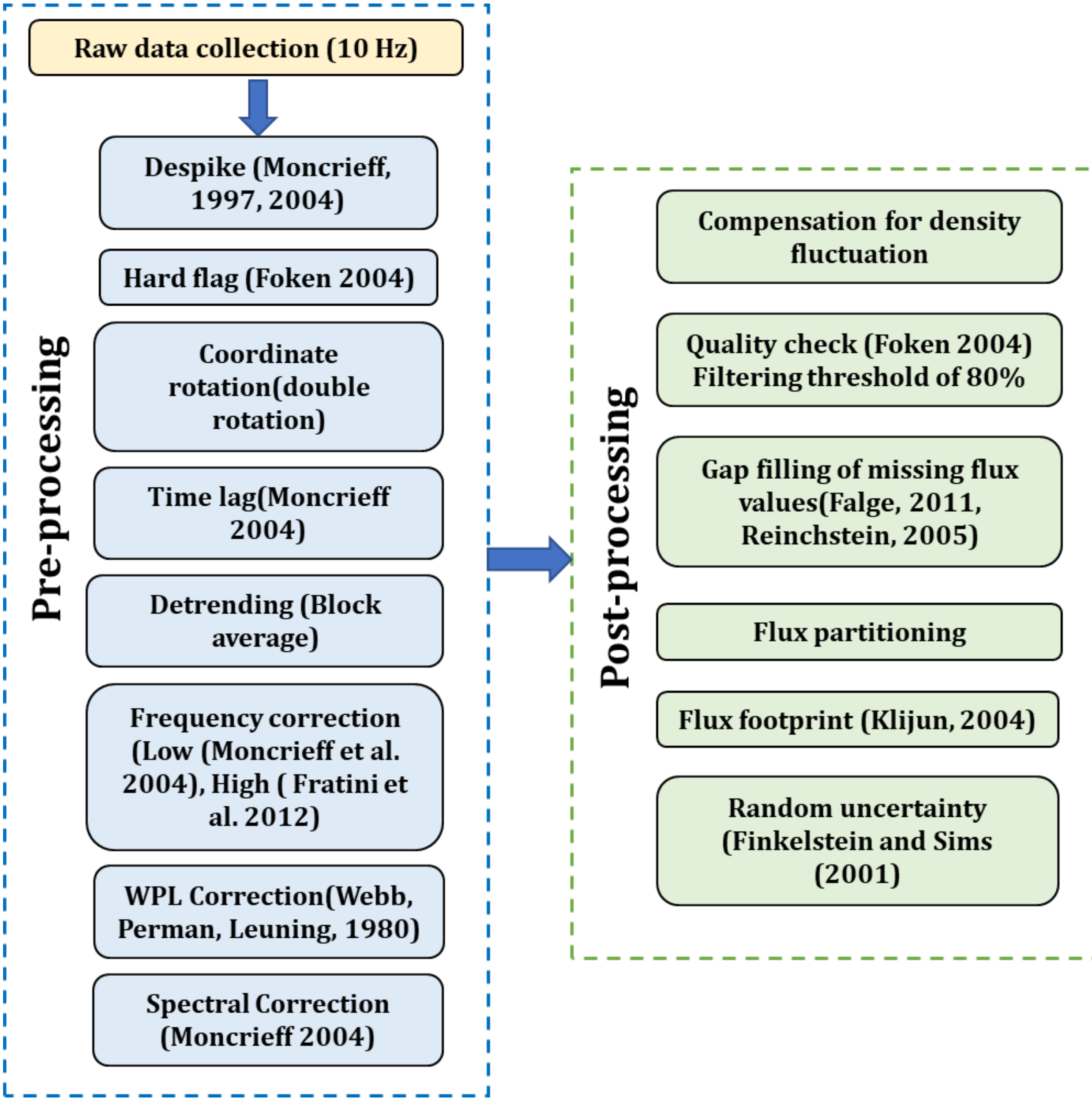

Figure 3. 6 A schematic showing the steps taken during the raw data pre-and post-processing of the eddy covariance data collected.

3.3 Methane measurements using chambers

Methane fluxes were measured at the three sites shown in Figure 3.1 using the LI-7810 $CH_4/CO_2/H_2O$ Trace Gas Analyzer (LI-COR Biosciences, Lincoln, Nebraska, USA). The LI-7810 is a high-precision, high-stability, laser-based gas analyzer that uses Optical Feedback-Cavity-Enhanced Absorption Spectroscopy (OF-CEAS) to measure gases in the air with a data acquisition rate of 1 Hz. The LI-7810 can measure CH_4 concentrations from 0.1 to 50 ppm and has a CO_2 measurement range of 1 - 10000 ppm. The LI-COR smart chamber was used to facilitate soil gas flux measurements in conjunction with the LI-7810 (Figure 3.8). The smart chamber also measures ancillary data such as soil moisture, soil temperature, and electrical conductivity using the Stevens HydraProbe.

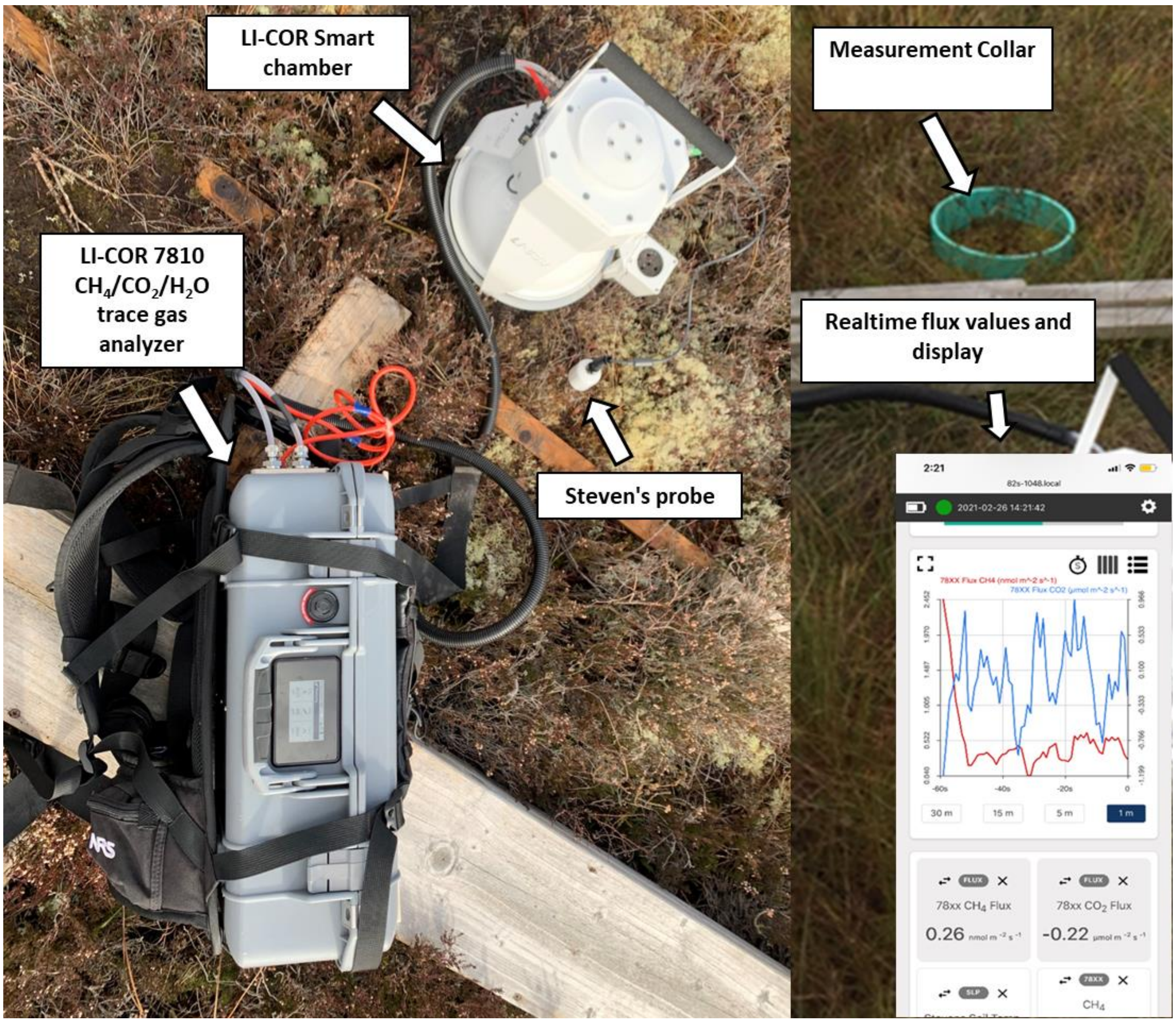

Figure 3. 7 LI-COR 7810 analyzer and smart chamber with collar and real-time measurement snapshot

The PVC collars (Figure 3.7) used in this study have an outer diameter of 21.34 cm and a height of 11.43 cm. The collar offset is measured as the distance between the soil surface and the top of the soil collar during every measurement to determine the volume of air inside the soil collar, which is in turn used to calculate the total system volume, one of the most important parameters for accurate flux estimation. The measurement duration was set to 180 seconds with dead band and post-purging. The chamber measurements were conducted at four major ecotopes i.e. central, subcentral, submarginal, and marginal at Clara bog as shown in Figure 3.2. Six collars were installed at each ecotope and measurements were collected fortnightly from January 2020 till December 2021. The representative vegetation for each ecotope is shown in Figure 3.8. The measurements were conducted fortnightly at three dominant vegetation communities at the Lulllymore site including Shrub mosaic, bog woodland, and at bare peat areas from May 2020 to December 2021. A total of 12 collars were installed at this site with four collars at each dominant vegetation community. At the Garryduff site measurements were conducted from May 2020 to December 2021 and a total of 16 collars were installed with 8 collars at bare peat and 8 collars at the vegetated spots which are covered with a mosaic of pioneer *Juncus, Eriophorum angustifolium,* and *Carex rostrata* dominated poor fen and emergent *Betula pubescens* and *Salix spp.* scrub. The representative vegetation at the site is shown in Figure 3.8.

Figure 3. 8 Representative dominant vegetation communities at all the sites where chamber measurements were conducted

The fluxes were calculated in the SoilFluxPro environment provided by LI-COR. Chapter 5 outlines methane dynamics for all three sites across the study period from the dominant vegetation communities locations and demonstrates a new methodology to upscale these fluxes from point to site scale using Planetscope imagery and machine learning algorithms.

3.4 Remote Sensing data

3.4.1 Sentinel-2 imagery

The Sentinel-2 Multispectral Instrument (MSI) samples 13 spectral bands: four bands at 10 meters, six bands at 20 meters, and three bands at 60 meters spatial resolution. The Sentinel-2 product Multispectral Instrument Level 2A (S2-MSIL2A) was made available in March 2018. The Level-2A images are bottom-of-atmosphere (BOA) reflectance in cartographic geometry and are atmospherically corrected. The satellite has a temporal resolution of 5 days, and the spatial resolution varies between 10m to 60m depending on the wavelengths. The S2 has three vegetation-red-edge bands (spatial resolution - 20m) dedicated specifically to identifying and analyzing vegetation on the ground. S2 imagery was acquired for the years 2018, 2019, and 2020 with a cloud filter of less than 10% through the Copernicus Open Access Hub, and all the bands were resampled to 10m spatial resolution using the bilinear interpolation technique in SNAP v.7.0. ("SNAP - ESA Sentinel Application Platform"). The images were then subset for Clara using the SNAP Subset tool. For this study, 9 images from 2018 (Table 3.2) were used for calibration and 11 images from 2019-2020 (Table 3.2) were used for validation. Chapter 6 shows the implementation of the Sentinel 2A data for modeling GPP using Light Use Efficiency models and the best combination of vegetation indices (hybrid models) for a near-natural raised bog was proposed.

Table 3. 2 Sentinel-2 imagery acquisition dates used for analysis in Chapter 6

Sr no.	Sentinel -2 Imagery acquisition date
1	15 February 2018
2	25 February 2018
3	21 April 2018
4	06 May 2018
5	16 May 2018
6	25 June 2018
7	30 June 2018
8	10 July 2018
9	18 October 2018
10	10 February 2019
11	21 April 2019
12	18 September 2019
13	28 October 2019
14	11 December 2019
15	22 December 2019
16	20 February 2020
17	15 April 2020
18	25 April 2020
19	27 November 2020
20	06 December 2020

3.4.2 PlanetScope

The PlanetScope satellite technology has evolved with Dove-Classic (PlanetScope-0), Dove-R (PlanetScope-1), and SuperDove (PlanetScope-2) sensors with distinct characteristics. The high-resolution PlanetScope imagery has been shown suitable to analyze and track changes in vegetation and forest cover, flood activity, and large construction projects. The data has a spatial resolution of 3.7 to 4.1 m and a temporal resolution of 1 day. In this study, the data is resampled and distributed to 3 m using PlanetScope-0 and PlanetScope-1 sensors. Atmospherically corrected products, based on the 6S model (Second Simulation of a Satellite Signal in the Solar Spectrum) were used in this study. Table 3.3 shows the four spectral bands and their wavelengths.

Table 3. 3 Spectral bands of PlanetScope sensors

Sensor	**Blue (nm)**	**Green (nm)**	**Red (nm)**	**NIR (nm)**
PlantScope - 0	455–515	500–590	590–670	780–860
PlanetScope -1	464-517	547-585	650-682	846-880

This work accessed PlanetScope-0 and -1 imagery via the Planet Education and Research Program (go.planet.com/research) and the API was used to obtain daily available PlanetScope-0 and 1 image for all three sites for the years 2020 and 2021 with a cloud filter of 10%. A total of 35 images were used for training and testing of the model at Clara, 19 images at Lullymore, and 19 images at the Garryduff site as shown in Table 3.4. Chapter 5 explains in detail the methodology used to create annual ecotope maps for all the sites with the help of planet Scope imagery and random forest algorithm.

Table 3. 4 PlanetScope imagery acquisition dates used for analysis in Chapter 5

Sr. no.	PlanetScope image acquisition date		
	CLARA	LULLYMORE	GARRYDUFF
1	12 January 2020	01 June 2020	03 May 2020
2	17 January 2020	08 June 2020	04 May 2020
3	10 March 2020	08 August 2020	27 September 2020
4	08 April 2020	20 September 2020	13 November 2020
5	15 April 2020	27 September 2020	04 December 2020
6	21 April 2020	01 September 2021	29 January 2021
7	11 May 2020	14 January 2021	10 February 2021
8	28 May 2020	23 January 2021	15 April 2021
9	18 September 2020	30 March 2021	24 April 2021
10	26 September 2020	06 April 2021	25 April 2021
11	02 October 2020	24 April 2021	07 May 2021
12	22 October 2020	25 April 2021	21 July 2021
14	24 December 2020	21 June 2021	26 August 2021
15	06 January 2021	20 July 2021	28 August 2021
16	14 January 2021	26 August 2021	07 September 2021
17	22 January 2021	28 August 2021	21 October 2021
18	28 February 2021	07 September 2021	21 November 2021
19	07 March 2021	30 October 2021	27 November 2021
20	24 April 2021		
21	25 April 2021		
22	31 May 2021		

Sr. no.	PlanetScope image acquisition date		
	CLARA	LULLYMORE	GARRYDUFF
23	20 July 2021		
24	25 July 2021		
25	24 August 2021		
26	27 August 2021		
27	07 September 2021		
28	29 September 2021		
29	21 October 2021		
30	04 November 2021		
31	21 November 2021		
32	22 November 2021		
33	27 November 2021		
34	04 December 2021		
35	10 December 2021		

Chapter 4: Multiyear carbon fluxes at a near-natural peatland in Ireland

Submitted: Global Change Biology

Primary author: Ruchita Ingle

Co-authors: Peter Cox Peter, Laurence Gill, Shane Regan and Matthew Saunders

Contributions: R.I. conceived the ideas, designed methodology, measured and analyzed the data and wrote the manuscript; P.C. provided the water table data; S.R. set up the water level monitoring network at the site; L.G. assisted in reviewing the manuscript; M.S. co-designed the experiment, processed the data and assisted in reviewing the manuscript.

4.1 Introduction

Peatlands are a type of wetland that can be found in almost every country covering 3% of the world's land area. These ecosystems store twice as much carbon stock compared to all the forests combined in the world (Global Peatland Initiative, 2019). Irish peatlands are estimated to store up to 75% of the total soil carbon (C) stocks (1064 –1503 Gt of C) on only 20% of the land area (Renou et al., 2018). Of the peatland systems in Ireland, raised bogs are of significant importance for national and global carbon budgets as they can store more carbon than blanket bogs and fens (Renou et al., 2006; Wilson and Müller, 2013; Tomlinson, 2005). The degradation of these systems through various anthropogenic activities, such as drainage for extraction, agriculture, and forestry, along with climate change is affecting the carbon sink potential of these ecosystems. In Ireland, only 10% of the raised bogs are remaining in an undisturbed state (Renou et al., 2018). The carbon dynamics of a natural peatland are governed by the hydrological conditions and it is crucial to keep the WTD close to the peat surface to maintain the carbon sink function of these systems (Evans et al., 2021).

Several studies have shown that exceptional dry interannual climatic events, referred to as drought hereafter in this chapter, are characterized by elevated summer temperatures and precipitation deficits, both of which can influence the carbon dioxide (CO_2) fluxes of peatland systems (Marcisz et al., 2020; Baldocchi et al., 2018; Lafleur et al., 2003; Aslan-Sungur et al., 2016; Drollinger et al., 2019). Such interannual changes in climate are becoming more prevalent across Europe and can alter the ecohydrological conditions of peatlands, as a result of water tables depletion coupled with increasing air and soil temperatures which tend to increase CO_2 emissions (Peters et al., 2020).

For example, Rinne et al. (2020) analyzed the effect of drought on carbon exchange at five northern European mire ecosystems, and three out of five raised bogs were shown to act as a carbon source during the drought of 2018. Another study by Lund et al. (2012) analyzed two drought events at a Swedish nutrient-poor peatland and the system acted as an annual source of carbon during the drought years but remained a carbon sink during the non-drought years. They concluded that the timing, severity, and duration of drought periods was the key driver of the CO_2 response of peatlands to climatic variability.

Other studies have seen an increase in CO_2 emissions due to enhanced rates of ecosystem respiration (R_{eco}) and the decrease of GPP during drought conditions (Helfter et al., 2015; Lafleur et al., 2003; McVeigh et al., 2014; Mikhaylov et al., 2019). The sensitivity of these systems to hydrological variability also depends on the vegetation communities present and their influence on both GPP and R_{eco}. Drollinger et al. (2019) showed that GPP at moss-dominated locations was more sensitive to WTD fluctuation than the vascular-dominated vegetation. The vascular vegetation can access water at lower depths due to their deeper root systems, making them less susceptible to changes in WTD (Lafleur et al., 2003; Antala et al., 2022). Radu et al. (2018) analyzed the impact of changing precipitation regimes on moss, sedge, and shrub communities in similar ecosystems. Their study suggests that changes in rainfall frequency will lead to increased vascular plant cover in peatlands which can positively impact the carbon-sink function by increasing the rate of C uptake through GPP.

All these studies highlight the fact that the underlying causes and dynamics affecting R_{eco} and GPP are not fully understood along with the resilience and adaptive capacity of these ecosystems to global change (Evans et al., 2016; Baldocchi et al., 2018). More long-term studies are still required to better understand the key drivers of net ecosystem exchange and to determine the resilience of peatlands across drainage gradients, particularly as peatland rehabilitation is being implemented as a climate mitigation tool at larger scales across Ireland.

In this research, we measured four years of net ecosystem exchange (NEE) data from a temperate, nutrient-poor peatland (raised bog) in the midlands of Ireland using the EC technique. The measurement period covers two drought events of 2018 and 2021 along with two normal wetter/humid years of 2019 and 2020. The main objectives were 1) to investigate the effects of drought conditions on rates of net ecosystem exchange and identify the key drivers responsible for carbon uptake and release and, 2) to assess the vulnerability and resilience of these ecosystems to climate change, particularly in the context of using peatlands as a nature-based climate mitigation tool.

4.2 Methods

4.2.1 Site

Clara bog is a near-natural raised bog located in County Offaly(Figure 4.1) in the midlands of Ireland (53°19 N, 7°36 W) and covering a total area of around 440 ha. The site is designated as a special area of conservation (SAC) under the European Union Habitats Directive (Council of the European Communities, 1992). It has an Atlantic temperate climate with an average annual rainfall of 883 mm and an average annual temperature of 9.6 °C (Hammond, 1981; Schaff & Streefkerk, 2011). The site is bisected by a road that splits the bog into two distinct areas Clara East (206 ha) and Clara West (234 ha): this study focuses on the West part of the bog and will be addressed further as Clara bog in this study.

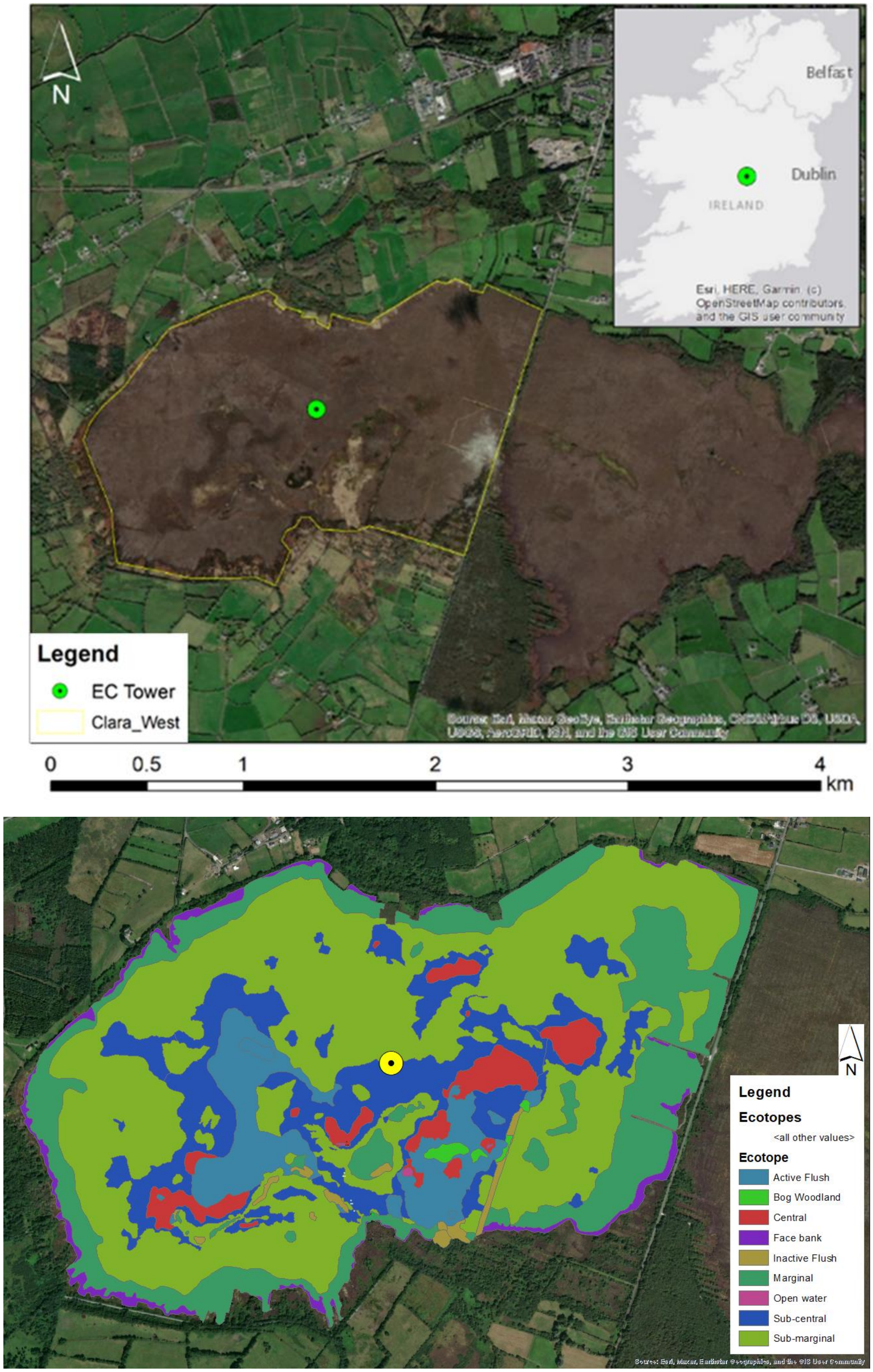

Figure 4. 1 (a) Clara bog with the location of the Eddy Covariance tower (b) Ecotopes at Clara bog with EC tower location

Despite being a near-natural bog, the site is significantly influenced by the surrounding land use and underlying hydrology. The site has been subject to continued subsidence which is attributed to the drainage of the regional groundwater table surrounding the bog and the hydrogeological complexity of the bog itself (Regan et al., 2020). The EC tower is located in a more stable area in the centre of the western part of the bog. The vegetation communities that constitute Clara bog have been categorized into a series of different 'ecotopes' (Fernandez et al., 2014). Ecotopes are categorized into nine ecotopes (Figure 4.1b) based on the combination of the plant species present, which are driven by the hydrological conditions across the site (wet to dry). The major five ecotopes and their dominant vegetation are described in detail in Table 4.1 and are marginal (M), submarginal (SM), subcentral (SC), central (Ce), and active flush and soaks (AF). (Crushell et al., 2008; van der Schaff and Streefkerk 2011; Fernandez et al., 2014).

Table 4. 1 Vegetation communities associated with the major ecotopes at Clara Bog

Ecotope	**Dominant vegetation**
Marginal	*Calluna vulgaris* and *Scirpus caespitosus*
Submarginal	*Narthecium ossifragum* and *Sphagnum tenellum*
Subcentral	*Sphagnum magellanicum*
Central	*Sphagnum cuspidatum*
Active Flush and Soak	*Sphagnum cuspidatum, Myrica gale, Betula pubescens* scrub woodland with *Sphagnum palustre* and *Polytrichum commune, Molinia caerulea tussocks*

4.2.2 Micrometeorological measurements

Eddy covariance measurements were carried out from February 1st, 2018, until December 31st, 2021 at the center of Clara West, as shown in Figure 1. The EC instrumentation consisted of an embedded closed path infra-red gas analyzer (LI-7200) and a sonic anemometer. The EC tower flux footprint predominately covers fetch from the major ecotopes. The raw EC data were collected at 10 Hz and processed using Eddy Pro version 7.0.6. Additional meteorological and environmental variables were also measured at the submarginal ecotope where the EC tower is installed. The additional sensors included precipitation, air temperature (T_a) and humidity, soil moisture (SOM), soil heat flux, soil temperature (T_s), Photosynthetically Active Radiation (PAR), and Net Radiation (NR). The meteorological data were recorded using a Campbell Scientific micro-logger (model-CR3000) at thirty minutes intervals. Water table height was recorded at hourly intervals using Orpheus Mini vented-pressure level transducers located in phreatic tubes. The EC processing and quality control procedures included spike removal and double coordinate rotation while tests on developed turbulence and stationery were also applied (Foken et al., 2004; Mauder, 2011; Reichstein et al., 2005; Baldocchi, et al., 2005). The flux data were gap-filled using semi-empirical models parameterized using high-quality flux data (Falge et al., 2001), while fluxes were partitioned through the extrapolation of night-time respiration (Reichstein et al., 2005; Baldocchi, et al., 2005). Missing meteorological data were gap-filled using the nearby meteorological weather station (Horseleap) which is 7.5 km to the north of the EC station. This study focuses on both annual and periodic carbon dynamics, and the seasonal assessment of the data is divided into three key periods following Helfter et al. (2015). The first period included the initial months of the growing season from March through June (M-J) followed by a second period which included the months of July to October (J-O). The third represented the dormant (D) period and included the months of November, December, January, and February.

4.3 Results

4.3.1 Environmental and Meteorological conditions

The seasonal and interannual fluctuations in the main meteorological parameters are shown in Figures 4.2 and 4.3. Daily values of mean T_a and total PAR showed characteristic seasonal patterns in all years (Figure 4.2b and c), with maximum measured incident daily radiation coinciding with maximum T_a, representing the peak of the summer period/growing season. The mean monthly T_a varied between 3.5°C to 17.1°C during the study period with the highest temperatures recorded in July of all the years. The seasonality in T_a follows the 30-year annual mean T_a (9.3°C) recorded at the closest Met Éireann station as shown in Figure 4.2b, with an annual mean T_a of 9.8°C, 9.9°C, 9.9°C, and 9.9°C for the years 2018, 2019, 2020 and 2021 respectively. During the study duration, the total annual precipitation follows the 30-year annual precipitation (989.32 mm) with the lowest annual precipitation recorded in 2021 (560 mm) followed by 2018 (733 mm), 2019 (1034.5 mm) and 2020 (1065.5 mm) as shown in Table 4.2. The highest monthly precipitation was observed in January 2018 (136mm) and 2021, August 2019 (158mm), and February 2020 (205mm) as shown in Figure 4.2a. Total monthly PAR ranged from 20 to 294 MJ m^{-2} with total annual incident radiation shown in Table 4.2. For all the years, PAR reached its peak during the M-J and J-O period with maxima during June in 2018, July in 2019 and 2021 and, May in 2020 (Figure 4.2c). Daily soil temperature (T_s) were ranging between -2°C to 21°C in 2018, 2°C to 18°C in 2019, 1°C to 18°C in 2020 and 0°C to 22°C in 2021 with annual average ranging between 10.2°C to 10.7°C throughout the study duration. The monthly soil temperature followed the seasonal trend with maximum soil temperature observed during the month of July coinciding with the maximum air temperature.

Table 4. 2 Meteorological and carbon flux data for all the four years

Parameter	**2018**	**2019**	**2020**	**2021**
Air temperature (°C)	-4 to 21	0 to 21	-1 to 20	-3 to 22
Soil temperature (°C)	-2 to 21	2 to 18	1 to 18	0 to 22
Total precipitation (mm)	733.3	1034.5	1065.5	560
Water table depth (cm)	-15 to 5.37	-9.6 to 7.9	-14.1 to 8.05	-19.1 to 2.7
Monthly total PAR (MJ m^{-2})	1318	1608.7	1581	1577
Soil moisture (%)	70 to 95	84 to 93	82 to 93	82 to 94
Total GPP (g C m^{-2})	-753.1	-824.3	-775.7	-726
Total R_{eco} (g C m^{-2})	806.6	699.1	689.8	676
Cumulative NEE (g C m^{-2})	53.5	-125.2	-85.88	-49.8
CDD (Days)	24	14	15	20
LWTD (Days)	147	70	81	205
CLWTD (Days)	109	28	81	79

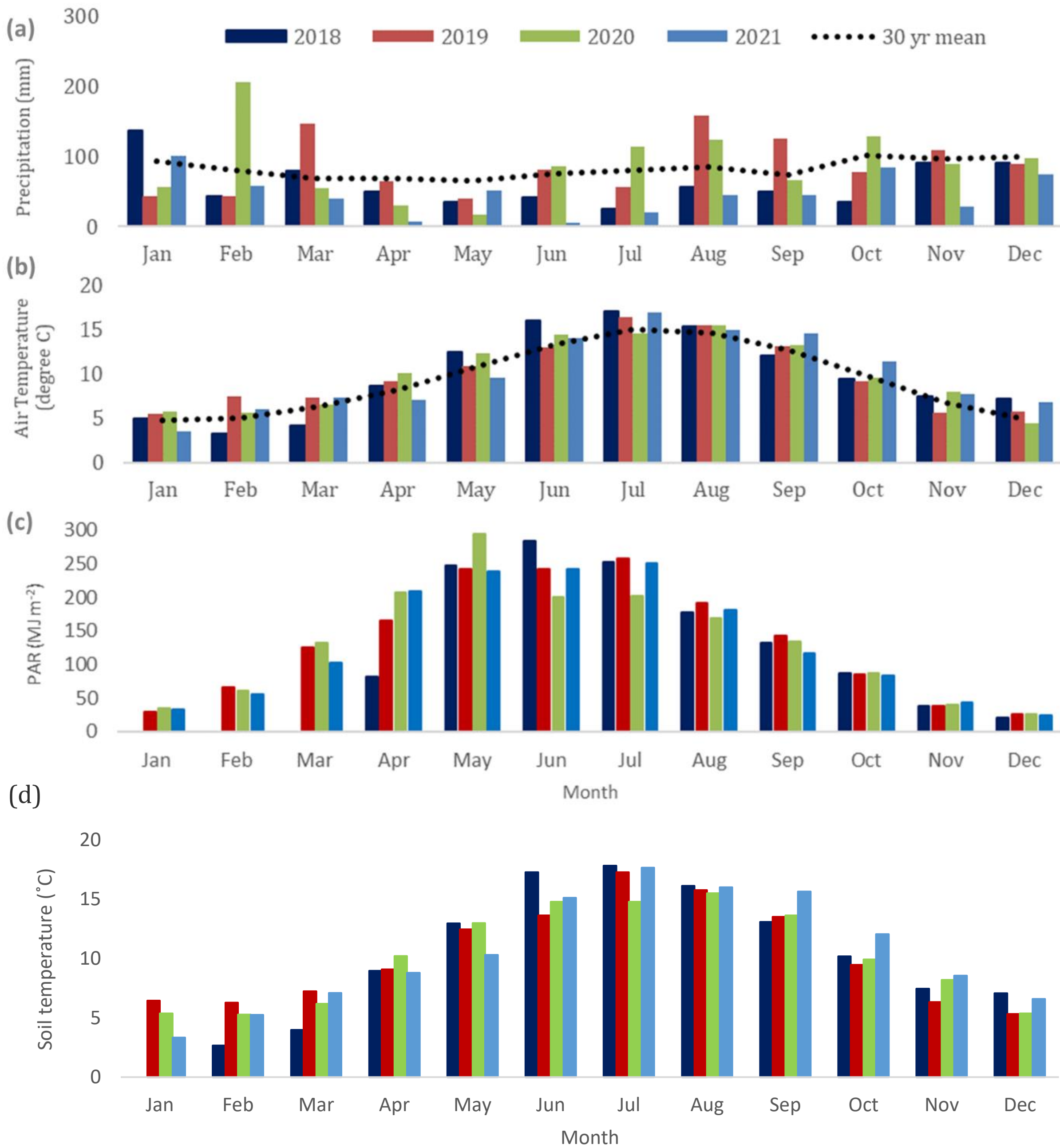

Figure 4. 2 Meteorological parameters at Clara West from 2018-2021 (a) total monthly precipitation (mm) (b) mean monthly air temperature (˚C) (c) total monthly photosynthetically active radiation (MJ m^{-2}) (d) mean monthly soil temperature (˚C)

The daily water table depth ranged from -19.13 to 8.05 cm throughout the study period as shown in Figure 4.3a. In 2018, the daily average WTD ranged between 5.4 cm to -15.07 cm thought the year, however, it dropped below the surface in April and remained there until November, leading to a consecutive period of 109 days where the WTD was below -5 cm which lasted from June through to September. However, the WTD in 2019, 2020, and 2021 also showed significant variability as shown in Figure 4.3a, with a number of consecutive days where the WTD was below -5 cm (28, 81, and 79 days respectively). Even though the deepest drawdown was observed in July 2021, the WTD was replenished to close to the surface sooner than in 2018. The total number of days when the WTD was below -5 cm (LWTD) is shown in Table 4.2. The dry periods were determined by the total number of consecutive days where the WTD fell below -5 cm (CLWTD) (Helfter et al., 2015). The total number of LWTD was highest in 2021 (205 days) followed by 2018 (147 days), 2020 (81 days), and 2019 (70 days), however, the longest consecutive days with WTD below -5 cm (CLWTD) was observed in 2018 (109 days) followed by 2020 (81 days), 2021 (79 days) and 2019 (28 days) (Table 4.2).

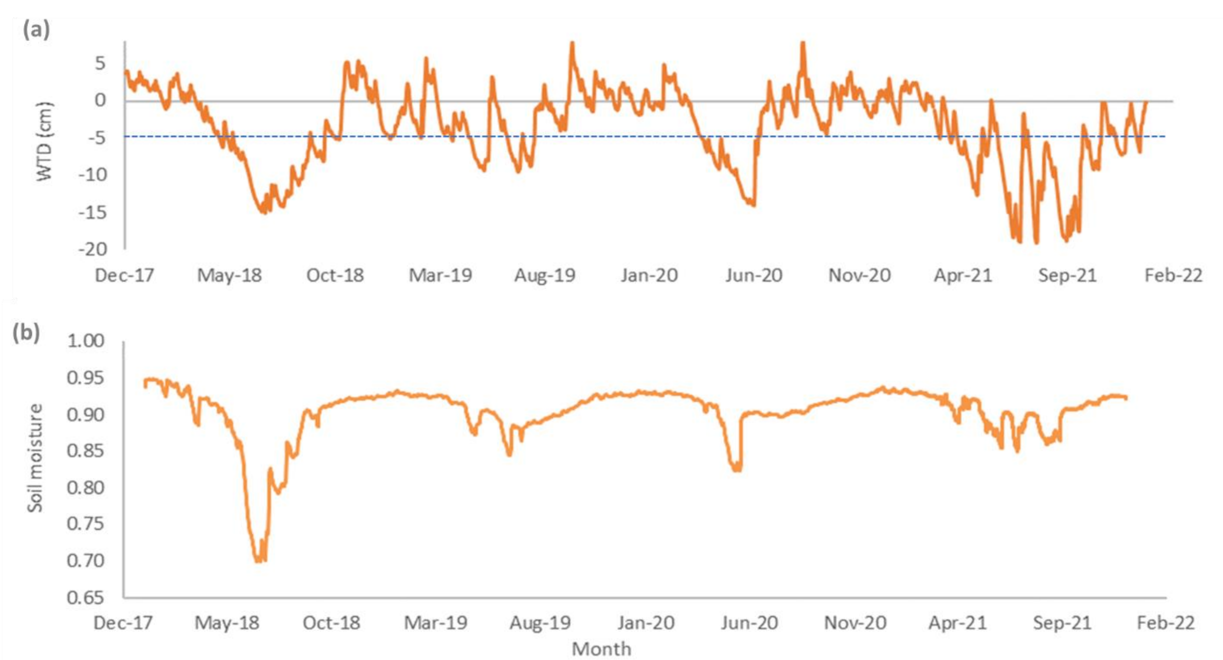

Figure 4. 3. Hydrological parameters at Clara West from 2018-2021 (a) Daily average water table depth (cm) (b) Daily average surface soil moisture content (%)

The average daily surface soil moisture content at the flux tower location is shown in Figure 4.3b and it varied between 70 and 95% throughout 2018-2021 with the lowest value of 70% recorded in May 2018. Overall, the highest number of consecutive days with soil moisture below 85% was also recorded in 2018 as 75 days followed by 19 days in 2020, 4 days in 2019, and zero days in 2021.

4.3.2 GPP and key drivers

The site showed interannual and seasonal variability in GPP throughout the measurement period with daily GPP ranging from -6.59 to 0.24 g C m^{-2}. GPP is CO_2 assimilated by the system and negative sign convention has been used to show assimilation and Ecosystem respiration (R_{eco}) is CO_2 released to the atmosphere and positive sign convention is used to show emissions in this thesis. The highest GPP values were recorded during the M-J and J-O periods and the lowest values were recorded in the D period as shown in Figure 4.4. Total annual GPP ranged between -726 g C m^{-2} to -825 g C m^{-2} across the study years with the highest rates of uptake observed in 2019 and the lowest in 2021 as shown in Table 4.2.

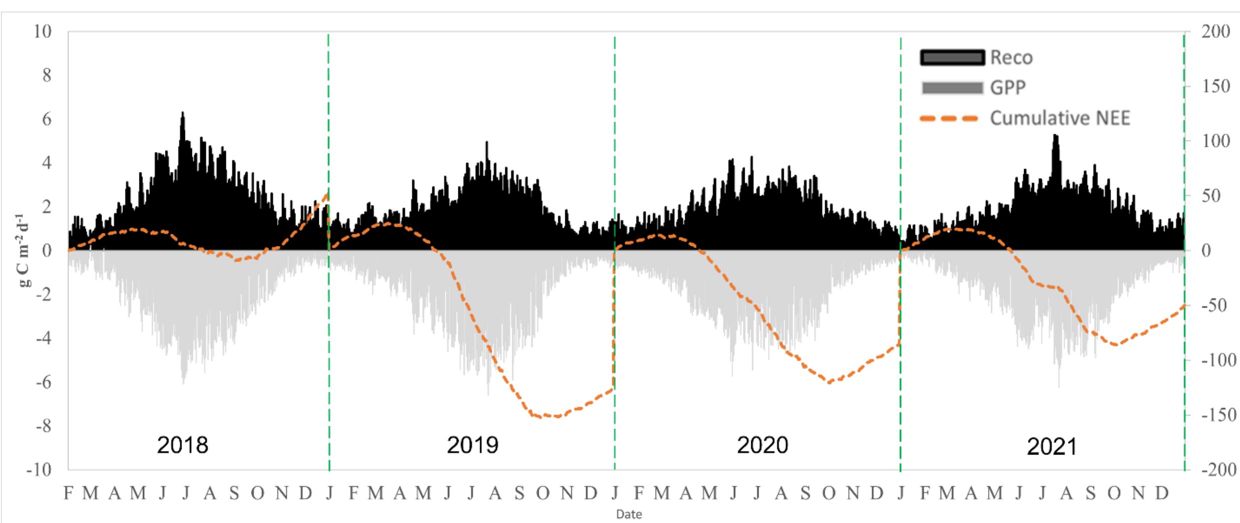

Figure 4. 4. Plot showing daily GPP (g C m^{-2}) in light grey colour, R_{eco} (g C m^{-2}) in black colour, and Cumulative NEE (g C m^{-2}) as an orange dotted line

Overall, annual rates of GPP showed varying correlation (Spearman) with environmental parameters ranging between 0.29 to 0.91, with the lowest correlation with precipitation (0.29 to 0.50) and highest correlation with soil temperature (0.91) throughout the study duration as shown in Table 4.3. The daily correlation of environmental parameters with GPP for the periods of M-J, J-O, and D is shown in Figure 4.5 giving an insight into key drivers. T_a (0.91), SOM (0.87), T_s (0.93), and WTD (0.9) were showing highest correlation with GPP during the M-J period of 2018 when compared to M-J, J-O, and D of all years(Figure 5). However, PAR showed strong correlation (0.9) with GPP during J-O of 2019. One of the key drivers WTD was showing the strongest correlation with GPP in M-J 2018 which was almost 30-40% higher than all the periods during the study duration (Figure 4.5a).

Table 4. 3 Annual correlations between GPP, Reco, and environmental parameters for all four years

Year	**2018**			**2019**			**2020**			**2021**		
Parameters	**GPP**	**R_{eco}**	**NEE**	**GPP**	**R_{eco}**	**NEE**	**GPP**	**R_{eco}**	**NEE**	**GPP**	**R_{eco}**	**NEE**
Ta	-0.84	0.97	-0.25	-0.81	0.95	-0.5	-0.78	0.96	-0.35	-0.83	0.96	-0.35
WTD	0.83	-0.82	0.49	0.45	-0.48	0.33	0.38	-0.34	0.38	0.73	-0.71	0.49
SOM	0.84	-0.88	0.41	0.8	-0.82	0.62	0.8	-0.85	0.53	0.84	-0.85	0.52
Ts	-0.91	0.96	-0.41	-0.88	0.94	-0.64	-0.85	0.92	-0.52	-0.9	0.94	-0.52
PAR	-0.83	0.79	-0.55	-0.9	0.71	-0.88	-0.89	0.66	-0.86	-0.81	0.66	-0.75
Rain	0.45	-0.28	0.5	0.3	-0.16	0.4	0.5	-0.35	0.52	0.29	-0.21	0.31

4.3.3 Reco and key drivers

Monthly R_{eco} followed a seasonal trend with the highest values during the M-J and J-O period and lowest values during the D period as shown in Figure 4.4. The daily rate of R_{eco} ranged between 0.25 to 6.29 g C m^{-2} throughout the study duration. Table 4.3 shows the correlation (Spearman) of annual rates of R_{eco} with environmental parameters ranging between 0.16 to 0.97, with the lowest annual correlation with precipitation (0.16 to 0.35) and the highest correlation with T_a (0.97) throughout the study duration.

Figure 4.5 shows the daily correlation of environmental parameters with R_{eco} for the periods of M-J, J-O, and D. Ta (0.98), SOM (0.87), T_s (0.97), PAR (0.82) and water table depth (0.86) were showing highest correlation with GPP during the M-J period of 2018 when compared to M-J, J-O and D of all the years(Figure 4.5). The WTD of M-J and J-O of 2018 showed a strong correlation with R_{eco} of 0.86 and 0.81 respectively. This correlation is almost 20-40% higher than all the periods during the study duration(Figure 4.5).

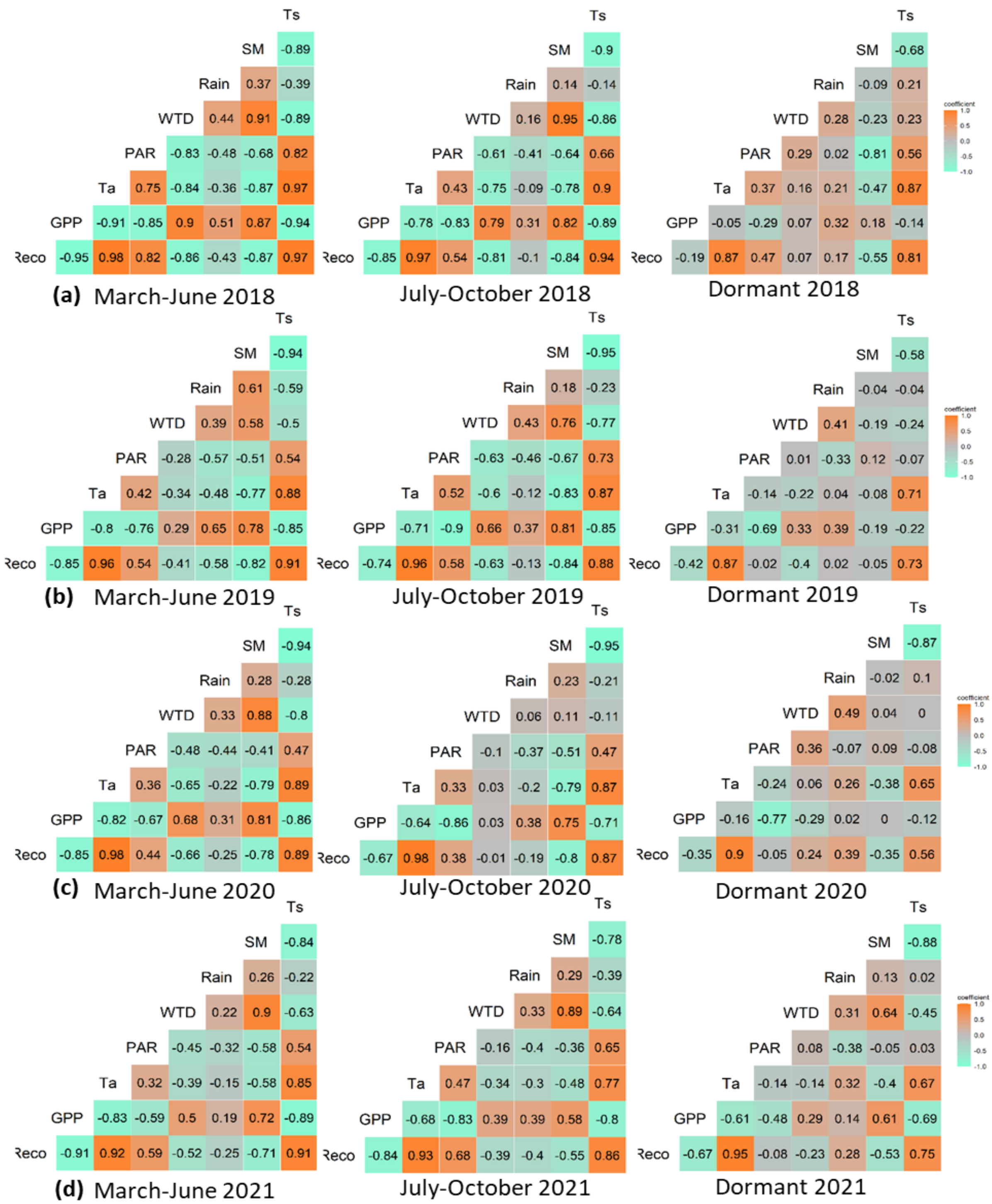

Figure 4. 5 Heat map based on correlation matrix between gross primary production (GPP), ecosystem respiration (R_{eco}), air temperature (Ta), soil temperature (Ts), (water table depth (WTD), soil moisture (SOM), photosynthetically active radiation (PAR) and precipitation (rain) for March-June, July-October and the Dormant period for (a) 2018 (b) 2019 (c) 2020 and (d) 2021. Warm colors represent positive correlation and cooler colors represent negative correlation based on the Spearman correlation test

4.3.4 NEE and key drivers

Seasonally, the site consistently alternated from being a net CO_2 sink in the growing season to being a net CO_2 source in the non-growing season with an overall cumulative net ecosystem exchange (NEE) of 53.5 g C m^{-2}, -125.2 g C m^{-2}, -85.88 g C m^{-2} and -49.8 g C m^{-2} in 2018, 2019, 2020 and 2021 respectively (Table 4.1). The switch from a net CO_2 source to a sustained CO_2 sink (point of inflection) generally occurred during late April or early May with an exception in 2018 when the system only switched to a CO_2 sink by the end of July. In 2018, the system reverted from being a CO_2 sink to a CO_2 source during mid-October and remained a source of CO_2 till the end of the year. However, the system continued to be a CO_2 sink after the first point of inflection (April or May) for all the other years (2019-2021). Annual NEE was correlated with all the environmental parameters (0.25 to 0.88) showing the highest correlation with PAR (0.88) in 2019 and the lowest correlation with annual T_a (0.25).

The ratio of GPP/R_{eco} is shown in Figure 4.6, with distinct differences observed between R_{eco} during the M-J and J-O period of 2018 as compared to other years. During these periods it was observed that carbon losses through respiration were close to exceeding rates of carbon assimilation through photosynthesis, while the opposite trend was observed for all subsequent years.

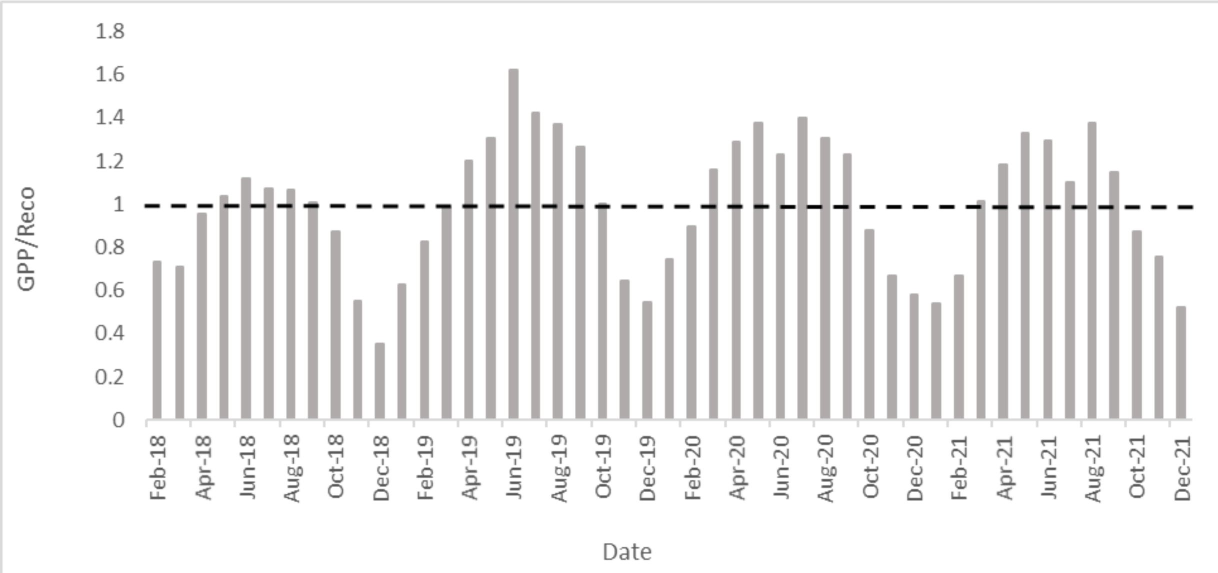

Figure 4. 6. The ratio of GPP/R_{eco} during the four-year study period (2018 to 2021)

4.4 Discussion

4.4.1 Impact of environmental factors on the carbon balance of peatlands

The carbon budget at Clara bog over the study period was driven by interannual variability in the hydrology at the site which resulted in Clara bog turning into a source of CO_2 in 2018 due to the prolonged depletion of the WTD which further influenced the surface soil moisture content during the M-J period due to higher temperatures. Annual rates of GPP and R_{eco} were correlating well with all the environmental parameters except precipitation. As shown in Table 4.3, the WTD of 2018 was showing the strongest correlation with both GPP and R_{eco} as compared to other years. the WTD during M-J in 2018 showed the strongest correlation of 90% with GPP and 86% with R_{eco} followed by J-O of 2018. This is mainly explained by the distinctly prolonged lowering of the WTD depletion and soil moisture during the M-J and J-O periods of 2018 combined with lower soil moisture and lower precipitation and, higher temperatures. The site was acting as a carbon sink in 2021 which was also a drought year marked by lower precipitation and significantly lower WTD for longer periods but there were enough periods of small amounts of rain to keep the soil moisture above 80%. The duration of the drawdown beyond a certain depth has characterized the drought of 2018 apart from 2021.

Out of all environmental drivers, WTD is one of the most studied hydrological drivers along with its sensitivity to the duration and severity of growing seasons of drought and flooding events (Aslan-Sungur et al. 2016; Lund et al. 2012; Evans et al. 2021). The 2018 drought caused a widespread water table drawdown across northern European mire ecosystems. Rinne et al. (2020) analyzed five natural peatlands equipped with EC systems and observed that three out of the four mires where the water table was significantly lowered turned from CO_2 sinks to sources during 2018. Furthermore, Evans et al. (2021) reported that the mean annual effective water table depth was a key driver controlling EC-derived CO_2 fluxes across 16 peatland sites in the UK and Ireland, and estimated that every 10 cm increase in the depth of the aerated peat layer could increase the net warming impact of CO_2 by at least 3 tonnes of CO_2 per hectare per year. This study observed the duration and timing of depletion in WTD that caused the soil moisture to fall below the threshold. Therefore, soil moisture along with the timing and duration of LWTD has influenced the carbon balance by converting the system from a carbon sink to a source in 2018.

Lund et al. (2012) analyzed two drought periods at a raised bog in Sweden and found that the timing, severity, and duration of drought periods regulate rates of GPP, Reco, and NEE. Short but severe summer drought can increase CO_2 emissions by enhancing rates of R_{eco} and reducing rates of GPP (Helfter et al. 2015; Lund et al. 2012b; McVeigh et al. 2014; Mikhaylov et al. 2019). Whether it is R_{eco} or GPP that plays a more significant role in driving interannual variability of NEE depends on the peatlands vegetation composition and hydrological conditions (Lafleur et al. 2003). In general, the GPP of moss-dominated peatlands appears more sensitive to changes in WTD than peatlands dominated by vascular vegetation, as the roots of vascular vegetation can reach deeper soil layers and access to water even during drought periods (Drollinger et al. 2019; Helfter et al. 2015; Lund et al. 2012; Rinne et al. 2020; Helbig et al. 2022). In this study, the predominant vegetation in the EC footprint is mosses but there are also significant areas of vascular plants, and the rates of GPP were found to be relatively consistent across years and exceeded R_{eco} in all years except for 2018. Drought events can stimulate peat decomposition due to the lowering of WTD and can strongly decrease the C sink strength of these ecosystems. Lund et al. (2012) reported that the drought years of 2006 (52.4±26.0 g CO_2 m^{-2}) and 2008 (86.4 g CO_2 m^{-2}) were C sources and suggests that the timing, severity, and duration of the drought period control the effect on GPP and Reco for temperate bogs. The findings of this study suggest that R_{eco} is more sensitive to warmer and drier summer conditions than photosynthesis and it aligns well with other previous studies on temperate bogs (Lund et al. 2012; Helfter et al. 2015; Fortuniak et al. 2021; Drollinger et al. 2019). This result does however contradict the findings that drought events strongly reduce GPP of near-natural peatlands due to the typical vegetation composition being adapted to high water levels (Lafleur et al. 2003; Chen et al. 2011; Baldocchi 2014). However, the effects of drought periods on the C balance have been found to differ widely between peatland types and latitudes (Minkkinen et al., 2018). Three years of measurements at a temperate peatland in Turkey showed that the peatland acted as a CO_2 source of 246, 244, and 663 g C m^{-2} yr^{-1} for the years 2011, 2012, and 2013 due to large interannual variability is driven by lowering of WTD and soil moisture (Aslan-Sungur et al. 2016). Fortuniak et al. (2021) observed that a temperate peatland in Poland acted as a significant sink of atmospheric carbon during wet years (−270 ±70 g C-CO_2 m^{-2} yr^{-1}) and a substantial source of carbon during dry years (+130 ± 70 g C-CO_2 $m^{-2}yr^{-1}$). However, a study based on one of the longest peatland EC study sites by Helfter et al. (2015) found that a temperate Scottish peatland acted as a consistent CO_2 sink (−5.2 to −135.9 g CO_2-C $m^{-2}yr^{-1}$) throughout the measurement span of 11 years. Consequently, the feedback of different climatic events on the C cycles of temperate peatlands may be affected by environmental and hydrological variation or plant physiological and phenological responses to drought conditions (Evans et al. 2021; Rinne et al. 2020; Nugent et al. 2018). Results from this study and Lund et al. (2012) have both highlighted the resilience of these systems to revert to acting as a carbon sink in the years after the occurrence of drought events and how soil moisture and timing of low WTD affect the C dynamics at these ecosystems.

4.4.2 Annual NEE

The average 4-year cumulative NEE over this study (-190.1± 243.5 g CO_2 m^{-2}) compares well with the annual NEE values reported for a raised bog (-212 ± 220 g CO_2 m^{-2} y^{-1}) in Ireland (Swenson et al. 2019). Previous measurements conducted at Clara bog during the years 2016 and 2017 using chamber technique indicated that the site was acting as a small source with NEE of 1.8 ± 15 g C-CO_2 m^{-2} y^{-1} in 2016 which was a normal climatic year and increased to being a source of 47.8 ± 16 g C-CO_2 m^{-2} y^{-1} in 2017 which was a dry year and this might have had an influence on the 2018 NEE. However, it is important to note that the chamber data were scaled to area based on ecotope maps while the EC footprint focuses on the dominant ecotopes on the bog.

Helfter et al. (2015) measured an 11-year mean NEE of -64.1 ± 33.6 g CO_2-C m^{-2} in a near-intact bog in Scotland and McVeigh et al. (2014) calculated a 9-year mean of -56 g Cm^{-2}

yr^{-1} (-32 to -79 g C m^{-2} yr^{-1}) in an Atlantic blanket bog in Ireland. Both these sites were acting as a carbon sink however, the annual net CO_2 ecosystem exchange at an intact bog in the Eastern Alps of Austria differed substantially between two measurement years, with a NEE of -24 ±13 g C m^{-2} yr^{-1} for a drought-affected year and -84 ± 13 g C m^{-2} yr^{-1} for the subsequent more humid year (Drollinger et al., 2019). The results from this study and that of Lund et al., 2012 and Drollinger et al., 2019 show that the temperate bogs exhibit strong interannual variation on NEE even for the same site and that the C balance is strongly affected by climatic variability. Large variations in interannual CO_2 fluxes could be an indicator of a transition in vegetation composition or shifting emphasis on the components of NEE at such ecosystems. (Wilson et al., 2016; Baldocchi et al., 2018; Alekseychik et al., 2021). This research highlights the strong influence that drought can have on carbon fluxes and emphasizes the potential sensitivity and vulnerability of peatland C stocks to predict the impacts of future climate change. Our results indicate that the prolonged lowering of the WTD due to drought can shift peatlands from carbon sinks to sources due to enhanced rates of C loss through R_{eco}. However, it also shows the resilience of these ecosystems to revert to being carbon sinks in subsequent years after drought events. This work and similar studies help provide insight into the sensitivity of peatland systems to interannual changes in climatic conditions. It also emphasizes the importance of timing and duration of hydrological changes such as WTD and soil moisture with their associated impacts on the carbon balance which might be a useful indicator while planning and implementing rehabilitation/rewetting activities on degraded sites.

4.5 Conclusion

This study underlines the importance of drought periods as regulators of interannual variation in CO_2 exchange at a near-natural bog in Ireland. Based on four years of eddy covariance CO_2 flux measurements, we found that the timing, severity, and duration of drought regulated the effect on the CO_2 dynamics. A short but severe drought period with a prolonged lowering of the water table depth and reduction in soil moisture during mid-summer 2018 increased rates of R_{eco} causing the study area to act as a source of C. The site reverted to being a CO_2 sink following the drought year and acted as a consistent carbon sink for the following two years and, the drought year of 2021 despite it being an even drier year as compared to 2018. This shows both the vulnerability and resilience/adaptive capacity of these ecosystems to act as a C sink. More studies with longer duration are however required to determine the long-term resilience of peatland systems across drainage gradients and rehabilitation techniques, particularly as peatland rewetting is a key climate mitigation tool in Ireland. The outputs of this work can be further used to study the effects of drought events on the biophysical processes responsible for the net CO_2 exchange in more detail, particularly using process-based peatland models with a high temporal resolution to better understand how these important C sinks might behave under future climate scenarios.

Chapter 5: Upscaling methane fluxes from peatlands across a drainage gradient in Ireland using PlanetScope imagery and machine learning tools

Published: Scientific Reports (https://www.nature.com/articles/s41598-023-38470-6)

Primary author: Ruchita Ingle

Co-authors: Wahaj Habib, John Connolly, Mark McCorry, Stephen Barry and Matthew Saunders

Contributions: R.I. conceived the ideas, designed overall and RS methodology, measured and analysed the data and wrote the full manuscript; W.H. contributed in RS methodology and GEE script. J. C. and M.S. supervised the research and assisted in reviewing and editing the manuscript. M.M. and S.B. contributed to the field research and manuscript review.

5.1 Introduction

Around 12% of global peatlands are degraded through anthropogenic activities (agriculture, forestry, and peat extraction) and contribute approximately 4% of the total global anthropogenic greenhouse gas emissions (Fluet-Chouinard et al., 2023). Furthermore, peatlands are an important source of atmospheric methane and contribute around 20-40% of the total global CH_4 emissions (Zhang et al., 2020). Methane dynamics of peatlands

involves production, consumption and transport of methane driven by various physical, chemical and biological processes (Lai, 2009). The methane production takes place in the anaerobic zone of peat soil via methanogens and is emitted to the atmosphere depending on the balance between methane production and consumption and the mode of methane transport (Lai, 2009). Methane is released from peat soil via diffusion, ebullition and plant mediated transport. The major key drivers of methane emissions from natural bogs are water table depth and temperature, however other processes like vascular transport in plants could partially override the effect of these controls for degraded and under rehabilitation peatland (Abdalla et al., 2016).

Quantification of these emissions is crucial to better understand the impacts of these systems on climatic feedback and to devise suitable mitigation strategies with a focus on the rehabilitation of these systems and their return to a net atmospheric cooling state. Closed chamber (CC) measurements and eddy covariance (EC) techniques are the most common field methods that are used to measure CH_4 emissions (Lees et al., 2018; Wang et al., 2013; Yu et al., 2013). EC towers typically measure trace gas fluxes with a high temporal resolution (10 Hz) across a footprint (250–3000m radius around flux towers) and deliver a single integrated flux value across the footprint area (Baldocchi, 2003; Chu et al., 2021). This can potentially bias or underestimate emission estimates particularly if the footprint area has heterogeneous vegetation (Matthes et al., 2014; Tuovinen et al., 2019; Zhang et al., 2020). Peatlands are naturally heterogeneous systems with vegetation changing at a scale of less than 1m which could significantly influence these flux measurements (Bhatnagar et al., 2020; Lai et al., 2014). Many EC studies do not take this vegetation variation into account within tower footprints nor the impact it has on integrated flux values when reporting annual carbon (C) and greenhouse gas (GHG) budgets (Levy et al., 2020; Tuovinen et al., 2019). The CC technique measures methane fluxes at chamber/collar scale (~0.25 m^2) with a higher spatial resolution compared to the EC as they can be distributed across the key vegetation communities present. However, the CC approach has lower temporal resolution and can also be labor intensive (Sachs et al., 2010; Zhang et al., 2012). Vegetation communities can act as a good predictor of seasonal methane fluxes as key plant species and associated communities grow in specific locations within the ecosystem and have characteristic emission profiles

(Bhatnagar et al., 2020; Lees et al., 2018; Räsänen & Virtanen, 2019). Therefore, to upscale methane fluxes from the chamber to site scale requires a better understanding of the spatial distribution of the vegetation within a study area (Bhatnagar et al., 2020; Erudel et al., 2017; Laine et al., 2007).

Remote sensing is a powerful tool for mapping vegetation distribution (Bhatnagar et al., 2020; Davidson et al., 2017; Räsänen et al., 2021; Zhang et al., 2020) and imagery can be acquired at a range of temporal and spatial scales ranging from near-Earth UAV at 5cm, up to remotely sensed data at 5-30m (Sentinel) or 500m (MODIS) (Lees et al., 2018). Erinjery et al. (2018) used a combination of Sentinel-2 (S2) MSI and Sentinel-1 (S1) data to discriminate different vegetation types in tropical rainforests with an overall accuracy of 75%. The S2 bands along with the machine-learning Bagged Trees ensemble classifier have also been used to map raised bogs, turloughs, and fens in Ireland with an overall accuracy of 87% (Bhatnagar et al., 2020). However, these studies are based on S2 imagery with 10m resolution. PlanetScope multispectral satellite imagery (PlanetScope-0 and -1) has a spatial resolution of 3.7 to 4.1 m and has been used to derive accurate fine-scale vegetation maps of peatlands (Räsänen et al., 2019, 2021, 2021). These higher-resolution images can capture the spatial distribution of plant species at a finer scale, unlike S2, Landsat, and MODIS. They can also capture seasonal changes due to the higher temporal resolution of a 3-5 day return period (Melack & Hess, 2023). Cheng et al. (2020) compared PlanetScope and Sentinel data to assess vegetation phenology for heterogeneous landscapes in Kenya and found that the PlanetScope data were able to better capture the spatial extent of changing phenology within the landscape than the Sentinel imagery.

Machine learning techniques are widely used with remote sensing approaches for wetland mapping (Bhatnagar et al., 2020; Chimner et al., 2019; Corcoran et al., 2013; Dayuf et al., 2017; Mahdavi et al., 2018; Sencaki et al., 2020). The Random Forest (RF) classification model (Breiman, 2001) based on an ensemble of several decision trees has been used in numerous global studies for mapping wetland ecology. The RF ensemble classifier was successfully used on 30,000 Landsat-8 images with the Google Earth Engine platform (GEE) to map the Canadian wetland inventory with an overall accuracy of 71% (Amani et al., 2019). A recent study by Chimner et al. (2019) focused on mapping the vegetation distribution in the mountain meadows of Peru using multi-sensor data and RF, achieving an overall accuracy of 92%. Bhatnagar et al. (2021) compared machine learning and deep learning algorithms to map peatland vegetation communities in Ireland and identified RF as the best pixel-based machine learning classifier with a mapping accuracy of 85%. The Statistical Machine Intelligence and Learning Engine (SMILE) is a comprehensive machine learning system and its platform implements machine learning algorithms for supervised and unsupervised classification. Sujud et al. (2021) provided a comparative analysis of four machine-learning classifiers implemented in Google Earth Engine (GEE) for mapping cannabis and other crop-type classifications and concluded that the SMILE Random forest (SMILE-RF) classifier outperformed all the other classifiers.

In this study, PlanetScope imagery along with the SMILE-RF algorithm was used to create annual vegetation maps of peatland systems across a drainage gradient. These maps were used to upscale chamber-based methane fluxes for various vegetation communities from the point-to-site scale using a weighted-area approach. Dominant vegetation communities were referred to as ecotopes in this work although the application of ecotopes to cutaway sites has not yet been defined. The annual ecotope maps for the years 2020 and 2021 were generated for three Irish midland peatlands (intact raised bog and two former raised bogs: now cutaway) across a drainage gradient. The drainage gradient defines the bog conditions due to degradation or management practices and this study focuses on sites degraded through recent industrial extraction, under rehabilitation, and near-natural bogs(Kiely et al., 2017; Renou-Wilson et al., 2018; Renou-Wilson & Wilson, 2018; Wilson et al., 2011).

5.2 Materials and methods

5.2.1 Site description

This study was undertaken at three raised bogs in Ireland as shown in Figure 5.1a using the LI-COR trace gas analyzer and smart chamber as shown in Figure 5.1b.

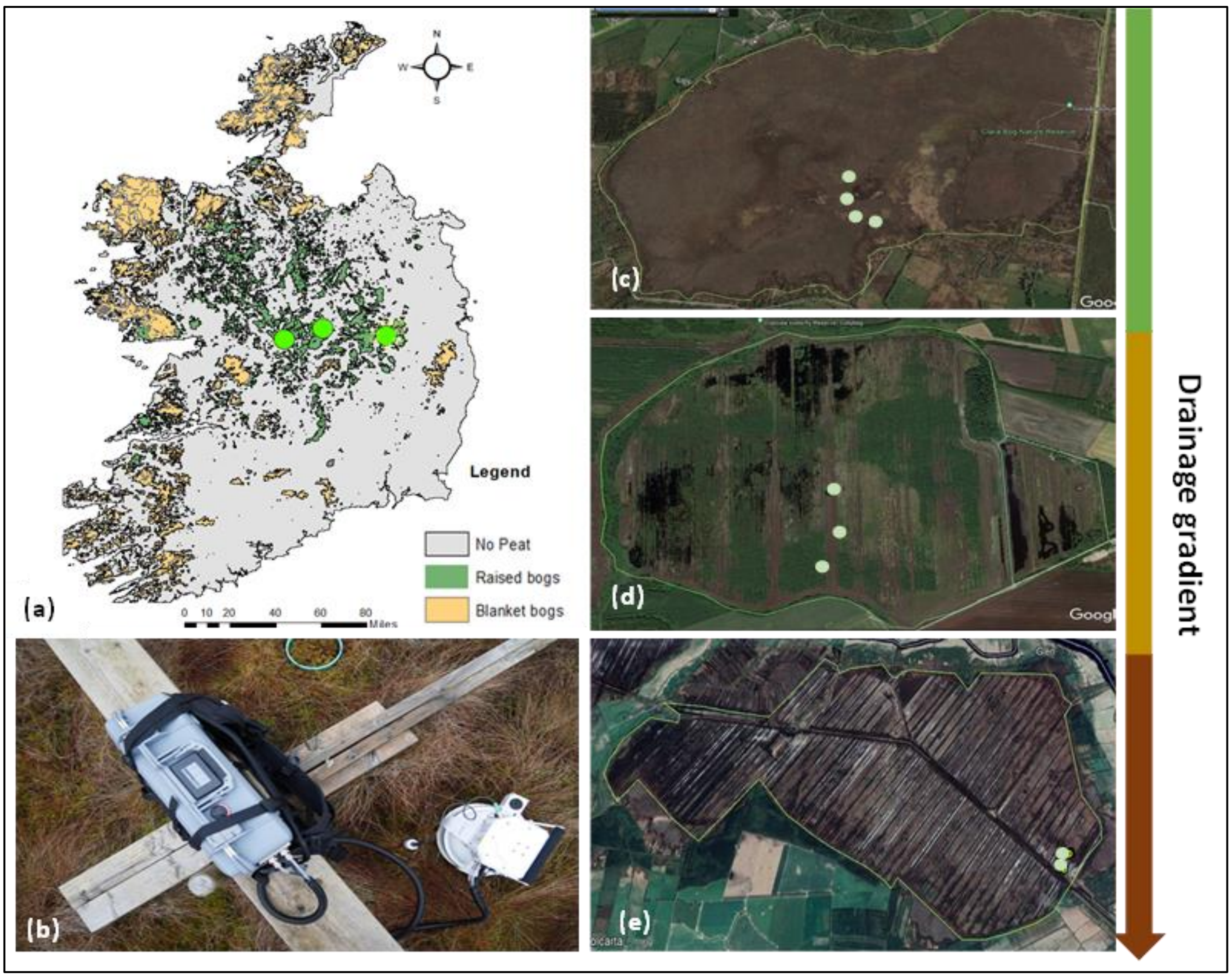

Figure 5. 1 (a) A map of Ireland showing the sites used and representing a drainage gradient; (b) The chamber measurement set up with the LI-COR (LI7810) trace gas analyzer, smart chamber, and PVC collar; c to e represent the sites across the drainage gradient (c) Clara bog (near-natural) (d) Lullymore (rehabilitation) (e) Garryduff (former industrial extraction), and the collar locations are shown as light green circles.

Clara Bog

Clara Bog is regarded as one of the largest near-natural raised bogs remaining in Ireland. It is located in County Offaly in the Irish Midlands and designated as a special area of conservation (SAC) under the European Union Habitats Directive (Council of the European Communities, 1992). The bog is bisected by a road that was put in place around the 18th Century and significantly impacted the hydrology of the bog (Crushell, 2008). For this study, measurements were conducted on the western part of the bog which will be referred to as Clara bog in this article (Figure 5.1c). Clara bog is divided into several ecotopes based on the vegetation community classification system proposed by Schouten in 2002 (Fernandez et al., 2014b). The ecotopes are characterized by the ecological differences that are linked to the variable hydrological characteristics of the bog and range from the ecologically pristine active raised bog (ARB) to central (Ce), subcentral (SC), active flush (AF) and soaks, submarginal (SM), marginal (M), Inactive flush (IF) and Bog woodland (BW). The bog woodland at Clara has high *Sphagnum* cover and has developed on deep peat. All the dominant species for each of the ecotopes are shown in Table 5.1. The chamber measurements were conducted fortnightly from January 2020 through December 2021. A total of 24 collars were installed at Clara Bog at the major dominant ecotopes (Ce, SC, SM, M) with 6 collars at each ecotope (Figure 5.1c).

Garryduff

Garryduff Bog (GD) is located in County Galway and represents a former industrial peat extraction (cutaway) site where peat production ceased in stages with complete closure in 2021 (Figure 5.1e). During the extraction period, it had a pumped drainage regime and the water table was significantly lower than the surrounding area (Bord Na Mońa Garryduff Decommissioning and Rehabilitation Plan, 2021). Much of the site comprises extensive areas dominated by bare peat and emerging pioneer vegetation. Parts of the cutaway now have well-developed wetlands and scrub vegetation. To understand the CH_4 dynamics from natural vegetation and bare peat, the site was categorized into two main ecotopes: bare peat (BP) and vegetation (V) as shown in Table 5.1, and chamber measurements were conducted fortnightly from May 2020 through December 2021. At this site, 16 collars were installed with 8 at the BP and 8 at V ecotopes (Figure 5.1e).

Lullymore

Lullymore in County Kildare is also a former industrial peatland extraction site (Figure 5.1d) that was previously mined but underwent rehabilitation through drain-blocking and rehabilitation on a phased basis over 15 years. Fortnightly chamber measurements were conducted from May 2020 through December 2021 at four dominant vegetation communities (Table 5.1) as follows: bare peat (BP), shrub (S), bog woodland (BW), and open water (OW), based on a Bord na Móna habitat map (Bord Na Mońa Lullymore Draft Rehabilitation Plan, 2017). Bog woodland at Lullymore is on shallow peat < 1 m deep and is defined by relatively dry peat conditions with no *Sphagnum.* All the dominant vegetation species are shown in Table 5.1. At the Lullymore site, 12 collars were installed with 4 collars each at the BP, S, and BW (Figure 5.1d).

Table 5. 1 Vegetation communities, assigned ecotopes, chamber measurements, and the number of collars for all the sites. NA: chamber measurements were not conducted

Site	Class	Ecotopes	Dominant vegetation	Chamber measurements (Yes/No)	No. of collars
Clara	1	Submarginal (SM)	*Narthecium ossifragum* and *Sphagnum tenellum*	Y	6
	2	Subcentral (SC)	*Sphagnum magellanicum*	Y	6
	3	Marginal (M)	*Calluna vulgaris* and *Trichophorum germanicum*	Y	6
	4	Central (C)	*Sphagnum cuspidatum*	Y	6
	5	Active flush (AF)	*Sphagnum cuspidatum, Myrica gale, Betula pubescens scrub woodland with Sphagnum palustre* and *Polytrichum commune, Molinia caerulea*	N	NA
	6	Bog woodland (BW)	*Betula pubescens, Frangula alnus, Pinus sylvestris, Pinus cortorta* and *Picea abies*	N	NA
	7	Inactive flush (IF)		N	NA
Lullymore	1	Bare peat (BP)	Bare peat	Y	4
	2	Shrub (S)	Mosaic of pioneer *Juncus, Eriophorum angustifolium*-dominated poor fen and emergent *Betula pubescens* and *Salix* spp. scrub	Y	4
	3	Bog woodland (BW)	*Betula pubescens, Pinus sylvestris, Pinus contorta* and	Y	4
	4	Open water (OW)	open water and emergent wetland vegetation	N	NA
Garryduff	1	Bare peat (BP)	Bare peat	Y	8
	2	Vegetation (V)	Mosaic of pioneer *Juncus, Eriophorum angustifolium andand Carex rostrata*-dominated poor fen and emergent *Betula pubescens* and *Salix* spp. scrub	Y	8

5.2.2 In-situ measurements

Methane fluxes were measured using the chamber technique(LAI, 2009; Laine et al., 2007) at Garryduff and Lullymore for 19 months and 24 months at Clara bog. A laser-based analyzer (LI-7810, CO_2/CH_4/H_2O Trace Gas Analyzer; LI-COR Biosciences) in conjunction with the LI-COR Smart Chamber portable unit (LI-8200-01S, Smart Chamber; LI-COR Biosciences) system was used to measure CH_4 concentrations (Figure 5.1b). The methane flux was calculated using a curvilinear function in the LICOR SoilFluxPro software version

5.2. In addition to the measurement of soil gas fluxes, an auxiliary HydraProbe (Stevens Water Monitoring System) provided simultaneous monitoring of soil temperature, moisture, and electrical conductivity. Methane measurements were recorded fortnightly except during the COVID-19 lockdown when travel across Ireland was restricted. The measured methane fluxes were converted from nmol CH_4 m^{-2} s^{-1} to g C m^{-2} y^{-1} to compare them with methane fluxes from similar systems in other reported studies.

5.2.3 Satellite data

The PlanetScope data was acquired by Planet labs Inc., with their low-cost constellation of satellites. The data has a spatial resolution of 3.7 to 4.1m which is resampled and distributed by two sensors i.e., PlanetScope–0 and PlanetScope-1 to achieve a 3m spatial resolution (Roy et al., 2021). The imagery was atmospherically corrected using the 6S model (Second Simulation of a Satellite Signal in the Solar Spectrum). The data was accessed and downloaded using the Planet Labs ArcGIS Pro add-in. The imagery consists of four bands: Red (590-682nm), Green (500-585nm), Blue (455-517nm), and NIR (780-880nm), and all the four bands were used for the analysis in this study. The images were collected in 2020 and 2021 for all three sites. A cloud filter of less than 10% was used and a total of 35 images were collected for Clara bog, 20 for Garryduff, and 19 for the Lullymore site. There were no cloud-free images available in the summer at Clara and Garryduff nor for the winter months at Lullymore in 2020. Three Vegetation Indices (NDVI, EVI, and GNDVI) were also calculated and added to the RF classification to improve the classification results.

5.2.4 Ecotope mapping

The PlanetScope data was used to map the ecotopes at the three study sites. A machine learning-based RF image classification SMILE technique was used in the Google Earth

Engine (GEE) platform to perform pixel-based image classification (Figure 5.2). All the available satellite images were ingested into GEE to create annual ecotope maps for 2020 and 2021. A combination of habitat maps provided by Bord na Móna (Lullymore and Garryduff sites) and National Parks and Wildlife Service (Clara bog) along with high-resolution Google Earth imagery (de Sousa et al., 2020; Noi Phan et al., 2020; Sellami & Rhinane, 2023) were used to train and test the models with a split of 70:30. A total number of 144 polygon samples (20578 pixels) were defined based on a random distribution across all the seven ecotopes at Clara bog. A similar approach was implemented at Lullymore with a total number of 166 polygons (30847 pixels) with random distribution over the four ecotopes. For the Garryduff site, a total number of 192 polygons (10922 pixels) were created using a random distribution across the two ecotopes. Furthermore, an accuracy assessment of the results was conducted and a confusion matrix with Overall validation Accuracy (OA), Producer Accuracy (PA), and user accuracy (UA) was developed (Table 5.2, 5.3, and 5.4). The Kappa coefficient was not reported for image classification as recommended by Foody (Foody, 2020) due to its limitation in the accuracy assessment of thematic maps. The annual ecotope maps generated for all three sites for the years 2020 and 2021 are shown in Figure 1. The area of each ecotope is estimated from the annual ecotope maps for the relevant year and was used for upscaling methane fluxes outlined in equation 1.

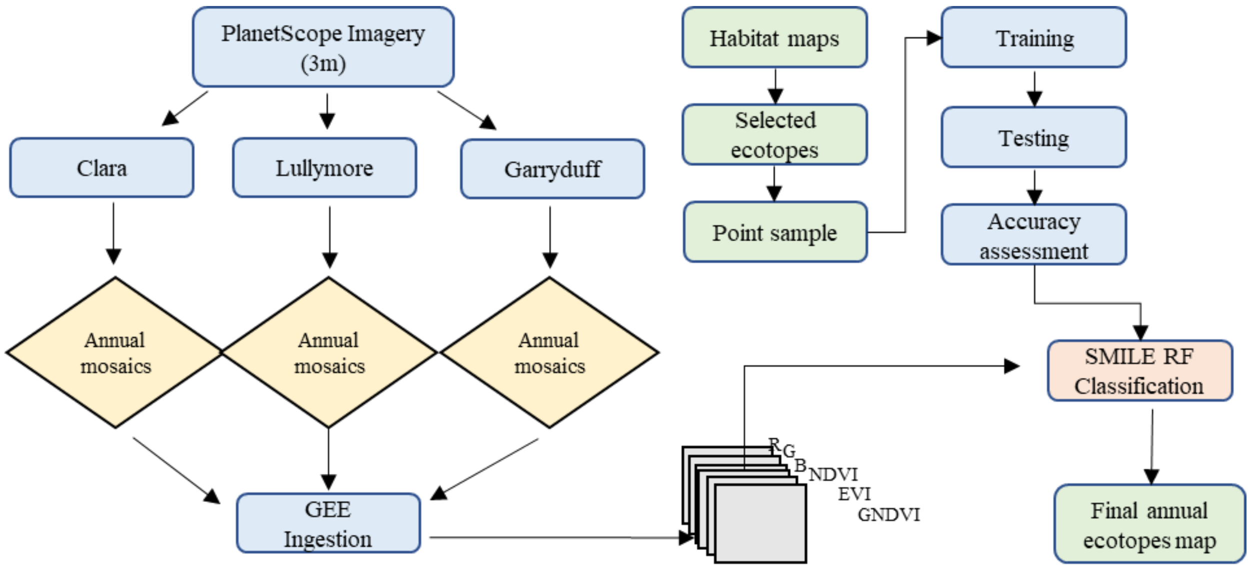

Figure 5. 2 Image classification workflow for annual ecotope map generation in GEE.

5.2.5 Upscaling

A simple area-weighted average method has been used previously in several studies and found to be an effective and simple upscaling approach (Davidson et al., 2017; Morozumi et al., 2019). The same approach is used here to upscale the chamber CH_4 fluxes, using equation 1 below:

$$\mathrm{Flux}_{\mathrm{upscaled}} = \frac{\text{mean chamber}-\text{derived flux} * \text{ecotope area}}{\text{Total area}} \qquad (1)$$

5.3 Results

5.3.1 Spectral Profiles

The spectral signatures of each ecotope at the three sites were plotted as shown in Figure 5.3. For Clara bog, the active flush ecotope showed the highest reflectance values followed by the central ecotope, bog woodland, inactive flush, submarginal and subcentral ecotopes, while the marginal ecotopes had the lowest reflectance values for most of the bands. The differences in reflectance between the central and marginal ecotope are notable. The submarginal, subcentral, and marginal ecotopes have similar reflectance values in RGB and NIR wavelengths (Figure 5.3a). The vegetation ecotope at the Garryduff site showed the highest reflectance value and bare peat showed the lowest reflectance value (Figure 5.3b). At the Lullymore site, the reflectance values of shrub and open water were noticeably different and Bog woodland showed the highest reflectance value for the NIR wavelength (Figure 5.3c). All the ecotopes, except the submarginal, subcentral, and marginal ecotopes at Clara can be distinguished based on their spectral signatures (Figure 5.3a).

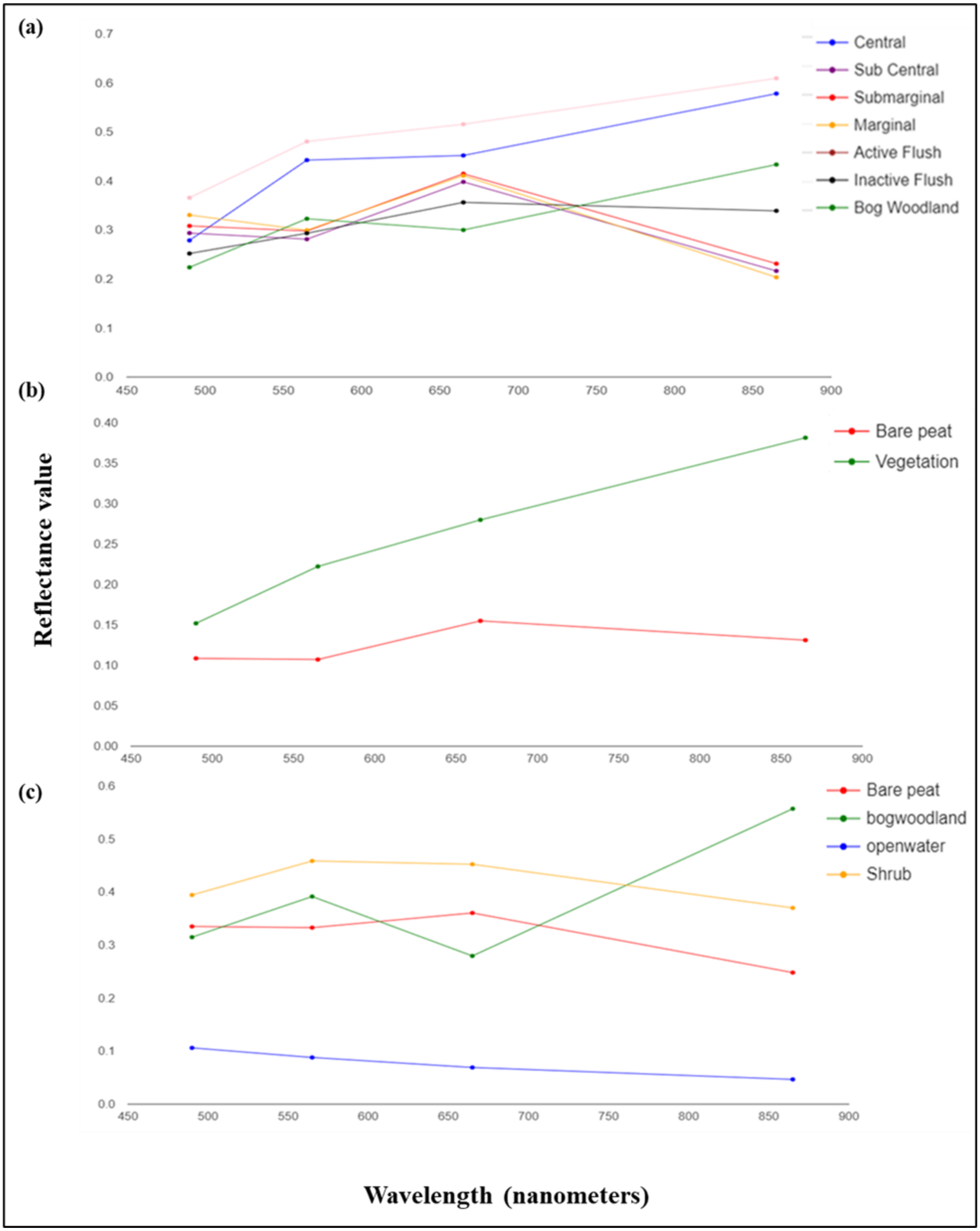

Figure 5. 3 A plot showing reflectance values across various wavelengths for the ecotopes at (a) Clara (b) Garryduff (c) Lullymore

5.3.2 Annual ecotopes map

Clara Bog

The annual ecotope maps derived from the PlanetScope imagery and SMILE-RF model showed variability between years (Figure 5.4a). The submarginal, subcentral, marginal, and bog woodland ecotopes showed a decline in area of 2.3%, 2.2%, 5%, and 35% respectively in 2021 as compared to 2020 (Table 5.5). However, the central, active flush and inactive flush ecotope areas were shown to increase by 53%, 20%, and 56% in 2021 when compared to 2020.

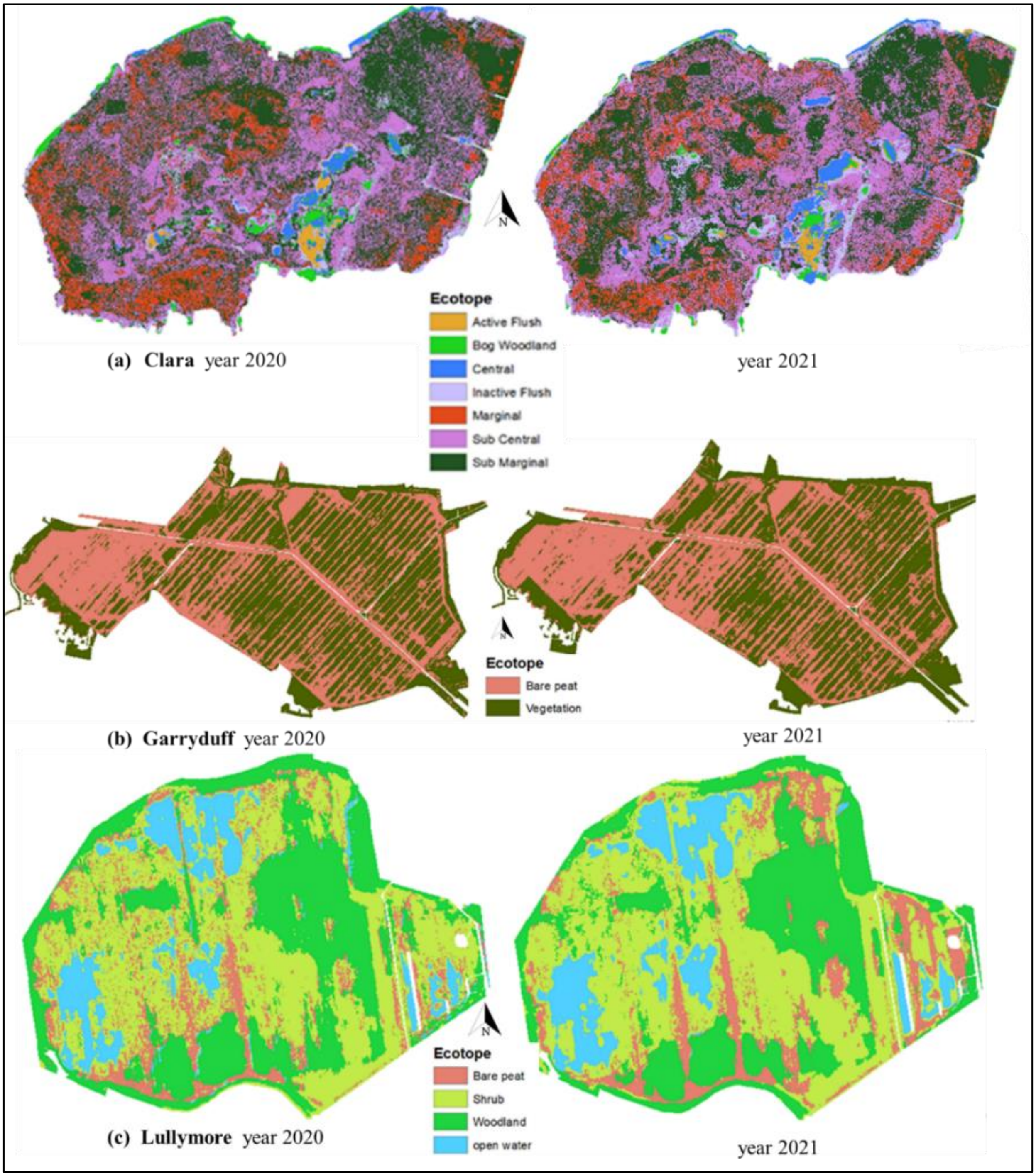

Figure 5. 4 Annual ecotope maps for years 2020 and 2021 at (a) Clara bog (b) Garryduff (c) Lullymore site

Accuracy assessment

In the 2020 assessment (Table 5.2), the highest producer's accuracy (PA), 91.14%, was seen for the bog woodland, and the lowest PA (60.30%) was observed for the inactive flush which was misclassified as submarginal and subcentral. The submarginal, subcentral, central, and marginal ecotopes were classified with PA ranging from 73.34 to 88.8%. The marginal ecotope had a PA of 73.34% and it was mostly misclassified as subcentral and submarginal. The user accuracy (UA) ranged from 79.89 to 92.64% with the lowest for the marginal ecotope and the highest for the active flush ecotope. In 2021, the highest PA was acquired at the central ecotope (95.75%) followed by active flush (94.88%) and bog woodland (93.03%) as shown in Table 5.2. The marginal ecotope was misclassified as submarginal and subcentral with a PA of 69.04% and the inactive flush was misidentified as submarginal and subcentral with a PA of 77.57%. The UA ranged from 80.42 to 96.21% with the highest accuracy for the central ecotope (96.21%) and the lowest for the marginal ecotope (80.42%). During both years, the active peat-forming ecotopes such as the central and subcentral areas were identified with PA and UA ranging from 82.05 to 96.21% for all the seasons. The overall validation accuracy (OA) of 83.20% was observed for 2020 and 84.20% for 2021 (Table 5.2). Table 5.5 shows the total estimated area in hectares for each ecotope for the years 2020 and 2021.

Table 5. 2 Validation accuracy assessment at Clara bog for 2020 and 2021

Clara 2020	SM	SC	M	C	AF	BW	IF	Total	PA(%)
SM	2099	246	88	0	0	2	0	2435	86.20
SC	285	1751	53	0	0	3	4	2096	83.54
M	116	89	564	0	0	0	0	769	73.34
C	0	3	0	211	9	15	6	244	86.48
AF	0	1	0	11	214	6	9	241	88.80
BW	1	4	0	10	1	216	5	237	91.14
IF	21	40	1	3	7	7	120	199	60.30
Total	2522	2134	706	235	231	249	144	6221	**OA**
UA(%)	83.23	82.05	79.89	89.79	92.64	86.75	83.33		**0.83**
Clara 2021	SM	SC	M	C	AF	BW	IF	Total	PA(%)
SM	2136	228	42	0	0	0	1	2407	88.74
SC	270	1748	87	0	0	0	5	2110	82.84
M	123	120	542	0	0	0	0	785	69.04
C	0	1	0	203	7	1	0	212	95.75
AF	0	0	0	6	204	2	3	215	94.88
BW	2	3	2	1	2	227	7	244	93.03
IF	18	14	1	1	7	7	166	214	77.57
Total	2549	2114	674	211	220	237	182	6187	**OA**
UA(%)	83.80	82.69	80.42	96.21	92.73	95.78	91.21		**0.84**

Garryduff

The annual ecotope maps are shown in Figure 5.4b and the total area for each ecotope for 2020 and 2021 is shown in Table 5.5. Here, an OA of 99% was observed for both years with PA and UA of almost 100% (Table 5.3). The vegetation and bare peat were mapped very well at this site for both years.

Table 5. 3 Validation accuracy assessment at Garryduff for 2020 and 2021

GD 2020	BP	V	Total	PA(%)
BP	4182	19	4201	99.55
V	8	5067	5075	99.84
Total	4190	5086	9276	**OA**
UA (%)	99.81	99.63		**0.99**
GD 2021	BP	V	Total	PA(%)
BP	4095	30	4125	99.27
V	17	5056	5073	99.66
Total	4112	5086	9198	**OA**
UA (%)	99.59	99.41		**0.99**

Lullymore

The annual ecotope maps are shown in Figure 5.4c and the total estimated area of each ecotope for 2020 and 2021 is shown in Table 5.5. The bare peat and open water ecotopes showed an increase in the area of 17% and 2% in 2021 compared to 2020. However, the shrub and bog woodland ecotopes showed a decrease of 2% and 4% in area, in 2021 vs 2020 respectively. An OA of 97.9% was observed for 2020 with the PA ranging from 90.27 to 100% (Table 5.4). The highest PA was seen for open water followed by bog woodland, shrub, and bare peat. The UA is also highest for open water followed by bog woodland, shrub, and bare peat. For 2021, an OA of 99.2% was observed. The PA of bare peat (96.86%) and shrub (97.50) was higher in 2021 as compared to 2020 and open water (98.87%) PA was lower in 2021 against 2020.

Table 5. 4 Validation accuracy assessment at Lullymore for 2020 and 2021

LM 2020	BP	S	BW	OW	Total	PA(%)
BP	167	17	1	0	185	90.27
S	10	380	7	1	398	95.48
BW	2	4	1766	0	1772	99.66
OW	0	0	0	261	261	100.00
Total	179	401	1774	262	2616	**OA**
UA (%)	93.30	94.76	99.55	99.62		**0.979**
LM 2021	BP	S	BW	OW	Total	PA(%)
BP	154	3	2	0	159	96.86
S	10	390	0	0	400	97.50
BW	0	0	1771	0	1771	100.00
OW	0	2	1	263	266	98.87
Total	164	395	1774	263	2596	**OA**
UA (%)	93.90	98.73	99.83	100.00		**0.992**

5.3.3 Upscaled methane flux

The upscaled methane flux for all the ecotopes at all the three sites for 2020 and 2021 is shown in Figure 5.5. The average annual methane flux values measured at the various ecotopes on Clara bog in 2021 were higher than in 2020. The average annual methane flux values ranged from 1.44 to 5.75 g C m^{-2} y^{-1} in 2020 and from 2.4 to 8.89 g C m^{-2} y^{-1} in 2021, with the highest fluxes measured at the central ecotope and lowest at the marginal ecotope during the study duration. The upscaled methane flux values ranged from 0.12 to 2.16 g C m^{-2} y^{-1} at Clara bog (Table 5.5). The lowest upscaled flux was observed at the central ecotope in 2020 followed by marginal, submarginal, and subcentral. The upscaled methane flux followed a similar trend in 2021 as shown in Table 5.5. At the Lullymore site, the average annual methane fluxes ranged from -1.08 to 1.14 g C m^{-2} y^{-1} in 2020 and -1.1 to 1.55 g C m^{-2} y^{-1} in 2021. The bog woodland soil was observed to be assimilating methane throughout the study duration and methane emissions from bare peat were close to zero. The upscaled methane fluxes at the ecotope and site scale are shown in Table 5.5.

The average annual methane fluxes at Garryduff ranged between 0 to 0.27 g C m^{-2} y^{-1} in 2020 and 0 to 0.53 g C m^{-2} y^{-1} in 2021, and the upscaled fluxes are shown in Table 5.5. As all the ecotopes assessed represent >88% of the total study area at each site, ecosystem-scale emissions are also provided in Table 5.5. Clara bog had the highest methane emissions followed by Lullymore and Garryduff where both the sites showed similar emission scenarios.

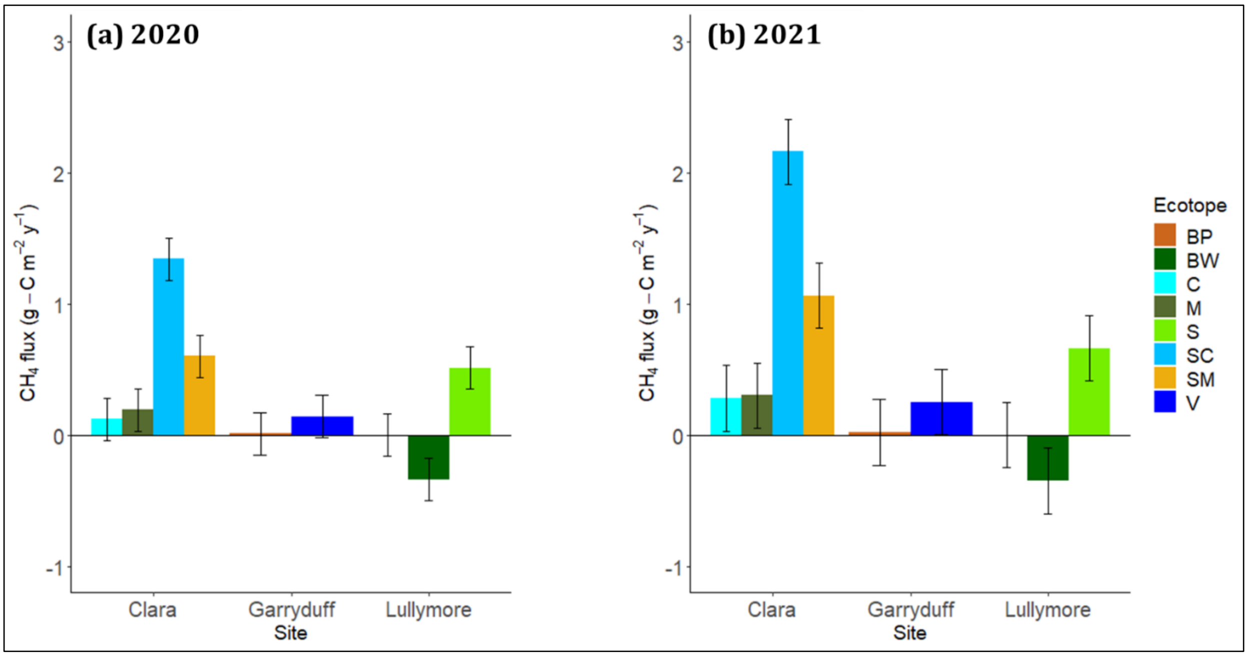

Figure 5. 5 Upscaled methane flux at all the ecotopes for all the three sites during the years (a) 2020 and (b) 2021

Table 5. 5 Upscaled annual methane fluxes at all locations

Site	**Ecotope**	**Area based on annual ecotope map 2020 (Ha)**	**Area covered by ecotopes in 2020 (%)**	**Upscaled methane flux in 2020 (g C m^{-2} y^{-1})**	**Upscaled methane flux in 2020 at site scale (g C m^{-2} y^{-1})**	**Area based on annual ecotope map 2021 (Ha)**	**Area covered by ecotopes in 2021 (%)**	**Upscaled methane flux in 2021 (g Cm^{-2} y^{-1})**	**Upscaled methane flux in 2021 at site scale (g Cm^{-2} y^{-1})**
Clara	SM	99.42	92.68	0.6	**2.25**	97.1	91.27	1.06	**3.8**
	SC	91.92		1.34		89.8		2.16	
	M	32.32		0.19		30.62		0.3	
	C	5.03		0.12		7.7		0.28	
Lullymore	BP	16.06	88.79	0	**0.17**	18.92	88.54	0	**0.31**
	S	58.43		0.51		57.02		0.66	
	BW	42.84		-0.34		41.06		-0.35	
Garryduff	BP	456.47	100	0.01	**0.15**	466.82	100	0.02	**0.27**
	V	480.83		0.14		470.49		0.25	

5.4 Discussion

5.4.1 Ecotope Mapping

Mapping peatland vegetation is very challenging due to the complex heterogeneity which can change over a few meters (Bhatnagar et al., 2020; Davidson et al., 2017; Räsänen & Virtanen, 2019). This study presents a novel, yet robust attempt to assess the potential of using high-resolution satellite imagery with the RF machine learning algorithm (SMILE) to create annual ecotopes maps for a variety of peatland ecosystems, and to use these maps to upscale chamber-based methane fluxes from point sources to the site/ecosystem scale. The mapping methodology developed here was successfully validated at all three sites with an overall validation accuracy of above 83%. Most temperate raised bogs tend to be located in geographical areas with significant cloud cover, which can lead to limited availability of satellite imagery. This makes it difficult to acquire satellite imagery for similar dates that align with field-based chamber measurements that track the phenological changes in the vegetation at similar temporal scales (Bhatnagar et al., 2020; Räsänen et al., 2019, 2021). The satellite imagery acquired for this study was selected to be as close as possible to the site-level flux measurement dates. Summer and winter imagery were not available for the year 2020, so this study focuses on developing annual ecotope maps for area estimation instead of adopting a seasonal perspective. The methodology proposed in this study accurately mapped all the ecotopes at the Lullymore and Garryduff sites, with overall accuracy above 95% for both sites in 2020 and 2021. However, the accuracy assessments were slightly lower at Clara bog. This may be due to Clara bog being a more complex site to map as there is a greater spatial heterogeneity in vegetation across the site. In Table 5.2, the central ecotope had a UA of 89.79 % in 2020 and 96.21% in 2021 and the inactive flush had a UA of 83.33% in 2020 and 91.21% in 2021. The bog woodland had a UA of 86.75% in 2020 and 95.78% in 2021. One of the reasons for an increase in UA in 2021 could be the inclusion of summer imagery while creating the annual ecotope maps which was not available for 2020 due to cloud cover. The marginal, subcentral, and submarginal ecotopes showed consistent UA ranging between 80.42 to 83.80% during both years. The UA at these ecotopes is lower as compared to other ecotopes at Clara and it might be due to their similar spectral signatures (Figure 5.3a). In the future, these challenges can be addressed by including a longer dataset and applying a multi-sensor approach while training and testing the models. However, the most important active raised bog (ARB) forming ecotopes e.g., the central and subcentral ecotopes (with the highest level of complexity) were classified in this study with PA of 86.48 - 95.75% and 82.84 - 83.54% respectively. Bhatnagar et al. (2021) used a nested drone-satellite approach to map Clara bog achieving a PA of 66% for subcentral and 86% for central ecotopes. In this study, the PA was improved with 83.54% for the subcentral and 95.75% for the central ecotope for 2021. Not opting for the majority voting approach which provides pixel value based on the majority of nearby pixels values and use of higher spatial resolution imagery could be responsible for getting higher accuracy ecotope maps at Clara bog in this study as compared to Bhatnagar et al. (2021) approach. Overall, the methodology suggested here was able to map the dominant vegetation communities across all the sites with an overall accuracy of ≥83%. This approach can be further developed and applied to more accurately define the key ecotopes on cutaway peatlands and to map the impact of rewetting and rehabilitation on ecological change and for the long-term monitoring of peatlands.

5.4.2 Upscaled Flux Chamber Measurements

The average annual methane fluxes measured at Clara bog during this study period were in the range with the chamber measurements previously conducted at Clara bog from 2015-2017 (Regan et al., 2020). The central ecotope average annual methane flux in 2020 (5.75 g C m^{-2} y^{-1}) and 2021 (8.89 g C m^{-2} y^{-1}) were in a similar range as those measured between 2015-2017 (7.95 ± 4.05 g C m^{-2} y^{-1}). Additionally, the measured methane flux in the subcentral ecotope in 2020 (3.6 g C m^{-2} y^{-1}) and 2021 (5.93 g C m^{-2} y^{-1}) is in the range with the 2015-2017 data (6.52 ± 2.1 g C m^{-2} y^{-1}). Similarly, the annual methane flux at the submarginal ecotope in 2020 (1.48 g C m^{-2} y^{-1}) and 2021 (2.7 g C m^{-2} y^{-1}) is also in the range with the 2015-2017 data (3.37 ± 1.18 g C m^{-2} y^{-1}) data. The fluxes from the marginal ecotope in 2020 (1.44 g C m^{-2} y^{-1}) and 2021 (2.44 g C m^{-2} y^{-1}) were slightly higher than the 2015-2017 range (0.82 ± 0.37 g C m^{-2} y^{-1}) (Regan et al., 2020). The upscaled, site scale methane flux at Clara bog (2.25 - 3.8 g C m^{-2} y^{-1}) also agreed with the median methane flux range of 3.3 - 3.6 g C m^{-2} y^{-1} from 108 sites across the world (Abdalla et al., 2016). The average annual methane flux measured at the Garryduff site was in the range with other similar bare peat sites in Ireland, with the flux values showing net zero methane emissions (Renou-Wilson et al., 2019). A range of rewetted and restored sites from Ireland and 16 sites from northern peatlands (latitude 40° to 70°N) showed a similar average annual methane emissions trend to the Lullymore site with nearly zero emissions from bare peat, and small emissions from shrub areas with assimilation from bog woodland soils (Abdalla et al., 2016; Renou-Wilson et al., 2019).

This study is the first attempt to use high-resolution satellite imagery and machine learning to upscale chamber fluxes in Ireland. There is potential to implement the framework developed in this study to upscale chamber and EC measurements across other types of peatlands such as blanket bogs, fens, and turloughs which are heterogenous and complex to map. Site-scale methane emissions from bare peat and natural vegetation can be useful to analyze the before and after impacts of rewetting and rehabilitation. Similarly, methane emissions from under-rehabilitation sites such as Lullymore provide us with information on emissions from various dominant vegetation communities and can act as a wider indicator for effective rehabilitation measures. To improve estimates of methane flux variations over time, an understanding of the phenological dynamics of vegetation communities and their spatial variation could be better than simply using measurements from one point in time (Helfter et al., 2022). The use of automatic chambers could potentially bridge the gap between EC tower measurements and spatial chamber measurements as they provide detailed flux measurements with a better temporal resolution. Additionally, the inclusion of key drivers such as water table depth and soil moisture while training the model could help refine the accuracy further.

5.5 Conclusion

This study tested the applicability of high-resolution multispectral satellite imagery and a mapping technique with machine learning algorithms to provide fine-scale vegetation maps. Furthermore, these maps were used to upscale chamber-based methane fluxes at peatland sites in Ireland across a drainage gradient. Our results provide evidence that upscaling is successful if the dominant vegetation communities are appropriately mapped. Results from this study highlight the complex spatial heterogeneity of peatlands and their impact on methane fluxes, and emphases the need to integrate dominant plant species into methane budget models and wider upscaling approaches. Overall, the novel use of remote sensing products and machine learning algorithms will continue to provide valuable data for improving the upscaling approach by understanding the impacts of key environmental drivers and vegetation dynamics on methane emissions to further inform effective rehabilitation measures.

Chapter 6: Development of hybrid models to estimate gross primary productivity at a near-natural peatland using Sentinel 2 data and a light-use efficiency model

Published: MDPI Biogeoscience and Remote sensing (https://www.mdpi.com/2072-4292/15/6/1673)

Primary author: Ruchita Ingle

Co-authors: Saheba Bhatnagar, Bidisha Ghosh, Laurence Gill, Shane Regan, John Connolly and Matthew Saunders

Contributions: R.I. conceived the ideas, designed the methodology, collected and analysed the data, and wrote the manuscript; S.B. contributed with Sentinel 2A imagery analysis; S.R. provided the water table data; M.S. supervised the research and contributed to the development of the manuscript; J.C. reviewed and helped with development of the manuscript; B.G., J.C., L.G., S.B. and S.R. assisted in reviewing the manuscript. All authors have read and agreed to the published version of the manuscript

---

6.1 Introduction

Peatlands are vital ecosystems in the global carbon (C) cycle, as they act as a significant store of carbon (Gorham, 1991) with estimates of soil organic carbon (SOC) stocks of between 500 to 700 billion tons of C globally (Scharlemann et al., 2014). However, these ecosystems are prone to degradation, primarily through drainage to facilitate a change in land use which results in a release of approximately 2–3 gigatons of carbon dioxide (CO_2) into the atmosphere every year (Tanneberger et al., 2017). To better understand how we can rehabilitate these systems and enhance their climate mitigation potential, it is important to quantify their C dynamics and the key drivers of C uptake and release at various spatial and temporal scales.

Natural and managed peatlands in Ireland are estimated to store up to 2320 Mt of C on ~ 20% of the land area (Connolly & Holden, 2009; Renou-Wilson et al., 2022). Irish peatlands have been extensively drained over the past number of decades for extraction for both energy and horticulture and conversion to agriculture and forestry (Connolly, 2018). These land-use conversions have significantly affected the greenhouse gas (GHG) dynamics of these ecosystems and they are estimated to release around 11–12.4 Mt CO_2 per year (Renou-Wilson et al., 2019). Furthermore, the conservation of near-natural peatlands and the rehabilitation of degraded peatlands is necessary to protect C stocks, reduce emissions and enhance their C assimilation capacity to further offset national GHG emissions.

Terrestrial Gross Primary Productivity (GPP) describes the total amount of CO_2 assimilated by plants in an ecosystem through photosynthesis and is considered the largest flux component of the global carbon cycle (Lees et al., 2018). Therefore detailed knowledge of the spatio-temporal extent of GPP dynamics and the key drivers such as air temperature, water table depth, and soil water content is imperative to improve our ability to quantify fluxes and upscale them across various spatial domains.

Current field-based methods of measuring annual carbon exchange, between peatlands and the atmosphere, include the use of static and dynamic chambers and eddy covariance (EC) towers (Kiely et al., 2018; Laine et al., 2006). The integration of both these techniques can encapsulate peatland carbon dynamics at a variety of temporal and spatial scales by capturing seasonal and interannual variability at the point-source and ecosystem scale. While EC techniques have proven to be of great importance in the measurement and modeling of C dynamics in peatlands (Baldocchi et al., 2018), these measurements only account for C fluxes within the footprint of the tower which typically spans over an area between 200 m^2 to 1 km^2. It is therefore challenging to scale up EC fluxes from the footprint-derived source to the regional/global scale due to the geographical distribution and the limited number of towers (Barba et al., 2018).

Light use efficiency (LUE) models based on Monteith's theory (1972) are extensively used to model GPP. This model expresses GPP as the product of the incident photosynthetically active radiation (PAR), the fraction of absorbed photosynthetically active radiation (f_{PAR}) by the vegetation canopy, and the light use efficiency parameter (ε). Spectral indices are important as they integrate nutrient and absorption characteristics, and are used as a proxy for f_{PAR}, which is one of the major parameters for the estimation of GPP in the LUE models (Joiner et al., 2018; Lees, et al., 2020). Rates of CO_2 assimilated by a plant canopy are strongly correlated with satellite-derived vegetation indices (Junttila et al., 2021; Schubert et al., 2008). The light use efficiency parameter (ε) can also vary depending on environmental conditions and plant physio-morphological changes (Hilker et al., 2008). It is also possible to calculate ε directly from the Photo-chemical Reflectance Index (PRI) however, the bands required for the PRI index are not available in Sentinel 2 data (Goerner et al., 2011; Peng et al., 2018; Schubert et al., 2008). There are also a limited number of studies available that report the derivation of ε values for peatlands using site-derived Light Response Curves (LRC) (Gan et al., 2021; Kross et al., 2016; Schwalm et al., 2006).

Remote sensing techniques provide a new opportunity to assess the C dynamics of peatlands and other remotely located ecosystems (Biudes et al., 2021; Lees et al., 2019). It can facilitate an assessment of multiple ecosystem attributes and can provide information across wider spatial scales. This is important as EC infrastructure is expensive, requires regular maintenance, and is limited to ecosystem scale perspectives, making direct measurements across multiple sites and spatial scales unfeasible. Because of this, the use of spectral indices as a proxy for carbon flux estimation is becoming more widely used (Bhatnagar et al., 2018; Couwenberg et al., 2011; Joiner et al., 2018).

Vegetation indices derived from satellite data such as the normalized difference vegetation index (NDVI) or enhanced vegetation index (EVI) have been correlated with GPP with varying degrees of success at grassland, cropland, and forested sites (Joiner et al., 2018; Schubert et al., 2008; Sims et al., 2006). The use of common MODIS-derived vegetation indices (250-500m), such as NDVI and EVI, can be challenging for GPP estimation over peatlands because of the narrow red absorption feature and narrow near-infrared reflectance peak, which is commonly observed in dominant peat-forming species such as *Sphagnum* mosses (Bhatnagar et al., 2018; Lafleur et al., 2003). Additionally, vegetation indices derived from MODIS data might incorporate forestry and grasslands into the peatland signals due to the coarse spatial resolution (250m-1000m) leading to an overestimation of GPP (Pei et al., 2022; Yuan et al., 2007). However, the use of higher spatial resolution sensors like Sentinel satellite imagery (10-30m) can help reduce the uncertainty in GPP estimation by providing greater insight into the carbon flux estimation of heterogenous landscapes (Lees et al., 2018).

The reflectance characteristics of peatlands are different from the forest, agricultural and grassland ecosystems due to the hydrological conditions, water content, and associated vegetation communities (Lin et al., 2019; Zheng et al., 2018). Moreover, the spectral signature of *sphagnum* mosses is characteristically different compared to the vascular vegetation in peatland ecosystems. The spectral reflectance of *sphagnum* species changes with the available moisture content and their reflectance increases during dry periods as *sphagnum* changes its color to yellow-brown (Harris, 2008; Lees et al., 2019; Van Gaalen et al., 2007; Vogelmann & Moss, 1993). Zhang et al. (2015) highlight the importance of using different indices within one model to properly understand the effect of water content on vegetation when using light-use efficiency models. Therefore, there is a need to assess the performance of widely used indices to predict GPP and develop a combination of indices specifically for raised bog ecosystems.

In this study, Sentinel-2 high-resolution satellite imagery was used to derive vegetation and water indices as it offers a new perspective in monitoring ecosystem phenology (Joiner et al., 2018; Lees et al., 2018; Lin et al., 2019). Six widely used indices which include four vegetation indices (NDVI, EVI, MCARI, REP2) and two water indices (LSWI, NDWI2) were used in this study to identify the best combination of indices for peatlands. Sentinel-2 images from a climatologically dry year in 2018 were used to derive indices as it provided an opportunity to acquire seasonal cloud-free imagery for GPP estimation and it was also useful to gain further insight into how the light use efficiency parameters performed during drier conditions. The objectives of this study were to (1) develop hybrid models using a combination of indices to estimate GPP using LUE models and validating them against EC-derived GPP for a near-natural peatland ecosystem and, (2) determine the site-specific light use efficiency parameters for a near-natural peatland under dry and normal conditions which could be used to refine estimates of LUE model based GPP from other sites in the future.

6.2 Materials and Methods

6.2.1 Study site

Clara bog (Fig.6.1a) is one of the largest remaining relatively intact raised bogs in Western Europe (Crushell et al., 2008), and is located in County Offaly in the midlands of Ireland (53°19 N, 7°36 W). The site is designated as a special area of conservation (SAC) under the European Union Habitats Directive (Council of the European Communities, 1992). It has an Atlantic temperate climate with an average annual rainfall of 883 mm and an average annual temperature of 9.6 °C (Hammond, 1981; van der Schaff & Streefkerk, 2011).

The site is bisected by a road into Clara East (206 ha) and Clara West (234 ha), and this study focuses on Clara West. Despite being a near-natural bog, the site has been subject to continued subsidence, which is attributed to the drainage of the regional groundwater table surrounding the bog and the hydrogeological complexity of the bog itself. This has resulted in the progressive loss of approximately 40% of the active raised bog (ARB) area since 1991 (Regan et al., 2019). The site is divided into nine ecotopes (van der Schaaf, 2002) based on the distribution of *Sphagnum* as shown in Figure 6.1b.

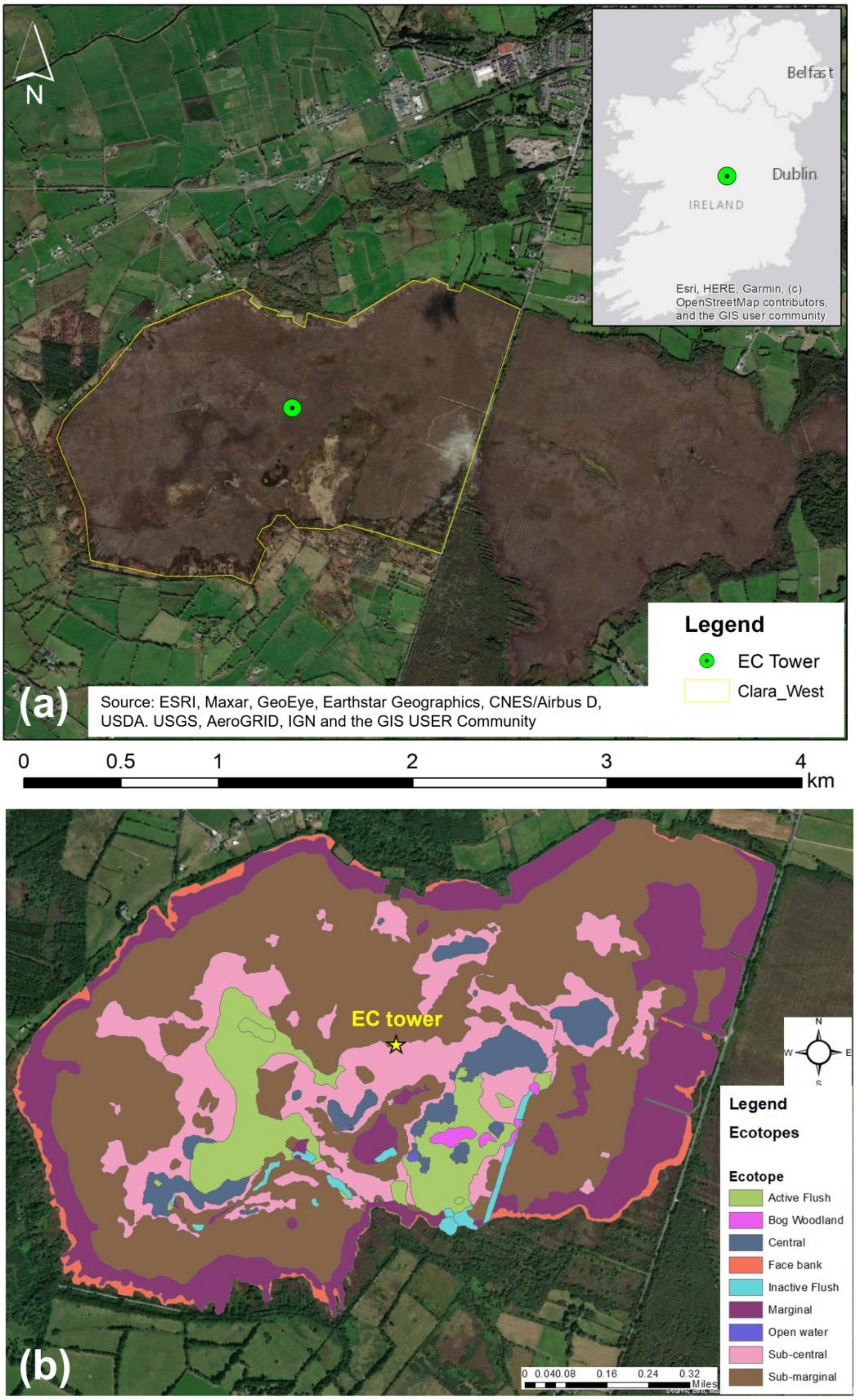

Figure 6. 1 (a) A map of Clara Bog showing the delineation of the bog into the eastern and western sections (the western section boundary is highlighted in yellow) and the location of the EC tower (b) Ecotope map of Clara Bog West (EU LIFE Irish Raised Bog Restoration Project) with EC tower location shown in yellow

6.2.2 Measurements of net ecosystem carbon dioxide exchange and ancillary variables

The EC instrumentation consisted of a Sonic Anemometer (Windmaster, Gill Instruments, Lymington, UK) which measures wind speed and direction in three dimensions, and an embedded closed path infra-red gas analyzer (LI-7200, LI-COR Lincoln, Nebraska, USA). The flux tower (Clara EC) is located at the center of Clara West (Fig. 6.1a) and the EC tower flux footprint predominantly covers the submarginal (SM) and subcentral (SC) ecotopes which constitute of *Narthecium ossifragum*, *Sphagnum tenellum,* and *Sphagnum magellanicum.* The submarginal and subcentral ecotopes constitute around 77% (191.34 ha) of the site and this study area was used to validate the modelled GPP with EC-derived GPP.

The raw EC data were collected at 10Hz and processed using Eddy Pro version 7.0.6. in advanced mode using site-specific parameters. Additional meteorological and environmental variables were also measured which included air temperature and humidity (CS215, Campbell Scientific, Shepshed, England), the Volumetric Water Content of the soil (VWC) (CS616 Water Reflectometer, Campbell Scientific, Shepshed, England), soil heat flux (HFP01 Hukseflux, Delft, The Netherlands), soil temperature (105E, Campbell Scientific, Shepshed, England), photosynthetically active radiation (PAR) (Skye Instruments, Llandrindod, Wales) and Net Radiation (NR) (NRLite, Kipp & Zonen, Delft, The Netherlands). The meteorological data were averaged and recorded using a Campbell Scientific micro-logger (model-CR3000) (Campbell Scientific, Shepshed, UK) at thirty minutes intervals. Water table height was recorded at the EC flux tower location using Orpheus Mini vented-pressure level transducers located in phreatic tubes. Precipitation data from the nearby Met Eireann weather station (Horseleap) was used during the study duration.

The EC processing and quality control procedures included spike removal and double coordinate rotation while tests on developed turbulence and stationarity were also applied (Foken et al., 2004; Mauder , 2011; Reichstein et al., 2005, Falge, et al., 2001). The flux data were gap-filled using semi-empirical models parameterized using high-quality flux data (Falge et al., 2001), while fluxes were partitioned through the extrapolation of night-time respiration (Reichstein et al., 2005, Falge, et al., 2001).

6.2.3 Modeling framework

Figure 6.2 shows the modeling framework used in this study and the model calibration and validation steps. As mentioned in the introduction, the main objective of this study is to find a combination of indices to be used with LUE models for GPP estimation at peatland sites. Additionally, a site-explicit Light Use Efficiency parameter (LUE) for this site was derived. Initially, GPP was modelled using equation 1 with six satellite-derived indices (Table 6.1), literature-based LUE parameter values (Table 6.2), and measured PAR for 2018. The results were then validated against field-based EC-derived GPP for 2018 to obtain the potential indices for the hybrid models. Overall, six hybrid models were developed based on regression analysis and modelled GPP were validated against EC-derived GPP for 2019 and 2020. Site-specific LUE parameters (ε_{site}) for drier (2018) and wetter years (2019-2020) for the near-natural peatland were established based on the analysis of light response curves at the site.

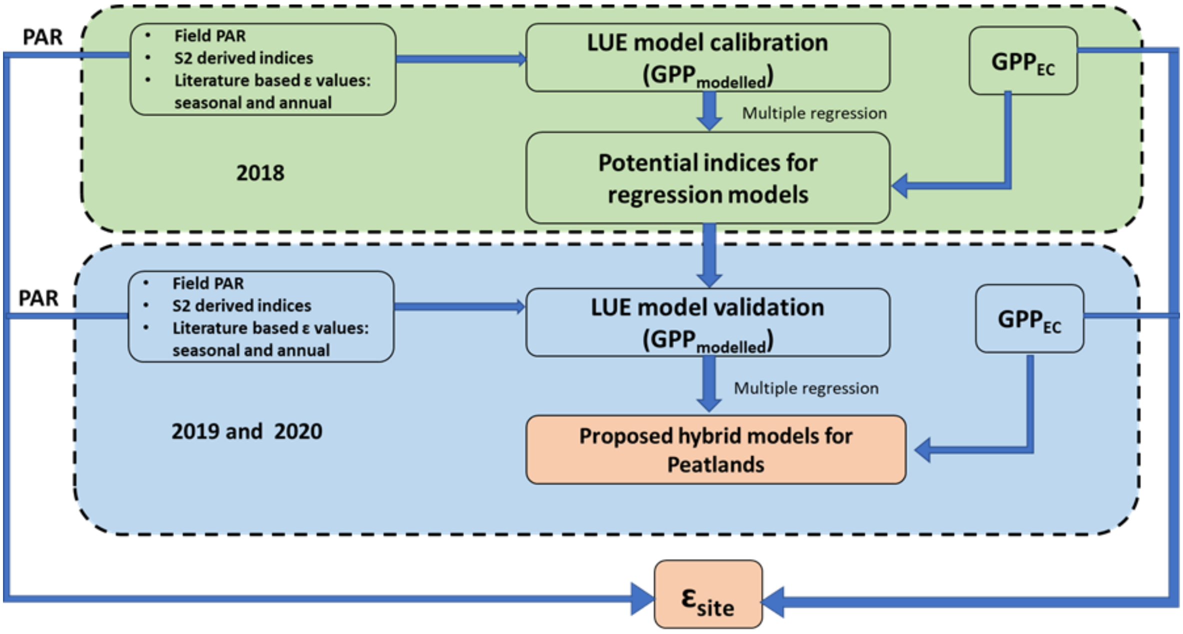

Figure 6. 2 The modeling framework showing calibration and validation steps to derive hybrid models and derive site-specific LUE parameters; light orange boxes show the objectives of this study; Blue and green boxes show the time frame for calibration and validation

6.2.4 Light Use Efficiency model

The most widely used model for estimating GPP from satellite data is the light use efficiency model developed by Monteith (1977), eq. (1). Clara West is located in the temperate climatic zone and for this study, it is assumed that the scaler effect of environmental drivers such as air temperature (T_a), and vapor pressure deficit (VPD) is negligible

$$GPP_{Modelled} = \varepsilon \times f_{PAR} \times PAR \qquad (1)$$

Where $GPP_{Modelled}$ is LUE modelled GPP; ε is the radiation use conversion efficiency of the vegetation (g C MJ^{-1}) also known as Light Use Efficiency (LUE) parameter, PAR is the photosynthetically active radiation incident at the canopy (MJ m^{-2}) and f_{PAR} is the fraction of incident PAR absorbed by the canopy (MJ m^{-2}). The f_{PAR} variable is usually modelled as a function of satellite-derived indices and can be expressed as in equation (2)

$$f_{PAR} = APAR/PAR \approx \text{indices} \quad (2)$$

Where APAR is Sentinel data and indices

The Sentinel-2 product Multispectral Instrument Level 2A (S2-MSIL2A) was made available in March 2018. The Level-2A images are bottom-of-atmosphere (BOA) reflectance in cartographic geometry and are atmospherically corrected. The satellite has a temporal resolution of 5 days, and the spatial resolution varies between 10m to 60m depending on the wavelengths. The S2 has three vegetation-red-edge bands (spatial resolution - 20m) dedicated specifically to identifying and analyzing vegetation on the ground. S2 imagery was acquired for the years 2018, 2019, and 2020 with a cloud filter of less than 10% through the Copernicus Open Access Hub (Copernicus Open Access Hub, 2020). The spatial resolution of S2 bands is 10m, 20m, and 60m (depending on the wavelength) and to maintain consistency all bands were resampled to 10m spatial resolution using the bilinear interpolation technique in SNAP v.7.0. ("SNAP - ESA Sentinel Application Platform"). The images were then subset for the location of Clara Bog using SNAP Subset tool specifically looking at the subcentral and submarginal ecotopes. The six widely used vegetation and water indices as mentioned in Table 1 were extracted from Sentinel 2 imagery using SNAP Raster toolbox and were averaged for each subset (using MATLAB v.2019a). These were then used as a proxy for f_{PAR} to model GPP using eq. 1. The formula and description of the indices are shown in Table 6.1.

Table 6. 1 List of vegetation and water indices used as a proxy for f_{PAR} to model GPP

Index	Formula	Description
Normalized Difference VI **(NDVI)** (Liu & Huete, 1995)	$NDVI = \frac{(NIR - Red)}{(NIR + Red)}$	1 ≥ NDVI > 0.1 describes the presence and condition (health) of vegetation. (dimensionless index)
Enhanced VI **(EVI)** (Gao et al., 1993)	$EVI = \frac{2.5 * (NIR - Red)}{((NIR + 6.0 * Red - 7.5 * Blue}$	0.8 ≥ EVI ≥ 0.2, improvement on NDVI - It uses blue band to minimize noise caused by canopy background and atmospheric effects and, describes the health of vegetation.
Land Surface Water Index **(LSWI)** (Gao et al., 1996)	$LSWI = \frac{(NIR - SWIR)}{(NIR + SWIR)}$	LSWI > 0.5; detects open water and highlights the wet-vegetation communities.
Normalized Difference Water Index **(NDWI2)** (McFeeters, 1996)	$NDWI2 = \frac{(NIR - Green)}{(NIR + Green)}$	NDWI2 is mainly used for the detection and delineation of water bodies from the soil and vegetation.
Modified Chlorophyll Absorption in Reflectance Index **(MCARI)** (Daughtry et al., 1993)	$MCARI = \left((REP1 - Red) - 0.2 * (REP1 - Green)\right) * \left(\frac{REP1}{Red}\right)$	MCARI depicts the leaf chlorophyll concentrations and responds to LAI-chlorophyll interactions.
Red Edge Position **(REP2)** (Curran et al., 1995)	REP2 = 740 nm	REP2 (red edge position-2) depicts the chlorophyll concentrations and highlights the green vegetation present in the area.

6.2.5 LUE parameter (ε)

Many remote sensing techniques, such as MODIS use look-up tables to derive ε values for specific biomes (Heinsch et al., 2006), and there is no class for wetlands or peatlands in the MODIS look-up table. ε is also often calculated from a constant of ε_{max} for specific biomes such as grassland, forests, and croplands by adjusting environmental stressors (Zhang et al., 2021). However, Connolly and Holden (2009) showed that ε in peatlands varies over space and time.

Given the dearth of information on LUE parameter (ε) for peatlands (Gan et al., 2021; Lees et al., 2018), this study uses ε values for the growing season and global fixed values based on available studies as shown in Table 6.2. For future research at similar near-natural sites, this study provides ε_{site} derived by rectangular hyperbolic curve fitting using a Michaelis–Menten equation with EC-derived GPP and in-situ field PAR data.

Table 6. 2 Literature-based LUE parameter values for peatlands

Time frame	ε (g C MJ^{-1})	Source
Growing season	0.61	[Schwalm et al., 2006]
Annual	1.21	[Kross et al., 2016]
Growing season	0.83	[Gan et al., 2021]

6.2.6 The hybrid model calibration

For model calibration (Fig. 6.2), the values for the spectral indices outlined in Table 6.1 were extracted from nine cloud-free Sentinel S2 images in 2018. All six indices (Table 6.1) were used as a proxy for f_{PAR} to model GPP using equation 1. Field-measured PAR for 2018 along with the literature-based LUE parameters (Table 6.2) were also used as an input in equation 1. As a next step, multiple linear regression was performed to test which indices significantly predicted the modelled GPP when compared with the EC-derived GPP. The results of the regression indicated that individually NDWI2, EVI, REP2, and NDVI showed a Spearman correlation between 0.8 to 0.95 whereas LSWI and MCARI showed a Spearman correlation of 0.77, as shown in

Fig. 3. Therefore, NDWI2, EVI, REP2, and NDVI were selected as potential candidates for the hybrid models and the fitted regression equations for all the three ε values are shown in Table 6.3. The adjusted R-squared ranged between 0.97 to 0.98 for all the models with a p-value below 0.05. All the analysis and modeling work was performed using R software (version 3.6.3) and relevant R packages.

Figure 6. 3 The correlation matrix of modelled GPP with EC-derived GPP for 2018 (red represents a stronger positive correlation, blue-yellow represents a moderate positive correlation and grey colour shows a correlation below 80%)

Table 6. 3 Multiple Regression based hybrid models

Model	ε = 0.61 (Schwalm et. al)	ε = 0.83 (Gan et. al)	ε = 1.2 (Kross et. al)
1	$3EVI - 1.1(NDWI2)$	$1.7EVI - 0.63(NDWI2)$	$2.5EVI - 0.9(NDWI2)$
2	$0.61NDVI + 0.44(NDWI2)$	$0.35NDVI + 0.25(NDWI2)$	$0.5NDVI + 0.36N(DWI2)$
3	$1.75(REP2) - 0.81(NDWI2)$	$(REP2) - 0.46(NDWI2)$	$1.4(REP2) - 0.67(NDWI2)$
4	$2.2EVI - 0.2NDVI$	$1.28EVI - 0.11NDVI$	$1.8EVI - 0.17NDVI$
5	$1.3(REP2) - 0.09NDVI$	$0.76(REP2) - 0.05NDVI$	$1.1(REP2) - 0.08NDVI$
6	$1.9(REP2) - 1.1EVI$	$1.1(REP2) - 0.61EVI$	$1.6(REP2) - 0.9EVI$

6.3 Results

6.3.1 Seasonal Dynamics of meteorological parameters

The seasonal fluctuations of the main meteorological parameters are shown in Figure 6.4. The average daily air temperature varied between -3.3°C to 21°C for the year 2018 and -1.2°C to 20°C for 2019 and 2020 (Fig 6.4a). The total annual precipitation received for 2019 was 1034 mm and 1065 mm for 2020, whilst the precipitation in 2018 (595 mm) was much lower highlighting that 2018 was a drought year (Fig 6.4b).

In 2018, the water table (Fig 6.4c) ranged between -15 cm (negative sign indicates below ground level) to 5.4 cm and it fluctuated between -14 cm to 8.05 cm for the years 2019 and 2020 (Fig 6.4c). However, the water table dropped to -5 cm on the 4th of June 2018 and remained 5 cm below the bog surface for 147 consecutive days in 2018 which is almost twice the number of consecutive days in 2020 (70 days) and 2020 (81 days). Daily values of air temperature and PAR showed characteristic seasonal patterns in all years (Fig 6.4a and 6.4d), with the maximum measured incident daily PAR coinciding with the maximum air temperatures representing the peak of the summer period/growing season.

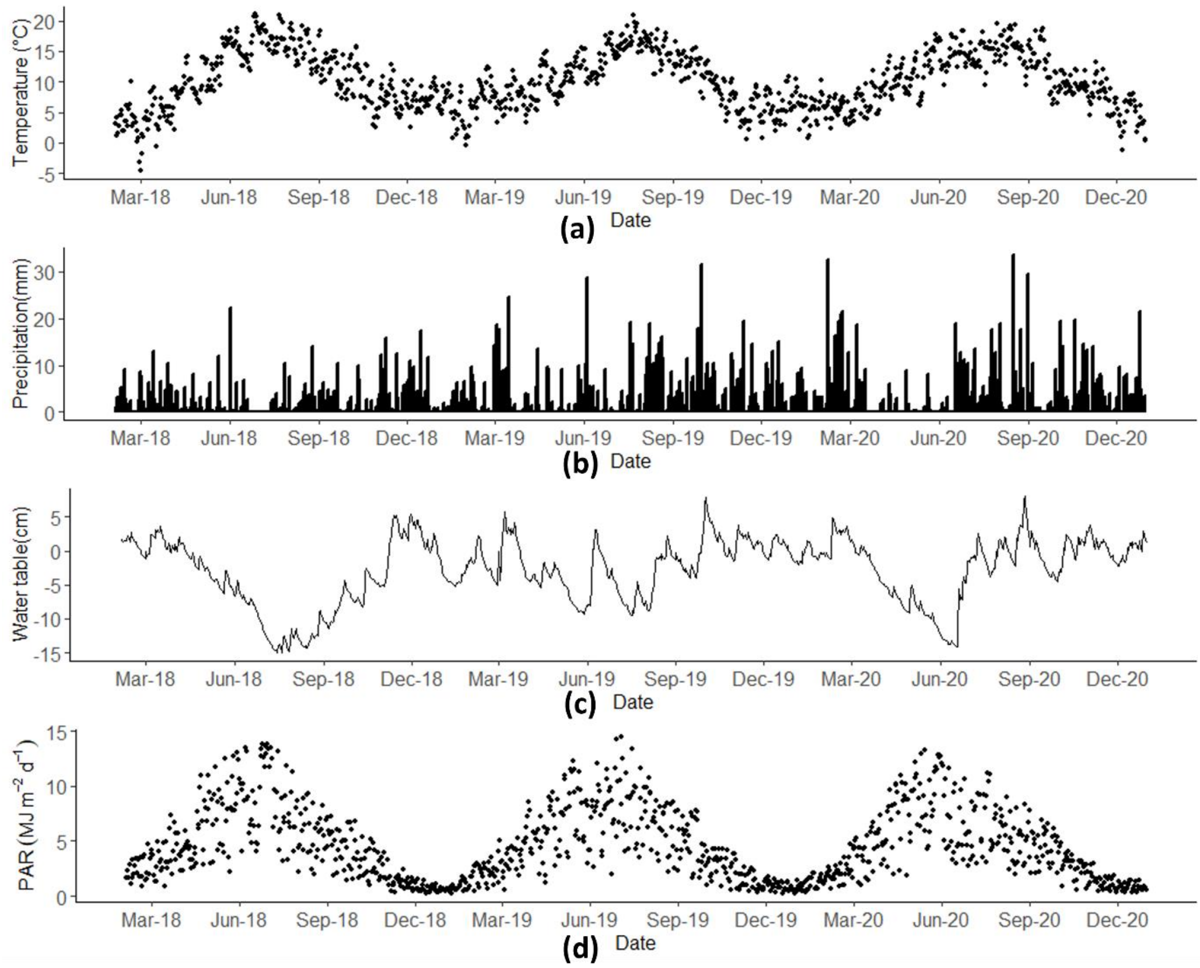

Figure 6. 4 The seasonal temporal dynamics of meteorological parameters (a) Average air temperature(°C) (b) Total daily precipitation (mm) (c) Water table depth (cm) (d) Total Daily PAR (MJ m^{-2} d^{-1})

6.3.2 Light Use Efficiency parameter (εsite) and Eddy Covariance GPP

The dynamics of GPP followed characteristic seasonal patterns in all years (Fig. 6.5a), with an increase in both carbon assimilation and release associated with increasing air temperatures and incident PAR during the spring and summer months. The total EC-based annual GPP for 2018, 2019, and 2020 was -773.9 g C m^{-2}, -824.33 g C $m^{-2,}$ and -775.7 g C m^{-2} respectively. GPP also showed seasonal variability with values for 2018 increasing to a maximum of -6.9 g C m^{-2} on 28th June 2018, while the maximum GPP (-6.6 g C m^{-2}) was observed on 23rd July 2019 and on 20th May 2020 (-5.7 g C m^{-2}).

Significant seasonal variability was also observed in the LUE parameter with LUE values following the seasonal dynamics of temperature and radiation with the highest values during summer (Fig. 6.5b). Values for 2018 ranged from 0.01g C MJ^{-1} in mid-February to 0.35g C MJ^{-1} in mid-June, returning to 0.01g C MJ^{-1} in December. The LUE parameter varied throughout the year from 0 to 0.41 g C MJ^{-1} for 2019 and 2020, with peaks reaching 28 June 2019 and 27 June 2020 (Fig. 6.5b). The annual ecosystem scale value is derived for 2018, 2019, and 2020 using the Michaelis–Menten curve fitting approach as 0.39, 0.42, and 0.38 g C MJ^{-1} d^{-1} with R^2 of 0.71, 0.78, and 0.77.

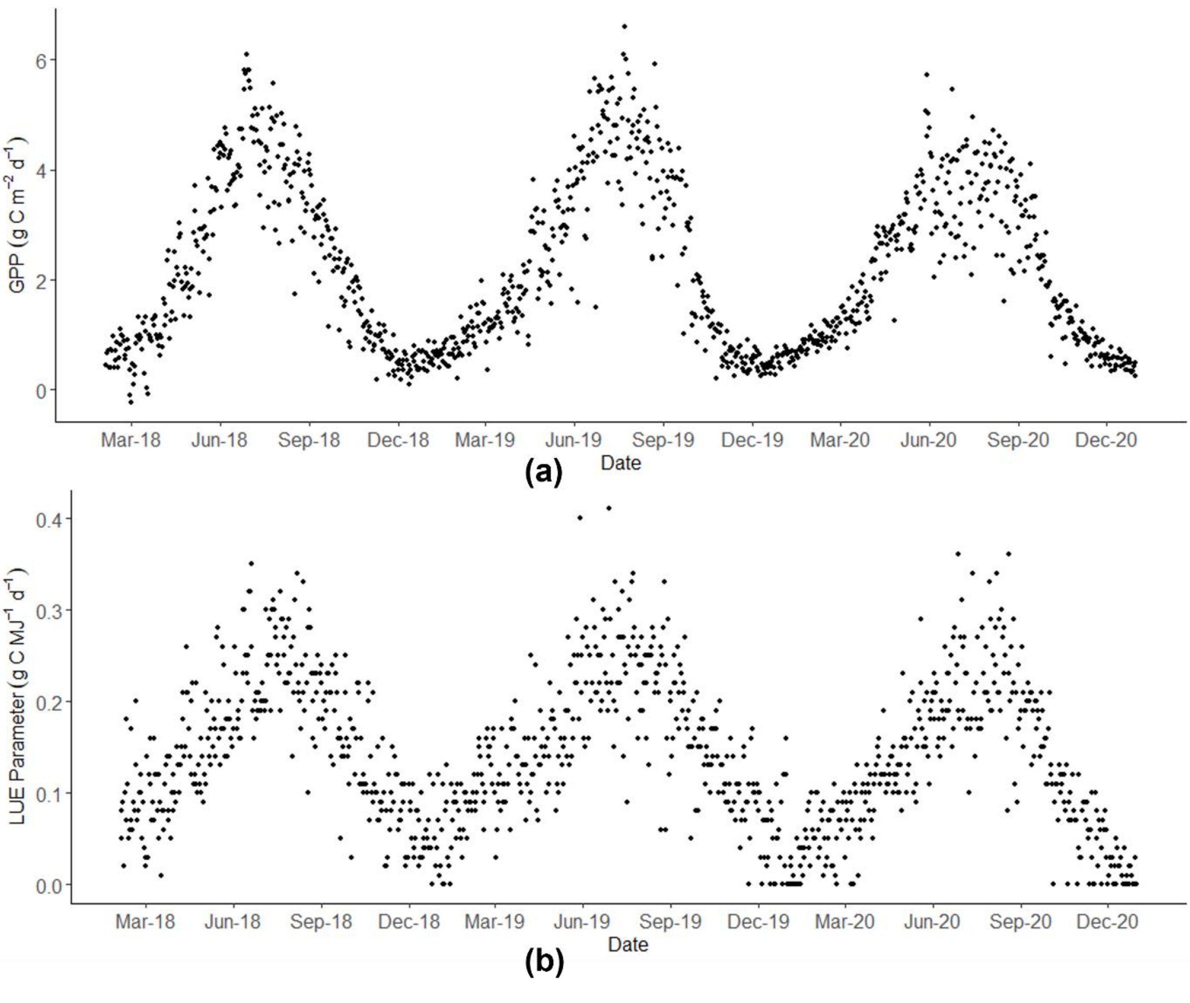

Figure 6. 5 The seasonal temporal dynamics of meteorological parameters (a) Daily Gross Primary Productivity (g C m^{-2} d^{-1}) (b) Light Use Efficiency parameter (ε_{site}) (g C MJ^{-1} d^{-1})

6.3.3 Validation of hybrid models

In total eleven cloud-free, Sentinel-2 images were used to derive indices for 2019 and 2020. All six hybrid models as shown in Table 6.3 were used as a proxy for f_{PAR} to model GPP using the light use efficiency model (equation 1) for the ε values presented in Table

6.2. The modelled GPP was validated against EC-derived GPP for the years 2019 and 2020 which were climatologically wet years (Table 6.4). GPP estimates using models 2 and 4 showed a strong correlation with the EC-derived GPP using all the literature-based ε values with a Spearman correlation coefficient of 0.96 and 0.89 respectively as shown in Figure 6.6. Models 5 and 6 exhibited a moderate correlation of around 0.61 to 0.69 with the EC-derived GPP while models 1 and 3 were poorly correlated with the EC GPP with Spearman coefficient of 0.2 to 0.25 respectively.

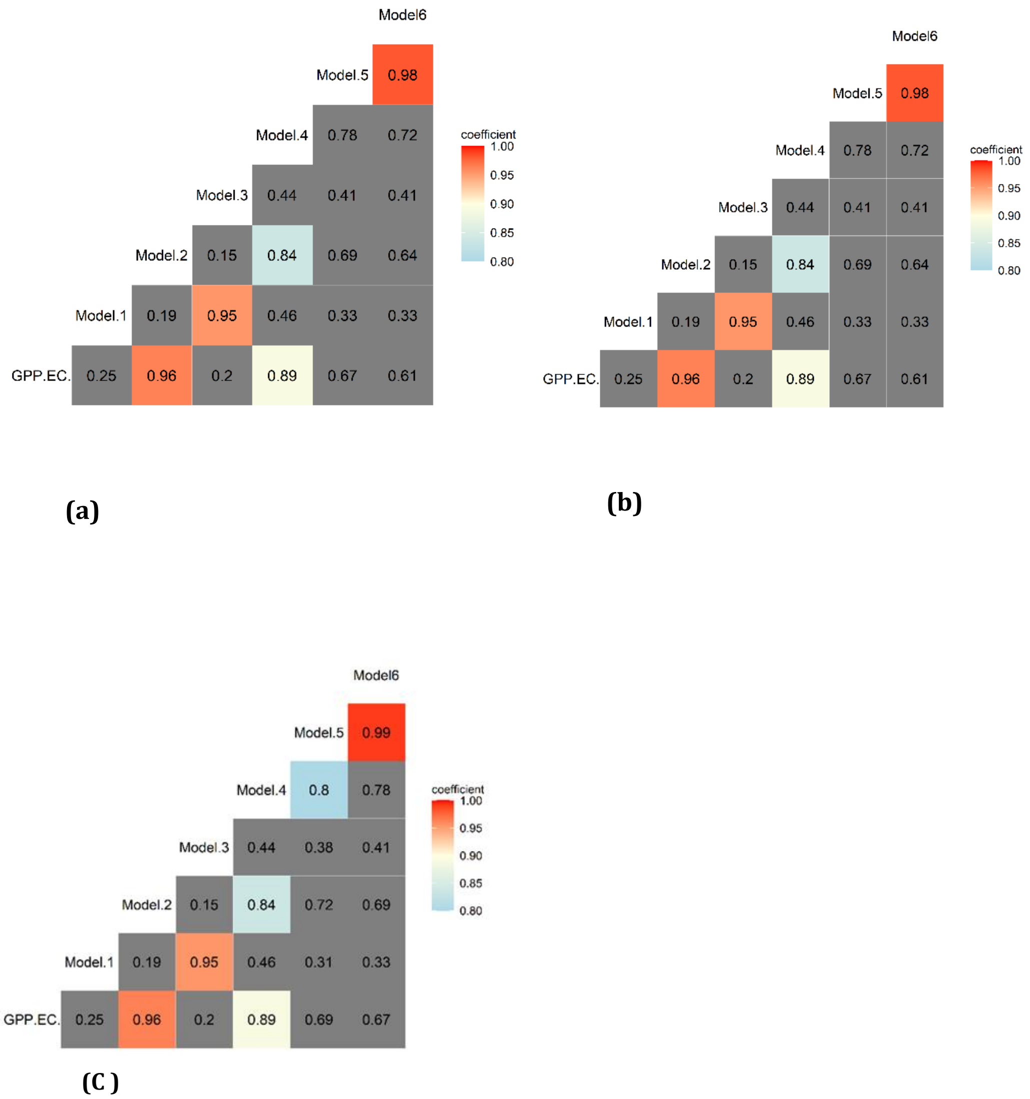

Figure 6. 6 The correlation matrix of modelled and EC-derived GPP for 2019 and 2020 (a) Correlation matrix for ε = 0.61 (b) Correlation matrix for ε = 0.83 (c) Correlation matrix for ε = 1.2 (warmer colour represents stronger positive correlation, cold colour represents moderate positive correlation and grey colour represents values lower than 80%)

6.4 Discussion

All of the six Sentinel-derived indices were used to develop hybrid models which were used as proxies for f_{PAR} to model GPP along with field-measured PAR and literature-based LUE parameters using the light use efficiency model approach. The global fixed annual value (Kross et al., 2016) and growing season values (Gan et al., 2021; Schwalm et al., 2006) of the LUE parameter (ε) were used to model GPP and these values were then compared with the EC-derived GPP to validate model performance. Model 2 which included NDVI and NDWI2 showed the highest correlation (0.96) with EC-derived GPP and one of the reasons might be that it was able to identify vegetation through NDVI and water bodies through NDWI2. Model 4 which included NDVI and EVI showed a correlation of 0.89 with the EC-derived GPP and was able to detect the vegetation well. A study by Madugundu et al. (2017) found that using a single index to model GPP under-estimated the flux values by 12% with EVI and overestimated the flux values by 20% with NDVI at an agricultural site. Similar studies highlight the importance of using hybrid models instead of a single index for estimating GPP.

Models 1,3,5 and 6 showed poor to moderate correlation with EC-derived GPP. Steenvoorden et al. (Steenvoorden et al., 2022) and Bhatnagar et al. (2018; 2020) also highlight the difference in spectral signatures of raised bogs and challenges for identifying ecotopes. A recent study by Lees et al. (2019) found that MOD17A2H GPP product overestimates GPP modelled from data collected by EC towers situated at two ex-forestry sites undergoing restoration in Scotland and at a near-natural blanket bog site in Ireland (Lees et al., 2019). Site-level validation studies have also shown moderate to low performance of MOD17A2H in capturing the seasonal and inter-annual variation in flux estimation (Zhang et al., 2017). Even though some models (Huang et al., 2019; Kang et al., 2018) have tried to incorporate remotely sensed variables to enhance performance such as land surface temperature (LST) and LSWI in the MODIS products, access to clear cloud cover-free imagery is a challenge that limits the application of these models across various scales.

In this study, the hybrid models were developed using three years of data that align with the deployment of the EC tower at this site in 2018, and this work represents a novel attempt to develop hybrid models exclusively for raised bog systems. The proposed models 2 and 4 in this study performed well with limited remote sensing data for a near-natural peatland and highlight the potential to apply the models developed across raised bogs with different management practices. Furthermore, these models could have utility for other wetland systems and could be tested on blanket bogs, fens, and turloughs and could also be used to spatially and temporally upscale GPP models using the site-specific LUE parameter developed here or the literature-based approach LUE parameter integration.

One of the limitations in this study was the availability of LUE parameter values in the wider literature for sites similar to the one in this study, as there are limited studies on peatlands that have reported seasonal, growing season, and annual LUE parameter values (Gan et al., 2021; Kross et al., 2016; Schwalm et al., 2006). Even though Sentinel-2 provides relatively high-resolution imagery, there is a need to use ε values from similar sites while using LUE models. Several studies use Photochemical Reflectance Index (PRI) as a direct proxy for ε however it is not possible with Sentinel 2 data due to limited band availability (Lees et al., 2018; 2020). This study reports site-specific ε_{site} values based on LRC curves for a near-natural peatland during extremely dry and normal climatic years which could be useful for the development of additional GPP models. The mean annual ecosystem-scale light use efficiency parameter values of 0.39 (dry year), 0.38-0.42 g C MJ^{-1} (normal years) were lower than the literature values ranging between 0.61 to 1.2 g C MJ^{-1} (Gan et al., 2021; Kross et al., 2016; Schwalm et al., 2006). The annual ecosystem-scale light use efficiency values reported for Clara west were not used to model GPP as it is calculated using EC-derived GPP and PAR. Validating modelled GPP with EC-derived GPP would have induced circularity into the model. However, the ε_{site} values from this study can be used for modeling similar sites across Ireland and other temperate peatlands. This study did not consider environmental stressors such as temperature and vapor pressure deficit while estimating GPP to reduce model complexity. As mentioned by

Kross et al. (2016) and Lees et al. (2018) scalars developed for other ecosystems may not be appropriate for peatlands and there is a need for longer datasets from multiple sites to develop or refine existing scalers. A recent study by Gan et al. (2021) uses a water use efficiency approach to estimate ecosystem maximum light use efficiency across 52 FLUXNET sites. Their results for seven biomes spread across the globe agree well with experimental and modeling methods (Gan et al., 2021). As a next step, the approach can be tested on satellites with limited band availability for remote locations and across the drainage gradient of peatlands.

6.5 Conclusion

In this paper, the GPP of a near-natural peatland was successfully modelled using Sentinel 2-derived vegetation indices and an LUE model. Six hybrid models based on multiple regression were developed and tested for various literature-based LUE parameter values specifically for raised bogs and modelled GPP using hybrid models 2 and 4 correlated well (0.89 to 0.96) with the EC-derived GPP. This study also reports site-specific LUE parameter values based on light response curves for an drought year and normal weather under normal climatological conditions years which could be useful in the future to help upscale estimates of GPP in other studies on near-natural peatlands. These results provide useful insights into the use of high-resolution derived vegetation indices and their potential to be used across various scales and peatland types. Additionally, this approach can be further refined using high-resolution imagery such as Planet scope to estimate carbon fluxes from remote locations. This information will also be useful as a reference for sensor selections and future sensor designs for ecosystem studies.

Chapter 7: General Discussion and Conclusion

7.1 Overview

Peatlands store a significant amount of terrestrial soil organic carbon (500 to 700 billion tonnes) as a part of the global carbon cycle (Gorham, 1991). Land-use conversion through drainage for peat harvesting, agriculture, and forestry are some of the main threats responsible for converting these ecosystems from a carbon sink to a source, by compromising the hydrological balance and increasing rates of mineralization and emissions (Blodau, 2002; Page & Baird, 2016). Climatic events such as shifts in temperature and precipitation patterns also act as a catalyst to alter the eco-hydrology of these ecosystems by further enhancing the rates of C and GHG emissions (Biancalani & Avagyan, 2014; Evans et al., 2021). It is crucial to understand the impacts of drainage and climate change on these ecosystems along with the key drivers of the emissions to fully understand their impact on climate feedback loops and to devise climate-smart mitigation strategies (Leifeld & Menichetti, 2018). Detailed information on C and GHG dynamics will aid in halting their emissions to the atmosphere by enhancing the mitigation potential of peatlands via conservation, effective rehabilitation, and restoration(UNEP, 2022; Wilson et al., 2022).

The primary aim of this PhD project was to develop an interdisciplinary approach to understand the impact of anthropogenic activities and climatic variability on the carbon and methane dynamics of raised bog ecosystems. This project represents a novel attempt to integrate innovative experimental and observational techniques to assess the impacts of various management activities across a drainage gradient in these ecosystems. This work has enhanced our understanding of how carbon dioxide and methane emissions vary both in space and time at sites across drainage gradients which included an industrial peat extraction site, a former extraction site on the rehabilitation trajectory, and a near-natural raised bog. Eddy covariance and closed chamber techniques were central to this research and were used to investigate the spatial-temporal extent of carbon and methane emissions and to better understand the key drivers of uptake or emissions. Chapter 3 describes the methodologies used to assess this while Chapter 4 focuses on the impacts of drought events on net ecosystem CO_2 fluxes using the EC technique at a near-natural raised bog in Ireland. This chapter also highlights the vulnerability and resilience of these ecosystems to drought events and elucidated the key drivers governing the system's response to such events. In Chapter 5, methane emissions from sites across the drainage gradient were measured using closed-chamber techniques. These emissions were upscaled from the point-to-site scale with the help of remote sensing and machine learning tools to broaden our knowledge of ecosystem-scale methane dynamics. A new/novel remote sensing approach was developed in Chapter 6 to model GPP (a major component of net ecosystem carbon exchange) using a light-use efficiency model and hybrid indices for raised bog ecosystems. This chapter (7) provides a synthesis of the research questions from the individual research chapters and discusses the context of the respective results with outputs from the wider scientific community (Section 7.2). To summarize, the conclusions (Section 7.3) and broader implications (Section 7.4) of the work are highlighted along with the limitations of the research, and suggestions for future research (Section 7.5) are also outlined.

7.2 Summary of the main findings

Research question 1: What are the impacts of climate change on the CO_2 dynamics of a near-natural bog and what are the key environmental and ecological drivers that influence uptake/release?

Chapter 4 underlines the importance of drought periods and changing water table height as key regulators of inter-annual variation in CO_2 exchange at a near-natural bog in Ireland. Based on four years of EC CO_2 flux measurements, I found that the timing, severity, and duration of drought have significant impacts on the water table height and soil moisture which then influenced the net ecosystem CO_2 uptake/release and controlled the effect on the CO_2 dynamics. A short but severe drought period marked by a prolonged lowering of water table depth and lower surface soil moisture conditions during mid-summer in 2018 increased rates of R_{eco} while rates of GPP remained constant, causing the study area to act as a source of C with an annual NEE and release of 53.5 g C m^{-2} in 2018. However, the site reverted to being a C sink following the drought year and consistently acted as a C sink with annual NEE ranging between -49.8 to -125.2 g C m^{-2} for the remaining three years, which highlights the vulnerability but also demonstrates the resilience and adaptive capacity of these ecosystems to return to their natural state as a C sink. However, it is worth noting that the lowest precipitation was recorded in 2021and the total number of days with a water table below 5 cm were highest in 2021. However, the system was still acting as a C sink and it might be due to sporadic precipitation events during the growing season that returned the water table close to the surface thus reducing C losses through Reco. This highlights the importance of more long-term studies to determine the resilience of peatlands to climate change and to better understand the role of key drivers of C dynamics in more detail. This research question is addressed and discussed in detail in Chapter 4.

Research question 2: How do methane emissions vary at peatland sites across a drainage gradient and how can these emissions be upscaled from the point to ecosystem/site scale when considering the spatial heterogeneity of the sites?

Chapter 5 assessed methane emissions at study sites covering a broad spectrum of various stages of bog condition and management practices which included near-natural, degraded, and sites under rehabilitation. Methane emissions were measured using closed chamber techniques at the dominant vegetation communities at all three sites throughout 18 to 24 months. The average annual methane emissions varied between 1.4 to 8.89 g C m^{-2} y^{-1} at the near-natural site; -1.1 to 1.55 g C m^{-2} y^{-1} at the site under rehabilitation and 0 to 0.5 g C m^{-2} y^{-1} at the degraded site. This study also tested the applicability of high-resolution multispectral satellite imagery and a variety of mapping techniques with machine learning algorithms to provide fine-scale vegetation maps. These maps were then used to upscale methane emissions from the point to ecosystem scale with an overall accuracy of over 83%. Our results provide evidence that upscaling is successful, as long as the dominant vegetation communities are appropriately mapped at heterogeneous sites. The highest average annual methane emissions were measured at the central ecotope at the near-natural site, and after upscaling the fluxes to the ecosystem scale, the central ecotope showed the lowest methane emissions due to the spatial extent covered, emphasizing the need to include the complex spatial heterogeneity of peatlands and report upscaled flux values for emission factor and site scale C budget estimation. Detailed information on this research question and comparison to other similar studies can be found in the discussion section of Chapter 5.

Research question 3: How can GPP be accurately estimated using remote sensing techniques and which combination of EO indices is most appropriate for use in peatland ecosystems? Furthermore, which light-use efficiency parameters can be used for near-natural peatlands and can they be applied to peatlands under variable hydrological conditions?

In Chapter 6, the GPP of a near-natural peatland was successfully modelled using Sentinel-2 derived indices and an LUE model. The model was calibrated during a dry year with six widely used vegetation and water indices as a proxy for f_{PAR}. Six hybrid models based on multiple regression were developed and validated during the wetter/humid/normal climatic years. The modelled GPP using model 2 (0.96) and model 4 (0.89) showed the highest Spearman correlation with the EC-derived GPP. This study also reported site-specific LUE parameter values based on light response curves for drought years and humid/wetter years which could be useful in the future to estimate GPP at similar sites independently and under variable climatic scenarios. These results provide useful insights into the use of high-resolution derived indices and their potential to be used across various scales and peatland types. This research question and our approach are addressed in detail in Chapter 6.

7.3 Limitations of research and suggestions for future work

- The global COVID-19 pandemic occurred during the second year of this research, and the associated travel restrictions delayed the installation of collars at the Lullymore and Garryduff sites reducing the measurement duration from 24 months to 18 months.
- The closed chambers were able to capture CH_4 emissions with high spatial coverage but their low temporal resolution might have missed episodic emissions during exceptional climatic events. As an example, missing data points due to limited access at particular sites due to flooding. The inclusion of floating chamber measurements would have been beneficial in this specific case to measure CO_2 and CH_4 emissions across the water/atmosphere interface.

There is potential to apply the framework proposed in Chapter 5 for upscaling chamber and eddy covariance measurements across other sites including blanket bogs, fens, and turloughs. Additionally, to enhance the upscaling approach proposed in Chapter 5, an understanding of the phenological dynamics of the vegetation communities present could be useful, rather than just the spatial variation at one point in time.

- The EC technique provides high-frequency, real-time measurements of GHG exchange across the soil, plant, and atmosphere continuum, however, the flux measurements are limited to the flux footprint and it might be challenging to upscale CO_2 fluxes at heterogenous sites and to determine full ecosystem scale budgets. The integration of closed chamber techniques with EC measurements is potentially useful to provide insight into the spatio-temporal extent of the fluxes. Another option would be the development of new flux footprint models which will integrate the heterogeneity of the site and associated uptake/emission characteristics in EC dynamics. The outputs of Chapter 4 can be further used to study the effects of droughts on the biophysical processes responsible for the net CO_2 exchange in more detail, particularly using process-based peatland models with the high temporal resolution to better understand how these important C sinks might behave under future climate scenarios.
- The availability of ground truth data such as ecological survey information for cross-checking satellite-derived maps is sparse. Generally, the ground truth surveys were conducted once a year at a particular point in time and they might not fully represent the seasonality in the vegetation. It would be useful to update ground truth data seasonally which will aid in the validation of satellite-derived maps.

- One of the major challenges in Ireland was the lack of available satellite images due to high cloud coverage. This is particularly problematic when looking for seasonal changes. During this study, summer and winter images were not available for some sites, however, this could be resolved by integrating seasonal UAV imagery. Additionally, the site-specific ε_{site} values estimated based on LRC curves for a near-natural peatland during dry and normal weather years could be used as a proxy for LUE-based GPP estimation at other similar sites.
- The amount of training data for machine learning algorithms play an essential role in the overall identification of vegetation communities. Seasonal drone/UAV imagery can aid in increasing the amount of training data sample size.

7.4 Implications of the research

7.4.1 Utility of long term observational platforms to assess the impacts of climatic variability

The results from Chapter 4 provides the first long-term EC flux and relevant meteorological data from a near-natural raised bog in Ireland and highlights the importance of long-term data for the estimation of emission factors and the global warming potential of these systems. A four-year CO_2 emission time series was shown to be useful in analysing the impacts of climate change on these ecosystems and highlighted both their vulnerability and resilience to these events. The study site was a carbon source during the drought year but regained its carbon sink function immediately in the following year and remained a carbon sink throughout the remaining study duration even though the climatic conditions continue to fluctuate. As outlined in Chapter 4, the timing and severity of WTD fluctuation resulting in deviation of soil moisture were one of the key drivers of the emissions in the dry year. Additionally, the research findings showed that R_{eco} is more sensitive to warmer and drier summer conditions than photosynthesis. Furthermore, this study has observed that the system remained a carbon sink even during the year 2021 which had the lowest total annual precipitation and the highest number of days where the water table was below 5 cm. This difference in the system behaving as a carbon source and a carbon sink during two drought events highlights the importance of long-term studies to capture multiple climatic events to understand the key drivers of these emissions over a longer duration, and to use this information to enhance our understanding of the climate mitigation potential of these systems. This and similar studies will also help in refining Tier 2 emission factors from peatlands which will lead to precise National emission inventory. The results from chapter 4 will also be helpful in validating process based models and aid in upscaling the emissions across at regional and national scales. This research provides first long-term carbon dioxide budget from near-natural raised bog in Ireland which will help set up a baseline scenario to measure the success of rehabilitation activities as numerous initiatives are underway from Bord na Móna (PCAS) and NPWS for effective rehabilitation of these ecosystems. Even though this study only spans over four year duration, it is an important first step towards understanding the vulnerability and resilience of near-natural peatlands to drought events. In future, such studies will be valuable for refining mitigation and adaptation framework and policies to harness impact of episodic climatic events such as drought, flooding and wildfires on peatlands.

7.4.2 Methane emissions from Irish raised bogs across drainage gradient and an approach to upscale fluxes

The results from Chapter 5 contribute to our understanding of the impact of drainage on the methane dynamics of peatlands. Closed chamber measurements at dominant vegetation communities helped assess hotspots of emissions which could lead to effective and more informed rehabilitation strategies. This study proposed and validated a novel, and to our knowledge, a first attempt to assess the potential of using high-resolution satellite imagery with the RF machine learning algorithm (SMILE) to upscale chamber-based methane fluxes from a point source to ecosystem scale across selected raised bogs in Ireland. This work demonstrated a methodology to map heterogeneous ecosystems with an overall accuracy of over 83%. There is potential to apply the framework proposed in this research to help upscale chamber and eddy covariance measurements across various types of peatlands such as blanket bogs, fens, and turloughs. Rehabilitation and restoration is gaining a lot of attention as emission reduction strategy globally and in Ireland. Methane emissions from near-natural, under rehabilitation and degraded sites will provide an insight on methane budgets along with hotspots of emissions. The emissions from sites across drainage gradient will be useful as a reference to evaluate effect of rewetting and rehabilitation. The mapping approach proposed in this thesis can aid in mapping detailed vegetation communities at heterogenous sites and the simpler upscaling approach proposed in chapter 5 can be easily extended across global peatlands to understand spatial extent of emissions at site scale which will be useful for refining Tier 2 emission factors .

7.4.3 Hybrid models for peatland ecosystems and a methodology to estimate GPP using remote sensing techniques

Chapter 6 demonstrates an approach to estimate GPP using remote sensing data at a near-natural peatland site with a potential for application at sites that are inaccessible and non-feasible for EC tower installation. Additionally, it also provides the best hybrid models to be used exclusively for peatland ecosystems. Six widely used Sentinel-derived indices were used to model GPP using multiple regression analysis and a light-use efficiency model. A global fixed annual value and growing season values of the LUE parameter (ε) were used to model GPP and these values were compared with EC-derived GPP to validate model performance. NDVI, NDWI2, and EVI-based hybrid models 2 and 4 performed well with an overall accuracy of over 89% throughout the validation for all the ε values. Results from this study show the potential of using Sentinel-2 derived indices for GPP estimation using LUE models for raised bogs. This study also reports site-specific ε values based on LRC curves for a near-natural peatland during drought and normal weather conditions, which could be useful for the development of additional GPP models that can account for and integrate climatic variability. The approach proposed in chapter 6 can be applied to estimate CO_2 budget from peatlands which are inaccessible or where measurements cannot be conducted as it will help in refining the country specific and global emission budgets.

Globally, nature based solutions (NBS) are gaining a lot of attention due to their potential to reduce carbon and GHG emissions on a shorter and longer time scale. In peatland context, conservation of near-natural peatlands is proposed as an effective NBS which is crucial for retaining ecosystem services provided by peatlands such as flood management, water quality management, fire risk management, land subsidence prevention, providing grazing and recreational areas. Additionally, rewetting followed by restoration is gaining a lot of attention as a NBS to tackle emissions from degraded peatlands. Peatland conservation and restoration also cuts across most United Nations Sustainable Development Goals (SDGs) and to accomplish effective management of these ecosystems, it is vital to achieve optimal tradeoff between CO_2 decrease and CH_4 increase. More detailed and long term studies are vital to increase our understanding of these complex ecosystems to increase their mitigation potential. Ireland is reporting GHG emissions and removals from managed wetlands to meet national, European and international climate change targets. The knowledge we have gained from the carbon and GHG dynamics from peatlands across drainage gradient as a part of this research (chapter 4, 5 and 6) has helped us better understand the impact of management practices and climate change on these sensitive ecosystems and it will help harness their mitigation potential along with refining tier 2 and 3 emission factors for Irish peatlands.

7.5 Conclusion

In conclusion, the work presented in this thesis has contributed to our understanding of carbon and GHG dynamics of these complex ecosystems along with key drivers of the emissions. The summary of key findings from this research is as follows: (1) This research has demonstrated how the EC technique along with an auxiliary sensor network can help understand the impact of climate change on CO_2 fluxes and the key drivers affecting the emissions at a near-natural bog. (2) It has shown that using closed chamber techniques to measure CH_4 emissions at sites across drainage gradients helps us understand emissions from dominant vegetation communities and has provided a new methodology to upscale these fluxes accurately using high-resolution remote sensing data and a machine learning approach (3) This research also suggested a new approach that can be used to estimate GPP with the help of high-resolution satellite imagery and combination of hybrid models proposed for raised bog ecosystems.

Overall, the research questions addressed in this thesis has helped enhance our knowledge on carbon and methane emissions from various states of peatlands which will help in optimising the trade-off between CO_2 and CH_4 emissions for effective rehabilitation. It is also importance to estimate emissions from inaccessible peatlands for precise emission inventory and I have proposed a way to estimate GPP using remote sensing based model with the help of hybrid models which are developed exclusively for raised bog ecosystems. Another important aspect that is covered in this

PhD is a simple upscaling approach is proposed and successfully implemented at sites across drainage gradient. All this information will be very useful in paving our way to enhance mitigation potential of peatlands by retaining their carbon sink function.

References

Abdalla, M., Hastings, A., Truu, J., Espenberg, M., Mander, Ü., and Smith, P. (2016). Emissions of methane from northern peatlands: a review of management impacts and implications for future management options. In *Ecology and Evolution* (Vol. 6, Issue 19, pp. 7080–7102). John Wiley and Sons Ltd. https://doi.org/10.1002/ece3.2469

Alekseychik, P., Korrensalo, A., Mammarella, I., Launiainen, S., Tuittila, E. S., Korpela, I., and Vesala, T. (2021). Carbon balance of a Finnish bog: Temporal variability and limiting factors based on 6 years of eddy-covariance data. *Biogeosciences*, *18*(16), 4681–4704. https://doi.org/10.5194/bg-18-4681-2021

Amani, M., Brisco, B., Afshar, M., Mirmazloumi, S. M., Mahdavi, S., Mirzadeh, S. M. J., Huang, W., and Granger, J. (2019). A generalized supervised classification scheme to produce provincial wetland inventory maps: an application of Google Earth Engine for big geo data processing. *Big Earth Data*, *3*(4), 378–394. https://doi.org/10.1080/20964471.2019.1690404

Antala, M., Juszczak, R., van der Tol, C., and Rastogi, A. (2022). Impact of climate change-induced alterations in peatland vegetation phenology and composition on carbon balance. In *Science of the Total Environment* (Vol. 827). Elsevier B.V. https://doi.org/10.1016/j.scitotenv.2022.154294

Aslan-Sungur, G., Lee, X., Evrendilek, F., and Karakaya, N. (2016). Large interannual variability in net ecosystem carbon dioxide exchange of a disturbed temperate peatland. *Science of the Total Environment*, *554–555*, 192–202. https://doi.org/10.1016/j.scitotenv.2016.02.153

Bain C.G, Bonn, A. , Stoneman, R. , Chapman, S. , Coupar, A. , Evans, M. , Gearey, B. , Howat, M. , Joosten, H. , Keenleyside, C., L. J. , Lindsay, R. , Littlewood, N. , Lunt, P. , Miller, C. J. , Moxey, A. , Orr, H. , Reed, M. , Smith, P. , … Worrall, F. (2011). *IUCN UK Commission of Inquiry on Peatlands*. Australasian Integrative Medicine Association. https://pearl.plymouth.ac.uk/bitstream/handle/10026.1/17516/IUCN%20UK%20Commission%20of%20Inquiry%20on%20Peatlands%20Full%20Report%20spv%20web.pdf?sequence=1andisAllowed=y

Baird, A., Green, S., Brown, E., and Dooling, G. (2019). Modelling time-integrated fluxes of CO2 and CH4 in peatlands: A review. *Mires and Peat*, *24*, 1–15. https://doi.org/10.19189/MaP.2019.DW.395

Baldocchi. (2003). Assessing the eddy covariance technique for evaluating carbon dioxide exchange rates of ecosystems: Past, present and future. *Global Change Biology*, *9*(4), 479–492. https://doi.org/10.1046/j.1365-2486.2003.00629.x

Baldocchi. (2014). Measuring fluxes of trace gases and energy between ecosystems and the atmosphere - the state and future of the eddy covariance method. *Global Change Biology*, *20*(12), 3600–3609. https://doi.org/10.1111/gcb.12649

Baldocchi, D., Chu, H., and Reichstein, M. (2018). Inter-annual variability of net and gross ecosystem carbon fluxes: A review. *Agricultural and Forest Meteorology*, *249*(May 2017), 520–533. https://doi.org/10.1016/j.agrformet.2017.05.015

Barba, J., Cueva, A., Bahn, M., Barron-Gafford, G. A., Bond-Lamberty, B., Hanson, P. J., Jaimes, A., Kulmala, L., Pumpanen, J., Scott, R. L., Wohlfahrt, G., and Vargas, R. (2018). Comparing ecosystem and soil respiration: Review and key challenges of tower-based and soil measurements. *Agricultural and Forest Meteorology*, *249*(March 2017), 434–443. https://doi.org/10.1016/j.agrformet.2017.10.028

Bhatnagar, S., Ghosh, B., Regan, S., Naughton, O., Johnston, P., and Gill, L. (2018). Monitoring environmental supporting conditions of a raised bog using remote sensing techniques. *Proceedings of the International Association of Hydrological Sciences*, *380*(2008), 9–15. https://doi.org/10.5194/piahs-380-9-2018

Bhatnagar, S., Gill, L., and Ghosh, B. (2020). Drone image segmentation using machine and deep learning for mapping raised bog vegetation communities. *Remote Sensing*, *12*(16). https://doi.org/10.3390/RS12162602

Bhatnagar, S., Gill, L., Regan, S., Naughton, O., Johnston, P., Waldren, S., and Ghosh, B. (2020). Mapping vegetation communities inside wetland using Sentinel-2 imagery in Ireland. *International Journal of Applied Earth Observation and Geoinformation*, *88*. https://doi.org/10.1016/j.jag.2020.102083

Bhatnagar, S., Gill, L., Regan, S., Waldren, S., and Ghosh, B. (2021). A nested drone-satellite approach to monitoring the ecological conditions of wetlands. *ISPRS Journal of Photogrammetry and Remote Sensing*, *174*, 151–165. https://doi.org/10.1016/j.isprsjprs.2021.01.012

Biancalani, R., and Avagyan, A. (2014). Towards climate-responsible peatlands management. In *Mitigation of Climate Change in Agriculture Series (MICCA)* (Issue 9). http://www.fao.org/3/a-i4029e.pdf

Biudes, M. S., Vourlitis, G. L., Velasque, M. C. S., Machado, N. G., Danelichen, V. H. de M., Pavão, V. M., Arruda, P. H. Z., and Nogueira, J. de S. (2021). Gross primary productivity of Brazilian Savanna (Cerrado) estimated by different remote sensing-based models. *Agricultural and Forest Meteorology*, *307*(April). https://doi.org/10.1016/j.agrformet.2021.108456

Blodau, C. (2002). Carbon cycling in peatlands - A review of processes and controls. In *Environmental Reviews* (Vol. 10, Issue 2, pp. 111–134). https://doi.org/10.1139/a02-004

Bord na Mońa Draft Rehabilitation Plan 2017 Lullymore Bog. http://www.bordnamona.ie/wp-

Bord na Mońa Garryduff Decommissioning and Rehabilitation Plan 2021 Garryduff Bog Cutaway Bog Decommissioning and Rehabilitation Plan.

Breiman, L. (2001). *Random Forests* (Vol. 45).

Bu, Z., Hans, J., Li, H., Zhao, G., Zheng, X., Ma, J., and Zeng, J. (2011). The response of peatlands to climate warming: A review. *Acta Ecologica Sinica*, *31*(3), 157–162. https://doi.org/10.1016/j.chnaes.2011.03.006

Bullock, C. H., Collier, M. J., and Convery, F. (2012). Peatlands, their economic value and priorities for their future management - The example of Ireland. In *Land Use Policy* (Vol. 29, Issue 4, pp. 921–928). https://doi.org/10.1016/j.landusepol.2012.01.010

Burba, G., and Anderson, D. (2008). A Brief Practical Guide to Eddy covariance CO2 flux measurements. *Ecological Applications : A Publication of the Ecological Society of America*, *18*(6), 1368–1378.

Chaichana, N., Bellingrath-Kimura, S. D., Komiya, S., Fujii, Y., Noborio, K., Dietrich, O., and Pakoktom, T. (2018). Comparison of closed chamber and eddy covariance methods to improve the understanding of methane fluxes from rice paddy fields in Japan. *Atmosphere*, *9*(9). https://doi.org/10.3390/atmos9090356

Chen, B., Black, T. A., Coops, N. C., Hilker, T., Trofymow, J. A., and Morgenstern, K. (2009). Assessing tower flux footprint climatology and scaling between remotely sensed and eddy covariance measurements. *Boundary-Layer Meteorology*, *130*(2), 137–167. https://doi.org/10.1007/s10546-008-9339-1

Chen, B., Coops, N. C., Fu, D., Margolis, H. A., Amiro, B. D., Barr, A. G., Black, T. A., Arain, M. A., Bourque, C. P. A., Flanagan, L. B., Lafleur, P. M., McCaughey, J. H., and Wofsy, S. C. (2011). Assessing eddy-covariance flux tower location bias across the Fluxnet-Canada Research Network based on remote sensing and footprint modelling. *Agricultural and Forest Meteorology*, *151*(1), 87–100. https://doi.org/10.1016/j.agrformet.2010.09.005

Cheng, Y., Vrieling, A., Fava, F., Meroni, M., Marshall, M., and Gachoki, S. (2020). Phenology of short vegetation cycles in a Kenyan rangeland from PlanetScope and Sentinel-2. *Remote Sensing of Environment*, *248*. https://doi.org/10.1016/j.rse.2020.112004

Chimner, R. A., Bourgeau-Chavez, L., Grelik, S., Hribljan, J. A., Clarke, A. M. P., Polk, M. H., Lilleskov, E. A., and Fuentealba, B. (2019). Mapping Mountain Peatlands and Wet Meadows Using Multi-Date, Multi-Sensor Remote Sensing in the Cordillera Blanca, Peru. *Wetlands*, *39*(5), 1057–1067. https://doi.org/10.1007/s13157-019-01134-1

Chu, H., Luo, X., Ouyang, Z., Chan, W. S., Dengel, S., Biraud, S. C., Torn, M. S., Metzger, S., Kumar, J., Arain, M. A., Arkebauer, T. J., Baldocchi, D., Bernacchi, C., Billesbach, D., Black, T. A., Blanken, P. D., Bohrer, G., Bracho, R., Brown, S., … Zona, D. (2021). Representativeness of Eddy-Covariance flux footprints for areas surrounding AmeriFlux sites. *Agricultural and Forest Meteorology*, *301–302*. https://doi.org/10.1016/j.agrformet.2021.108350

Cole, B., McMorrow, J., and Evans, M. (2014). Spectral monitoring of moorland plant phenology to identify a temporal window for hyperspectral remote sensing of peatland. *ISPRS Journal of Photogrammetry and Remote Sensing*, *90*, 49–58. https://doi.org/10.1016/j.isprsjprs.2014.01.010

Connolly, J. (2018). Mapping land use on Irish peatlands using medium resolution satellite imagery. *Irish Geography*, *51*(2), 187–204. https://doi.org/10.2014/igj.v51i2.1371

Connolly, J., and Holden, N. M. (2009). Mapping peat soils in Ireland: Updating the derived Irish peat map. *Irish Geography*, *42*(3), 343–352. https://doi.org/10.1080/00750770903407989

Connolly, J., and Holden, N. M. (2011). Object oriented classification of disturbance on raised bogs in the Irish Midlands using medium- and high-resolution satellite imagery. *Irish Geography*, *44*(1), 111–135. https://doi.org/10.1080/00750778.2011.615558

Connolly, J., and Holden, N. M. (2017). Detecting peatland drains with Object Based Image Analysis and Geoeye-1 imagery. *Carbon Balance and Management*, *12*(1). https://doi.org/10.1186/s13021-017-0075-z

Corcoran, J. M., Knight, J. F., and Gallant, A. L. (2013). Influence of multi-source and multi-temporal remotely sensed and ancillary data on the accuracy of random forest classification of wetlands in northern Minnesota. *Remote Sensing*, *5*(7), 3212–3238. https://doi.org/10.3390/rs5073212

Couwenberg, J., Thiele, A., Tanneberger, F., Augustin, J., Bärisch, S., Dubovik, D., Liashchynskaya, N., Michaelis, D., Minke, M., Skuratovich, A., and Joosten, H. (2011). Assessing greenhouse gas emissions from peatlands using vegetation as a proxy. *Hydrobiologia*, *674*(1), 67–89. https://doi.org/10.1007/s10750-011-0729-x

Crushell, P. (2008). *Soak systems of an Irish raised bog: A multidisciplinary study of their origin, ecology, conservation and restoration*.

Crushell, P., Connolly, A., Schouten, M., and Mitchell, F. J. G. (2008). The changing landscape of Clara Bog: The history of an Irish raised bog. *Irish Geography*, *41*(1), 89–111. https://doi.org/10.1080/00750770801915596

Curran, P. J., Windham, W. R., and Gholz, H. L. (1995). *Exploring the relationship between reflectance red edge and chlorophyll concentration in slash pine leaves*. *3*, 203–206.

Czapiewski, S., and Szumińska, D. (2022). An overview of remote sensing data applications in peatland research based on works from the period 2010–2021. In *Land* (Vol. 11, Issue 1). MDPI. https://doi.org/10.3390/land11010024

Daughtry, C. S. T., Walthall, C. L., Kim, M. S., and Colstoun, E. B. De. (1993). *Estimating Corn Leaf Chlorophyll Concentration from Leaf and Canopy Reflectance*. *4257*(00).

Davidson, E. A., Savage, K., Verchot, L. V., and Navarro, R. (2002). Minimizing artifacts and biases in chamber-based measurements of soil respiration. *Agricultural and Forest Meteorology*, *113*(1–4), 21–37. https://doi.org/10.1016/S0168-1923(02)00100-4

Davidson, S. J., Santos, M. J., Sloan, V. L., Reuss-Schmidt, K., Phoenix, G. K., Oechel, W. C., and Zona, D. (2017). Upscaling CH4 fluxes using high-resolution imagery in Arctic Tundra ecosystems. *Remote Sensing*, *9*(12). https://doi.org/10.3390/rs9121227

Dayuf Jusuf, M., Danoedoro, P., Muljo Sukojo, B., and Hartono. (2017). Model of Peatland Vegetation Species using HyMap Image and Machine Learning. *IOP Conference Series: Earth and Environmental Science*, *98*(1). https://doi.org/10.1088/1755-1315/98/1/012050

de Sousa, C., Fatoyinbo, L., Neigh, C., Boucka, F., Angoue, V., and Larsen, T. (2020). Cloud-computing and machine learning in support of country-level land cover and ecosystem extent mapping in Liberia and Gabon. *PLoS ONE*, *15*(1). https://doi.org/10.1371/journal.pone.0227438

Desai, A. R., Xu, K., Tian, H., Weishampel, P., Thom, J., Baumann, D., Andrews, A. E., Cook, B. D., King, J. Y., and Kolka, R. (2015). Landscape-level terrestrial methane flux observed from a very tall tower. *Agricultural and Forest Meteorology*, *201*, 61–75. https://doi.org/10.1016/j.agrformet.2014.10.017

Dondini, M., Richards, M. I. A., Pogson, M., McCalmont, J., Drewer, J., Marshall, R., Morrison, R., Yamulki, S., Harris, Z. M., Alberti, G., Siebicke, L., Taylor, G., Perks, M., Finch, J., McNamara, N. P., Smith, J. U., and Smith, P. (2016). Simulation of greenhouse gases following land-use change to bioenergy crops using the ECOSSE model: a comparison between site measurements and model predictions. *GCB Bioenergy*, *8*(5), 925–940. https://doi.org/10.1111/gcbb.12298

Dooling, G. P. (2014). *The effects of peatland restoration on methane and carbon dioxide fluxes*.

Drollinger, S., Maier, A., and Glatzel, S. (2019). Interannual and seasonal variability in carbon dioxide and methane fluxes of a pine peat bog in the Eastern Alps, Austria. *Agricultural and Forest Meteorology*, *275*(September 2018), 69–78. https://doi.org/10.1016/j.agrformet.2019.05.015

Erinjery, J. J., Singh, M., and Kent, R. (2018). Mapping and assessment of vegetation types in the tropical rainforests of the Western Ghats using multispectral Sentinel-2 and SAR Sentinel-1 satellite imagery. *Remote Sensing of Environment*, *216*, 345–354. https://doi.org/10.1016/j.rse.2018.07.006

Erudel, T., Fabre, S., Houet, T., Mazier, F., and Briottet, X. (2017). Criteria Comparison for Classifying Peatland Vegetation Types Using In Situ Hyperspectral Measurements. *Remote Sensing*, *9*(7), 748. https://doi.org/10.3390/rs9070748

Eugster, W. (2012). Eddy Covariance. In *Eddy Covariance* (Issue January). https://doi.org/10.1007/978-94-007-2351-1

Evans, C. D., Peacock, M., Baird, A. J., Artz, R. R. E., Burden, A., Callaghan, N., Chapman, P. J., Cooper, H. M., Coyle, M., Craig, E., Cumming, A., Dixon, S., Gauci, V., Grayson, R. P., Helfter, C., Heppell, C. M., Holden, J., Jones, D. L., Kaduk, J., … Morrison, R. (2021). Overriding water table control on managed peatland greenhouse gas emissions. *Nature*, *November 2020*. https://doi.org/10.1038/s41586-021-03523-1

Evans, C. D., Peacock, M., Baird, A. J., Artz, R. R. E., Burden, A., Callaghan, N., Chapman, P. J., Cooper, H. M., Coyle, M., Craig, E., Cumming, A., Dixon, S., Gauci, V., Grayson, R. P., Helfter, C., Heppell, C. M., Holden, J., Jones, D. L., Kaduk, J., … Morrison, R. (2021). Overriding water table control on managed peatland greenhouse gas emissions. *Nature*, *593*(7860), 548–552. https://doi.org/10.1038/s41586-021-03523-1

Evans, C., Morrison, R., Burden, A., Williamson, J., Baird, A., Brown, E., Callaghan, N., Chapman, P., Cumming, A., Dean, H., Dixon, S., Dooling, G., Evans, J., Gauci, V., Grayson, R., Haddaway, N., He, Y., Heppel, K., Holden, J., … Worrall, F. (2016). *Lowland peat systems in England and Wales - evaluating greenhouse gas fluxes and carbon balances (DEFRA Project SP1210)*. 1–170.

Falge, E., Baldocchi, D., Olson, R., Anthoni, P., Aubinet, M., Bernhofer, C., Burba, G., Ceulemans, R., Clement, R., Dolman, H., Granier, A., Gross, P., Grünwald, T., Hollinger, D., Jensen, N. O., Katul, G., Keronen, P., Kowalski, A., Lai, C. T., … Wofsy, S. (2001). Gap filling strategies for defensible annual sums of net ecosystem exchange. *Agricultural and Forest Meteorology*, *107*(1), 43–69. https://doi.org/10.1016/S0168-1923(00)00225-2

Fernandez, F., Connolly, K., Crowley, W., Denyer, J., Duff, K., and Smith, G. (2014). *Raised Bog Monitoring and Assessment Survey* (Issue 81). Irish Wildlife Manuals.

Fernandez Valverde, F., Connolly, K., Crowley, W., Denyer, J., Duff, K., and Smith, G. (2014). Raised Bog Monitoring and Assessment Survey 2013. *Irish Wildlife Manuals No. 81*, *81*, 198.

Fluet-Chouinard, E., Stocker, B. D., Zhang, Z., Malhotra, A., Melton, J. R., Poulter, B., Kaplan, J. O., Goldewijk, K. K., Siebert, S., Minayeva, T., Hugelius, G., Joosten, H., Barthelmes, A., Prigent, C., Aires, F., Hoyt, A. M., Davidson, N., Finlayson, C. M., Lehner, B., … McIntyre, P. B. (2023). Extensive global wetland loss over the past three centuries. *Nature*, *614*(7947), 281–286. https://doi.org/10.1038/s41586-022-05572-6

Foken, T., Mathias, G., Mauder, M., Mahrt, L., Amiro, B., and Munger, W. (2004). *Chapter 9 POST-FIELD DATA QUALITY CONTROL*. *1988*, 181–208.

Foody, G. M. (2020). Explaining the unsuitability of the kappa coefficient in the assessment and comparison of the accuracy of thematic maps obtained by image classification. *Remote Sensing of Environment*, *239*. https://doi.org/10.1016/j.rse.2019.111630

Forbrich, I., Kutzbach, L., Wille, C., Becker, T., Wu, J., and Wilmking, M. (2011). Cross-evaluation of measurements of peatland methane emissions on microform and ecosystem scales using high-resolution landcover classification and source weight modelling. *Agricultural and Forest Meteorology*, *151*(7), 864–874. https://doi.org/10.1016/j.agrformet.2011.02.006

Fortuniak, K., Pawlak, W., Siedlecki, M., Chambers, S., and Bednorz, L. (2021). Temperate mire fluctuations from carbon sink to carbon source following changes in water table. *Science of the Total Environment*, *756*. https://doi.org/10.1016/j.scitotenv.2020.144071

Fossitt, J. A. (2000). A guide to habitats in Ireland. *Heritage Council. NPWS*, 115.

Frolking, S., Talbot, J., Jones, M. C., Treat, C. C., Kauffman, J. B., Tuittila, E., and Roulet, N. (2011). *Peatlands in the Earth ' s 21st century climate system*. *September*. https://doi.org/10.1139/a11-014

Gan, R., Zhang, L., Yang, Y., Wang, E., Woodgate, W., Zhang, Y., Haverd, V., Kong, D., Fischer, T., Chiew, F., and Yu, Q. (2021). Estimating ecosystem maximum light use efficiency based on the water use efficiency principle. *Environmental Research Letters*, *16*(10). https://doi.org/10.1088/1748-9326/ac263b

Gao B C. (1996). A normalized difference water index for remote sensing of vegetation liquid water from space Bo-Cai Gao Joint Center for Earth System Sciences Code 913, NASA Goddard Space Flight Center, Greenbelt, MD 20771. *Remote Sensing of Environment*, *58*(3), 257–266.

Gao, X., Huete, A. R., Ni, W., and Miura, T. (1993). *Optical – Biophysical Relationships of Vegetation Spectra without Background Contamination*. *4257*(00).

Gatis, N., Luscombe, D. J., Carless, D., Parry, L. E., Fyfe, R. M., Harrod, T. R., Brazier, R. E., and Anderson, K. (2019). Mapping upland peat depth using airborne radiometric and lidar survey data. *Geoderma*, *335*(September), 78–87. https://doi.org/10.1016/j.geoderma.2018.07.041

Gilabert, M. A., Sánchez-Ruiz, S., and Moreno, álvaro. (2017). Annual gross primary production from vegetation indices: A theoretically sound approach. *Remote Sensing*, *9*(3). https://doi.org/10.3390/rs9030193

Goerner, A., Reichstein, M., Tomelleri, E., Hanan, N., Rambal, S., Papale, D., Dragoni, D., and Schmullius, C. (2011). Remote sensing of ecosystem light use efficiency with MODIS-based PRI. *Biogeosciences*, *8*(1), 189–202. https://doi.org/10.5194/bg-8-189-2011

Gorham, E. (1991). Northern peatlands: role in the carbon cycle and probable responses to climatic warming. *Ecological Applications*, *1*(2), 182–195. https://doi.org/10.2307/1941811

Günther, A., Barthelmes, A., Huth, V., Joosten, H., Jurasinski, G., Koebsch, F., and Couwenberg, J. (2020). Prompt rewetting of drained peatlands reduces climate warming despite methane emissions. *Nature Communications*, *11*(1). https://doi.org/10.1038/s41467-020-15499-z

Hammond, R. F. (1981). The Peatlands of Ireland. In *Soil Survey Bulletin No. 35* (2nd ed.). An Foras Taluntais.

Harris, A. (2008). Spectral reflectance and photosynthetic properties of Sphagnum mosses exposed to progressive drought. *Ecohydrology*, *1*(1), 35–42. https://doi.org/10.1002/eco.5

Harris, A., and Bryant, R. G. (2009). A multi-scale remote sensing approach for monitoring northern peatland hydrology: Present possibilities and future challenges. *Journal of Environmental Management*, *90*(7), 2178–2188. https://doi.org/10.1016/j.jenvman.2007.06.025

Heinsch, F. A., Zhao, M., Running, S. W., Kimball, J. S., Nemani, R. R., Davis, K. J., Bolstad, P. v, Cook, B. D., Desai, A. R., Ricciuto, D. M., Law, B. E., Oechel, W. C., Kwon, H., Luo, H., Wofsy, S. C., Dunn, A. L., Munger, J. W., Baldocchi, D. D., Xu, L., … Flanagan, L. B. (2006). Evaluation of remote sensing based terrestrial productivity from MODIS using regional tower eddy flux network observations. *IEEE Transactions on Geoscience and Remote Sensing*, *44*(7), 1908–1923. https://doi.org/10.1109/TGRS.2005.853936

Helbig, M., Živković, T., Alekseychik, P., Aurela, M., Euskirchen, E. S., Flanagan, L. B., Griffis, T. J., Hanson, P. J., Hattakka, J., Helfter, C., Hirano, T., Humphreys, E. R., Kiely, G., Kolka, R. K., Laurila, T., Leahy, P. G., and Lohila, A. (2022). *Warming response of peatland CO2 sink is sensitive to seasonality in warming trends*. *12*(August). https://doi.org/10.1038/s41558-022-01428-z

Helfter, C., Campbell, C., Dinsmore, K. J., Drewer, J., Coyle, M., Anderson, M., Skiba, U., Nemitz, E., Billett, M. F., and Sutton, M. A. (2015). Drivers of long-term variability in CO2 net ecosystem exchange in a temperate peatland. *Biogeosciences*, *12*(6), 1799–1811. https://doi.org/10.5194/bg-12-1799-2015

Helfter, C., Gondwe, M., Murray-Hudson, M., Makati, A., Lunt, M. F., Palmer, P. I., and Skiba, U. (2022). Phenology is the dominant control of methane emissions in a tropical non-forested wetland. *Nature Communications*, *13*(1). https://doi.org/10.1038/s41467-021-27786-4

Hilker, T., Coops, N. C., Hall, F. G., Andrew Black, T., Chen, B., Krishnan, P., Wulder, M. A., Seilers, P. J., Middleton, E. M., and Huemmrich, K. F. (2008). A modeling approach for upscaling gross ecosystem production to the landscape scale using remote sensing data. *Journal of Geophysical Research: Biogeosciences*, *113*(3), 1–15. https://doi.org/10.1029/2007JG000666

Hilker, T., Coops, N. C., Wulder, M. A., Black, T. A., and Guy, R. D. (2008). The use of remote sensing in light use efficiency based models of gross primary production: A review of current status and future requirements. *Science of the Total Environment*, *404*(2–3), 411–423. https://doi.org/10.1016/j.scitotenv.2007.11.007

Hiraishi, T., Krug, T., Tanabe, K., Srivastava, N., Jamsranjav, B., Fukuda, M., and Troxler, T. G. (2014). 2013 Supplement to the 2006 IPCC Guidelines for National Greenhouse Gas Inventories: Wetlands. Chapter 4: Coastal Wetlands.Hiraishi, T., Krug, T., Tanabe, K., Srivastava, N., Baasansuren, J., Fukuda, M. and Troxler, T.G. (eds). Published: IPCC, Switzerlan. In *Comprehensive OrganicSynthesis*.

Huang, X., Xiao, J., and Ma, M. (2019). Evaluating the performance of satellite-derived vegetation indices for estimating gross primary productivity using FLUXNET observations across the globe. *Remote Sensing*, *11*(15). https://doi.org/10.3390/rs11151823

Huete, A. R., Liu, H., and van Leeuwen, W. J. D. (n.d.). *The Use of Vegetation Indices in Forested Regions: Issues of Linearity and Saturation*.

Järvi, L., Rannik, U., Kokkonen, T. V., Kurppa, M., Karppinen, A., Kouznetsov, R. D., Rantala, P., Vesala, T., and Wood, C. R. (2018). Uncertainty of eddy covariance flux measurements over an urban area based on two towers. *Atmospheric Measurement Techniques*, *11*(10), 5421–5438. https://doi.org/10.5194/amt-11-5421-2018

Jensen, L. S., Mueller, T., Tate, K. R., Ross, D. J., Magid, J., and Nielsen, N. E. (1996). Soil surface CO2 flux as an index of soil respiration in situ: A comparison of two chamber methods. *Soil Biology and Biochemistry*, *28*(10–11), 1297–1306. https://doi.org/10.1016/S0038-0717(96)00136-8

Joiner, J., Yoshida, Y., Zhang, Y., Duveiller, G., Jung, M., Lyapustin, A., Wang, Y., and Tucker, C. J. (2018). Estimation of terrestrial global gross primary production (GPP) with satellite data-driven models and eddy covariance flux data. *Remote Sensing*, *10*(9), 1–38. https://doi.org/10.3390/rs10091346

Joosten, H., and Clarke, D. (2002). Wise Use of Mires and Peatlands. In *International Mire Conservation Group and International Peat Society, Helsinki* (Issue June). https://doi.org/10.1016/s0925-8574(98)00046-9

Junttila, S., Kelly, J., Kljun, N., Aurela, M., Klemedtsson, L., Lohila, A., Nilsson, M. B., Rinne, J., Tuittila, E. S., Vestin, P., Weslien, P., and Eklundh, L. (2021). Upscaling northern peatland co2 fluxes using satellite remote sensing data. *Remote Sensing*, *13*(4), 1–23. https://doi.org/10.3390/rs13040818

Jurasinski, G., Ahmad, S., Anadon-Rosell, A., Berendt, J., Beyer, F., Bill, R., Blume-Werry, G., Couwenberg, J., Günther, A., Joosten, H., Koebsch, F., Köhn, D., Koldrack, N., Kreyling, J., Leinweber, P., Lennartz, B., Liu, H., Michaelis, D., Mrotzek, A., … Wrage-Mönnig, N. (2020). From Understanding to Sustainable Use of Peatlands: The WETSCAPES Approach. *Soil Systems*, *4*(1), 14. https://doi.org/10.3390/soilsystems4010014

Kang, X., Yan, L., Zhang, X., Li, Y., Tian, D., Peng, C., Wu, H., Wang, J., and Zhong, L. (2018). Modeling gross primary production of a typical Coastal Wetland in China using MODIS time series and CO2 Eddy Flux Tower Data. *Remote Sensing*, *10*(5). https://doi.org/10.3390/rs10050708

Kiely, G., Leahy, P., Lewis, C., Sottocornola, M., Laine, A., and Koehler, A.-K. (2018). *GHG Fluxes from Terrestrial Ecosystems in Ireland* (Issue 227). www.epa.ie

Kiely, G., Leahy, P., Sottocornola, M., and Saunders, M. (2017). *Peatland Carbon Fluxes and the Lullymore Measurement Site*. *February*.

Kross, A., Seaquist, J. W., and Roulet, N. T. (2016). Light use efficiency of peatlands: Variability and suitability for modeling ecosystem production. *Remote Sensing of Environment*, *183*, 239–249. https://doi.org/10.1016/j.rse.2016.05.004

Lafleur, P. M., Roulet, N. T., Bubier, J. L., Frolking, S., and Moore, T. R. (2003). Interannual variability in the peatland-atmosphere carbon dioxide exchange at an ombrotrophic bog. *Global Biogeochemical Cycles*, *17*(2). https://doi.org/10.1029/2002gb001983

LAI, D. Y. F. (2009). Methane Dynamics in Northern Peatlands: A Review. *Pedosphere*, *19*(4), 409–421. https://doi.org/10.1016/S1002-0160(09)00003-4

Lai, D. Y. F., Moore, T. R., and Roulet, N. T. (2014). Spatial and temporal variations of methane flux measured by autochambers in a temperate ombrotrophic peatland. *Journal of Geophysical Research: Biogeosciences*, *119*(5), 864–880. https://doi.org/10.1002/2013JG002410

Laine, A., Sottocornola, M., Kiely, G., Byrne, K. A., Wilson, D., and Tuittila, E. S. (2006). Estimating net ecosystem exchange in a patterned ecosystem: Example from blanket bog. *Agricultural and Forest Meteorology*, *138*(1–4), 231–243. https://doi.org/10.1016/j.agrformet.2006.05.005

Laine, A., Wilson, D., Kiely, G., and Byrne, K. A. (2007). Methane flux dynamics in an Irish lowland blanket bog. *Plant and Soil*, *299*(1–2), 181–193. https://doi.org/10.1007/s11104-007-9374-6

Lanigan, G. J., Donnellan, T., Hanrahan, K., Paul, C., Shalloo, L., Krol, D., Forrestal, P., Farrelly, N., O'brien, D., Ryan, M., Murphy, P., Caslin, B., Spink, J., Finnan, J., Boland, A., Upton, J., and Richards, K. (2018). *An Analysis of Abatement Potential of Greenhouse Gas Emissions in Irish Agriculture 2021-2030 Prepared by the Teagasc Greenhouse Gas Working Group Authors*. *March 2019*, 1–80.

Lee, S. C., Christen, A., Black, A. T., Johnson, M. S., Jassal, R. S., Ketler, R., Nesic, Z., and Merkens, M. (2017). Annual greenhouse gas budget for a bog ecosystem undergoing restoration by rewetting. *Biogeosciences*, *14*(11), 2799–2814. https://doi.org/10.5194/bg-14-2799-2017

Lees, K. J., Artz, R. R. E., Khomik, M., Clark, J. M., Ritson, J., Hancock, M. H., Cowie, N. R., and Quaife, T. (2020). Using Spectral Indices to Estimate Water Content and GPP in Sphagnum Moss and Other Peatland Vegetation. *IEEE Transactions on Geoscience and Remote Sensing*, 1–11. https://doi.org/10.1109/tgrs.2019.2961479

Lees, K. J., Clark, J. M., Quaife, T., Khomik, M., and Artz, R. R. E. (2019). Changes in carbon flux and spectral reflectance of Sphagnum mosses as a result of simulated drought. *Ecohydrology*, *12*(6). https://doi.org/10.1002/eco.2123

Lees, K. J., Lees, K. J., Artz, R. R. E., Khomik, M., Clark, J. M., Ritson, J., Hancock, M. H., Cowie, N. R., and Quaife, T. (2020). Using spectral indices to estimate water content and GPP in sphagnum moss and other peatland vegetation. *IEEE Transactions on Geoscience and Remote Sensing*, *58*(7), 4547–4557. https://doi.org/10.1109/TGRS.2019.2961479

Lees, K. J., Quaife, T., Artz, R. R. E., Khomik, M., and Clark, J. M. (2018). Potential for using remote sensing to estimate carbon fluxes across northern peatlands – A review. *Science of the Total Environment*, *615*, 857–874. https://doi.org/10.1016/j.scitotenv.2017.09.103

Lees, K. J., Quaife, T., Artz, R. R. E., Khomik, M., Sottocornola, M., Kiely, G., Hambley, G., Hill, T., Saunders, M., Cowie, N. R., Ritson, J., and Clark, J. M. (2019). A model of gross primary productivity based on satellite data suggests formerly afforested peatlands undergoing restoration regain full photosynthesis capacity after five to ten years. *Journal of Environmental Management*, *246*(July 2018), 594–604. https://doi.org/10.1016/j.jenvman.2019.03.040

Leifeld, J., and Menichetti, L. (2018). The underappreciated potential of peatlands in global climate change mitigation strategies /704/47/4113 /704/106/47 article. *Nature Communications*, *9*(1). https://doi.org/10.1038/s41467-018-03406-6

Levy, P., Drewer, J., Jammet, M., Leeson, S., Friborg, T., Skiba, U., and Oijen, M. van. (2020). Inference of spatial heterogeneity in surface fluxes from eddy covariance data: A case study from a subarctic mire ecosystem. *Agricultural and Forest Meteorology*, *280*. https://doi.org/10.1016/j.agrformet.2019.107783

Limpens, J., Berendse, F., Blodau, C., Canadell, J. G., Freeman, C., Holden, J., Roulet, N., Rydin, H., and Schaepman-Strub, G. (2008). Peatlands and the carbon cycle: From local processes to global implications - A synthesis. *Biogeosciences*, *5*(5), 1475–1491. https://doi.org/10.5194/bg-5-1475-2008

Lin, S., Li, J., Liu, Q., Li, L., Zhao, J., and Yu, W. (2019). Evaluating the effectiveness of using vegetation indices based on red-edge reflectance from Sentinel-2 to estimate gross primary productivity. *Remote Sensing*, *11*(11). https://doi.org/10.3390/rs11111303

Liu, H. Q., and Huete, A. (1995). A Feedback Based Modification of the NDVI to Minimize Canopy Background and Atmospheric Noise. In *IEEE TRANSACTIONS ON GEOSCIENCE AND REMOTE SENSING* (Vol. 33, Issue 2).

Loisel, J., Gallego-Sala, A. V., Amesbury, M. J., Magnan, G., Anshari, G., Beilman, D. W., Benavides, J. C., Blewett, J., Camill, P., Charman, D. J., Chawchai, S., Hedgpeth, A., Kleinen, T., Korhola, A., Large, D., Mansilla, C. A., Müller, J., van Bellen, S., West, J. B., … Wu, J. (2021). Expert assessment of future vulnerability of the global peatland carbon sink. *Nature Climate Change*, *11*(1), 70–77. https://doi.org/10.1038/s41558-020-00944-0

Lund, M., Christensen, T. R., Lindroth, A., and Schubert, P. (2012). Effects of drought conditions on the carbon dioxide dynamics in a temperate peatland. *Environmental Research Letters*, *7*(4). https://doi.org/10.1088/1748-9326/7/4/045704

Mackin, F., Barr, A., Rath, P., Eakin, M., Ryan, J., Jeffrey, R., Fernandez Valverde, F., and Valverde, F. (2017). Best practice in raised bog restoration in Ireland. *Irish Wildlife Manuals*, *99*(99).

Madugundu, R., Al-Gaadi, K. A., Tola, E. K., Kayad, A. G., and Jha, C. S. (2017). Estimation of gross primary production of irrigated maize using Landsat-8 imagery and Eddy Covariance data. *Saudi Journal of Biological Sciences*, *24*(2), 410–420. https://doi.org/10.1016/j.sjbs.2016.10.003

Mahdavi, S., Salehi, B., Granger, J., Amani, M., Brisco, B., and Huang, W. (2018). Remote sensing for wetland classification: a comprehensive review. In *GIScience and Remote Sensing* (Vol. 55, Issue 5, pp. 623–658). Taylor and Francis Inc. https://doi.org/10.1080/15481603.2017.1419602

Marcisz, K., Kołaczek, P., Gałka, M., Diaconu, A. C., and Lamentowicz, M. (2020). Exceptional hydrological stability of a Sphagnum-dominated peatland over the late Holocene. *Quaternary Science Reviews*, *231*. https://doi.org/10.1016/j.quascirev.2020.106180

Matthes, J. H., Sturtevant, C., Verfaillie, J., Knox, S., and Baldocchi, D. (2014). Parsing the variability in CH4 flux at a spatially heterogeneous wetland: Integrating multiple eddy covariance towers with high-resolution flux footprint analysis. *Journal of Geophysical Research: Biogeosciences*, *119*(7), 1322–1339. https://doi.org/10.1002/2014JG002642

Mauder M., F. T. (2011). *Documentation and Instruction Manual of the Eddy Covariance Software Abt . Mikrometeorologie Documentation and Instruction Manual of the Eddy-Covariance Software Package Matthias Mauder Thomas Foken Arbeitsergebnisse*. *May 2014*. https://doi.org/10.5194/bg-5-451-2008

McFeeters, S. K. (1996). The use of the Normalized Difference Water Index (NDWI) in the delineation of open water features. *International Journal of Remote Sensing*, *17*(7), 1425–1432. https://doi.org/10.1080/01431169608948714

McVeigh, P., Sottocornola, M., Foley, N., Leahy, P., and Kiely, G. (2014). Meteorological and functional response partitioning to explain interannual variability of CO2 exchange at an Irish Atlantic blanket bog. *Agricultural and Forest Meteorology*, *194*, 8–19. https://doi.org/10.1016/j.agrformet.2014.01.017

Melack, J. M., and Hess, L. L. (2023). Areal extent of vegetative cover: A challenge to regional upscaling of methane emissions. In *Aquatic Botany* (Vol. 184). Elsevier B.V. https://doi.org/10.1016/j.aquabot.2022.103592

Mikhaylov, O. A., Zagirova, S. v, and Miglovets, M. N. (2019). Seasonal and inter-annual variability of carbon dioxide exchange at a boreal peatland in north-east European Russia. *Mires and Peat*, *24*, 1–16. https://doi.org/10.19189/MaP.2017.OMB.293

Minasny, B., Berglund, Ö., Connolly, J., Hedley, C., de Vries, F., Gimona, A., Kempen, B., Kidd, D., Lilja, H., Malone, B., McBratney, A., Roudier, P., O'Rourke, S., Rudiyanto, Padarian, J., Poggio, L., ten Caten, A., Thompson, D., Tuve, C., and Widyatmanti, W. (2019). Digital mapping of peatlands – A critical review. *Earth-Science Reviews*. https://doi.org/10.1016/j.earscirev.2019.05.014

Minkkinen, K., Ojanen, P., Penttilä, T., Aurela, M., Laurila, T., Tuovinen, J. P., and Lohila, A. (2018). Persistent carbon sink at a boreal drained bog forest. *Biogeosciences*, *15*(11), 3603–3624. https://doi.org/10.5194/bg-15-3603-2018

Moffat, A. M., Papale, D., Reichstein, M., Hollinger, D. Y., Richardson, A. D., Barr, A. G., Beckstein, C., Braswell, B. H., Churkina, G., Desai, A. R., Falge, E., Gove, J. H., Heimann, M., Hui, D., Jarvis, A. J., Kattge, J., Noormets, A., and Stauch, V. J. (2007).

Comprehensive comparison of gap-filling techniques for eddy covariance net carbon fluxes. *Agricultural and Forest Meteorology*, *147*(3–4), 209–232. https://doi.org/10.1016/j.agrformet.2007.08.011

Morin, T. H., Bohrer, G., Stefanik, K. C., Rey-Sanchez, A. C., Matheny, A. M., and Mitsch, W. J. (2017). Combining eddy-covariance and chamber measurements to determine the methane budget from a small, heterogeneous urban floodplain wetland park. *Agricultural and Forest Meteorology*, *237–238*, 160–170. https://doi.org/10.1016/j.agrformet.2017.01.022

Morozumi, T., Shingubara, R., Suzuki, R., Kobayashi, H., Tei, S., Takano, S., Fan, R., Liang, M., Maximov, T. C., and Sugimoto, A. (2019). Estimating methane emissions using vegetation mapping in the taiga–tundra boundary of a north-eastern Siberian lowland. *Tellus, Series B: Chemical and Physical Meteorology*, *71*(1), 1–17. https://doi.org/10.1080/16000889.2019.1581004

Myklebust, M. C., Hipps, L. E., and Ryel, R. J. (2008). Comparison of eddy covariance, chamber, and gradient methods of measuring soil CO2 efflux in an annual semi-arid grass, Bromus tectorum. *Agricultural and Forest Meteorology*, *148*(11), 1894–1907. https://doi.org/10.1016/j.agrformet.2008.06.016

Noi Phan, T., Kuch, V., and Lehnert, L. W. (2020). Land cover classification using google earth engine and random forest classifier-the role of image composition. *Remote Sensing*, *12*(15). https://doi.org/10.3390/RS12152411

Novick, K. A., Walker, J., Chan, W. S., Schmidt, A., Sobek, C., and Vose, J. M. (2013). Eddy covariance measurements with a new fast-response, enclosed-path analyzer: Spectral characteristics and cross-system comparisons. *Agricultural and Forest Meteorology*, *181*, 17–32. https://doi.org/10.1016/j.agrformet.2013.06.020

NPWS. (2014). *National Raised Bog SAC Management Plan Draft*. *January*.

Nugent, K. A., Strachan, I. B., Strack, M., Roulet, N. T., and Rochefort, L. (2018). Multi-year net ecosystem carbon balance of a restored peatland reveals a return to carbon sink. *Global Change Biology*, *24*(12), 5751–5768. https://doi.org/10.1111/gcb.14449

Oertel, C., Matschullat, J., Zurba, K., Zimmermann, F., and Erasmi, S. (2016). Greenhouse gas emissions from soils—A review. *Chemie Der Erde*, *76*(3), 327–352. https://doi.org/10.1016/j.chemer.2016.04.002

Paço, T. A., Ferreira, M. I., and Conceição, N. (2006). Peach orchard evapotranspiration in a sandy soil: Comparison between eddy covariance measurements and estimates by the FAO 56 approach. *Agricultural Water Management*, *85*(3), 305–313. https://doi.org/10.1016/j.agwat.2006.05.014

Page, S. E., and Baird, A. J. (2016). Peatlands and Global Change: Response and Resilience. *Annual Review of Environment and Resources*, *41*(1), 35–57. https://doi.org/10.1146/annurev-environ-110615-085520

Parish, F. Sirin, A. Charman, D. Joosten, H. Minayeva, T. Silvius, M. and Stringer, L. (2008). *Assessment on Peatlands, Biodiversity and Climate Change: Main Report.*

Global Environment Centre, Kuala Lumpur and Wetlands International, Wageningen.

Pei, Y., Dong, J., Zhang, Y., Yuan, W., Doughty, R., Yang, J., Zhou, D., Zhang, L., and Xiao, X. (2022). Evolution of light use efficiency models: Improvement, uncertainties, and implications. *Agricultural and Forest Meteorology*, *317*(March), 108905. https://doi.org/10.1016/j.agrformet.2022.108905

Peng, D., Zhang, H., Yu, L., Wu, M., Wang, F., Huang, W., Liu, L., Sun, R., Li, C., Wang, D., and Xu, F. (2018). Assessing spectral indices to estimate the fraction of photosynthetically active radiation absorbed by the vegetation canopy. *International Journal of Remote Sensing*, *39*(22), 8022–8040. https://doi.org/10.1080/01431161.2018.1479795

Peters, W., Bastos, A., Ciais, P., and Vermeulen, A. (2020). A historical, geographical and ecological perspective on the 2018 European summer drought: Perspective on the 2018 European drought. In *Philosophical Transactions of the Royal Society B: Biological Sciences* (Vol. 375, Issue 1810). Royal Society Publishing. https://doi.org/10.1098/rstb.2019.0505

Petrescu, A. M. R., Lohila, A., Tuovinen, J. P., Baldocchi, D. D., Desai, A. R., Roulet, N. T., Vesala, T., Dolman, A. J., Oechel, W. C., Marcolla, B., Friborg, T., Rinne, J., Matthes, J. H., Merbold, L., Meijide, A., Kiely, G., Sottocornola, M., Sachs, T., Zona, D., … Cescatti, A. (2015). The uncertain climate footprint of wetlands under human pressure. *Proceedings of the National Academy of Sciences of the United States of America*, *112*(15), 4594–4599. https://doi.org/10.1073/pnas.1416267112

Pirk, N., Mastepanov, M., Parmentier, F. J. W., Lund, M., Crill, P., and R. Christensen, T. (2016). Calculations of automatic chamber flux measurements of methane and carbon dioxide using short time series of concentrations. *Biogeosciences*, *13*(4), 903–912. https://doi.org/10.5194/bg-13-903-2016

Poyda, A., Reinsch, T., Skinner, R. H., Kluß, C., Loges, R., and Taube, F. (2017). Comparing chamber and eddy covariance based net ecosystem CO2 exchange of fen soils. *Zeitschrift Fur Pflanzenernahrung Und Bodenkunde*, *180*(2), 252–266. https://doi.org/10.1002/jpln.201600447

Pumpanen, J., Kolari, P., Ilvesniemi, H., Minkkinen, K., Vesala, T., Niinistö, S., Lohila, A., Larmola, T., Morero, M., Pihlatie, M., Janssens, I., Yuste, J. C., Grünzweig, J. M., Reth, S., Subke, J. A., Savage, K., Kutsch, W., Østreng, G., Ziegler, W., … Hari, P. (2004). Comparison of different chamber techniques for measuring soil CO 2 efflux. *Agricultural and Forest Meteorology*, *123*(3–4), 159–176. https://doi.org/10.1016/j.agrformet.2003.12.001

Radu, D. D., and Duval, T. P. (2018). Precipitation frequency alters peatland ecosystem structure and CO2 exchange: Contrasting effects on moss, sedge, and shrub communities. *Global Change Biology*, *24*(5), 2051–2065. https://doi.org/10.1111/gcb.14057

Räsänen, A., Juutinen, S., Tuittila, E. S., Aurela, M., and Virtanen, T. (2019). Comparing ultra-high spatial resolution remote-sensing methods in mapping peatland vegetation. *Journal of Vegetation Science*, *30*(5), 1016–1026. https://doi.org/10.1111/jvs.12769

Räsänen, A., Manninen, T., Korkiakoski, M., Lohila, A., and Virtanen, T. (2021). Predicting catchment-scale methane fluxes with multi-source remote sensing. *Landscape Ecology*, *36*(4), 1177–1195. https://doi.org/10.1007/s10980-021-01194-x

Räsänen, A., and Virtanen, T. (2019). Data and resolution requirements in mapping vegetation in spatially heterogeneous landscapes. *Remote Sensing of Environment*, *230*. https://doi.org/10.1016/j.rse.2019.05.026

Rastogi, A., Bandopadhyay, S., Stróżecki, M., and Juszczak, R. (2018). Monitoring the Impact of Environmental Manipulation on Peatland Surface by Simple Remote Sensing Indices. *ITM Web of Conferences*, *23*, 30. https://doi.org/10.1051/itmconf/20182300030

Rebmann, C., Aubinet, M., Schmid, H., Arriga, N., Aurela, M., Burba, G., Clement, R., De Ligne, A., Fratini, G., Gielen, B., Grace, J., Graf, A., Gross, P., Haapanala, S., Herbst, M., Hörtnagl, L., Ibrom, A., Joly, L., Kljun, N., … Franz, D. (2018). ICOS eddy covariance flux-station site setup: A review. *International Agrophysics*, *32*(4), 471–494. https://doi.org/10.1515/intag-2017-0044

Regan, A. S., Swenson, M., Connor, M. O., and Gill, L. (2020). Ecohydrology , Greenhouse Gas Dynamics and Restoration Guidelines for Degraded Raised Bogs. In *EPA Report* (Issue 342).

Regan, S., Flynn, R., Gill, L., Naughton, O., and Johnston, P. (2019). Impacts of Groundwater Drainage on Peatland Subsidence and Its Ecological Implications on an Atlantic Raised Bog. *Water Resources Research*, *55*(7), 6153–6168. https://doi.org/10.1029/2019WR024937

Reichstein, M., Falge, E., Baldocchi, D., Papale, D., Aubinet, M., Berbigier, P., Bernhofer, C., Buchmann, N., Gilmanov, T., Granier, A., Grünwald, T., Havránková, K., Ilvesniemi, H., Janous, D., Knohl, A., Laurila, T., Lohila, A., Loustau, D., Matteucci, G., … Valentini, R. (2005). On the separation of net ecosystem exchange into assimilation and ecosystem respiration: Review and improved algorithm. In *Global Change Biology* (Vol. 11, Issue 9, pp. 1424–1439). https://doi.org/10.1111/j.1365-2486.2005.001002.x

Renou, F., Egan, T., and Wilson, D. (2006). Tomorrow's landscapes: Studies in the after-uses of industrial cutaway peatlands in Ireland. *Suo*, *57*(4), 97–107.

Renou-wilson, F. (2018). Peatlands. In R. Creamer and L. O'Sullivan (Eds.), *The Soils of Ireland* (pp. 141–152). Springer International.

Renou-Wilson, F., Byrne, K. A., Flynn, R., Premrov, A., Riondato, E., Saunders, M., Walz, K., and Wilson, D. (2022). *Peatland Properties Influencing Greenhouse Gas Emissions and Removal* (Issue 401). www.epa.ie

Renou-Wilson, F., Moser, G., Fallon, D., Farrell, C. A., Müller, C., and Wilson, D. (2019). Rewetting degraded peatlands for climate and biodiversity benefits: Results from two raised bogs. *Ecological Engineering*, *127*, 547–560. https://doi.org/10.1016/j.ecoleng.2018.02.014

Renou-Wilson, F., and Wilson, D. (2018). *EPA - Vulnerability Assessment of Peatlands: Exploration of Impacts and Adaptation Options in Relation to Climate Change and Extreme Events (VAPOR)* (Issue 250).

Renou-Wilson, F., Wilson, D., Rigney, C., Byrne, K., Farrell, C., and Müller, C. (2018). *EPA - Network Monitoring Rewetted and Restored Peatlands/Organic Soils for Climate and Biodiversity Benefits (NEROS)* (Issue Report No.236).

Rinne, J., Tuovinen, J., Klemedtsson, L., Aurela, M., Holst, J., Lohila, A., Weslien, P., Vestin, P., Ł, P., Peichl, M., Tuittila, E., Heiskanen, L., Laurila, T., Li, X., Alekseychik, P., Mammarella, I., Ström, L., Crill, P., and Nilsson, M. B. (2020). *Effect of the 2018 European drought on methane and carbon dioxide exchange of northern mire ecosystems*.

Rinne, J., Tuovinen, J. P., Klemedtsson, L., Aurela, M., Holst, J., Lohila, A., Weslien, P., Vestin, P., Łakomiec, P., Peichl, M., Tuittila, E. S., Heiskanen, L., Laurila, T., Li, X., Alekseychik, P., Mammarella, I., Ström, L., Crill, P., and Nilsson, M. B. (2020). Effect of the 2018 European drought on methane and carbon dioxide exchange of northern mire ecosystems: 2018 drought on northern mires. *Philosophical Transactions of the Royal Society B: Biological Sciences*, *375*(1810). https://doi.org/10.1098/rstb.2019.0517

Rowson, J. G., Worrall, F., and Evans, M. G. (2013). Predicting soil respiration from peatlands. *Science of the Total Environment*, *442*, 397–404. https://doi.org/10.1016/j.scitotenv.2012.10.021

Roy, D. P., Huang, H., Houborg, R., and Martins, V. S. (2021). A global analysis of the temporal availability of PlanetScope high spatial resolution multi-spectral imagery. *Remote Sensing of Environment*, *264*. https://doi.org/10.1016/j.rse.2021.112586

Ruiz, S. S. (2019). Remote sensing and ecosystem modeling to simulate terrestrial carbon fluxes. *Revista de Teledeteccion*, *2019*(53), 87–91. https://doi.org/10.4995/raet.2019.11220

Sachs, T., Giebels, M., Boike, J., and Kutzbach, L. (2010). Environmental controls on CH4 emission from polygonal tundra on the microsite scale in the Lena river delta, Siberia. *Global Change Biology*, *16*(11), 3096–3110. https://doi.org/10.1111/j.1365-2486.2010.02232.x

Schaff, S. van der, and Streefkerk, J. G. (2011). *Relationships between ecotopes, hydrological position and subsidence on Clara Bog*. 127–136.

Scharlemann, J. P. W., Tanner, E. V. J., Hiederer, R., and Kapos, V. (2014). Global soil carbon: Understanding and managing the largest terrestrial carbon pool. *Carbon Management*, *5*(1), 81–91. https://doi.org/10.4155/cmt.13.77

Schubert, P., Lund, M., and Eklundh, L. (2008). Estimation of gross primary productivity of an ombrotrophic bog in southern sweden. *International*

Geoscience and Remote Sensing Symposium (IGARSS), *4*(1), 866–869. https://doi.org/10.1109/IGARSS.2008.4779860

Schwalm, C. R., Black, T. A., Amiro, B. D., Arain, M. A., Barr, A. G., Bourque, C. P. A., Dunn, A. L., Flanagan, L. B., Giasson, M. A., Lafleur, P. M., Margolis, H. A., McCaughey, J. H., Orchansky, A. L., and Wofsy, S. C. (2006). Photosynthetic light use efficiency of three biomes across an east-west continental-scale transect in Canada. *Agricultural and Forest Meteorology*, *140*(1–4), 269–286. https://doi.org/10.1016/j.agrformet.2006.06.010

Sellami, E. M., and Rhinane, H. (2023). A NEW APPROACH FOR MAPPING LAND USE / LAND COVER USING GOOGLE EARTH ENGINE: A COMPARISON OF COMPOSITION IMAGES. *The International Archives of the Photogrammetry, Remote Sensing and Spatial Information Sciences*, *XLVIII-4/W6-2022*, 343–349. https://doi.org/10.5194/isprs-archives-XLVIII-4-W6-2022-343-2023

Sencaki, D. B., Prayogi, H., Arfah, S., and Arif Pianto, T. (2020). Machine learning approach for peatland delineation using multi-sensor remote sensing data in Ogan Komering Ilir Regency. *IOP Conference Series: Earth and Environmental Science*, *500*(1). https://doi.org/10.1088/1755-1315/500/1/012005

Sims, D. A., Rahman, A. F., Cordova, V. D., El-Masri, B. Z., Baldocchi, D. D., Flanagan, L. B., Goldstein, A. H., Hollinger, D. Y., Misson, L., Monson, R. K., Oechel, W. C., Schmid, H. P., Wofsy, S. C., and Xu, L. (2006). On the use of MODIS EVI to assess gross primary productivity of North American ecosystems. *Journal of Geophysical Research: Biogeosciences*, *111*(4), 1–16. https://doi.org/10.1029/2006JG000162

Steenvoorden, J., Limpens, J., Crowley, W., and Schouten, M. G. C. (2022). There and back again: Forty years of change in vegetation patterns in Irish peatlands. *Ecological Indicators*, *145*. https://doi.org/10.1016/j.ecolind.2022.109731

Sujud, L., Jaafar, H., Haj Hassan, M. A., and Zurayk, R. (2021). Cannabis detection from optical and RADAR data fusion: A comparative analysis of the SMILE machine learning algorithms in Google Earth Engine. *Remote Sensing Applications: Society and Environment*, *24*. https://doi.org/10.1016/j.rsase.2021.100639

Swenson, M. M., Regan, S., Bremmers, D. T. H., Lawless, J., Saunders, M., and Gill, L. W. (2019). Carbon balance of a restored and cutover raised bog: Implications for restoration and comparison to global trends. *Biogeosciences*, *16*(3), 713–731. https://doi.org/10.5194/bg-16-713-2019

Tanneberger, F., Tegetmeyer, C., Busse, S., Barthelmes, A., Shumka, S., Mariné, A. M., Jenderedjian, K., Steiner, G. M., Essl, F., Etzold, J., Mendes, C., Kozulin, A., Frankard, P., Milanović, Ganeva, A., Apostolova, I., Alegro, A., Delipetrou, P., Navrátilová, J., … Joosten, H. (2017). The peatland map of Europe. *Mires and Peat*, *19*(2015), 1–17. https://doi.org/10.19189/MaP.2016.OMB.264

Thom, T., Hanlon, A., Lindsay, R., Richards, J., Stoneman, R., and Brooks, S. (2018). *Conserving Bogs: The Management Handbook*. 207.

Tomlinson, R. W. (2005). Soil carbon stocks and changes in the Republic of Ireland. *Journal of Environmental Management*, *76*(1), 77–93. https://doi.org/10.1016/j.jenvman.2005.02.001

Tuovinen, J. P., Aurela, M., Hatakka, J., Räsänen, A., Virtanen, T., Mikola, J., Ivakhov, V., Kondratyev, V., and Laurila, T. (2019). Interpreting eddy covariance data from heterogeneous Siberian tundra: Land-cover-specific methane fluxes and spatial representativeness. *Biogeosciences*, *16*(2), 255–274. https://doi.org/10.5194/bg-16-255-2019

UNEP. (2022). *Global Peatlands Assessment – The State of the World's Peatlands: Evidence for action toward the conservation, restoration, and sustainable management of peatlands.* https://www.unep.org/resources/global-peatlands-

van der Schaaf, S. (2002). Bog Hydrology. In M. G. C. Schouten (Ed.), *Conservation and Restoration of Raised Bogs* (Issue 4, pp. 54–109). Staatsbosbeheer, Geological Survey of Ireland.

van der Schaff, S., and Streefkerk, J. G. (2011). *Relationships between ecotopes, hydrological position and subsidence on Clara Bog*. 127–136.

van Gaalen, K. E., Flanagan, L. B., and Peddle, D. R. (2007). Photosynthesis, chlorophyll fluorescence and spectral reflectance in Sphagnum moss at varying water contents. *Oecologia*, *153*(1), 19–28. https://doi.org/10.1007/s00442-007-0718-y

Vanikiotis, T., Stagakis, S., and Kyparissis, A. (2018). Effects of satellite spatial resolution on gross primary productivity estimation through light use efficiency modeling. *Sixth International Conference on Remote Sensing and Geoinformation of the Environment (RSCy2018)*, *10773*(August), 62. https://doi.org/10.1117/12.2326605

Veber, G., Kull, A., Villa, J. A., Maddison, M., Paal, J., Oja, T., Iturraspe, R., Pärn, J., Teemusk, A., and Mander, Ü. (2018). Greenhouse gas emissions in natural and managed peatlands of America: Case studies along a latitudinal gradient. *Ecological Engineering*, *114*, 34–45. https://doi.org/10.1016/j.ecoleng.2017.06.068

Vitt, D. H. (2008). Peatlands. In *Encyclopedia of Ecology, Five-Volume Set* (pp. 2656–2664). https://doi.org/10.1016/B978-008045405-4.00318-9

Vogelmann, J. E., and Moss, D. M. (1993). *Spectral Reflectance Measurements in the Genus Sphagnum* (Vol. 45).

Wagle, P., Xiao, X., and Suyker, A. E. (2015). Estimation and analysis of gross primary production of soybean under various management practices and drought conditions. *ISPRS Journal of Photogrammetry and Remote Sensing*, *99*, 70–83. https://doi.org/10.1016/j.isprsjprs.2014.10.009

Wang, J. M., Murphy, J. G., Geddes, J. A., Winsborough, C. L., Basiliko, N., and Thomas, S. C. (2013). Methane fluxes measured by eddy covariance and static chamber techniques at a temperate forest in central Ontario, Canada. *Biogeosciences*, *10*(6), 4371–4382. https://doi.org/10.5194/bg-10-4371-2013

Wang, M., Guan, D. X., Han, S. J., and Wu, J. L. (2010). Comparison of eddy covariance and chamber-based methods for measuring CO2 flux in a temperate mixed forest. *Tree Physiology*, *30*(1), 149–163. https://doi.org/10.1093/treephys/tpp098

Warmenbol, C., and Smith, M. (2018). International union for conservation of nature (IUCN). *The Wetland Book: I: Structure and Function, Management, and Methods*, 665–669. https://doi.org/10.1007/978-90-481-9659-3_110

Webster, K. L., Bhatti, J. S., Thompson, D. K., Nelson, S. A., Shaw, C. H., Bona, K. A., Hayne, S. L., and Kurz, W. A. (2018). Spatially-integrated estimates of net ecosystem exchange and methane fluxes from Canadian peatlands. *Carbon Balance and Management*, *13*(1). https://doi.org/10.1186/s13021-018-0105-5

Wilson, D., Dixon, S. D., Artz, R. R. E., Smith, T. E. L., Evans, C. D., Owen, H. J. F., Archer, E., and Renou-Wilson, F. (2015). Derivation of greenhouse gas emission factors for peatlands managed for extraction in the Republic of Ireland and the United Kingdom. *Biogeosciences*, *12*(18), 5291–5308. https://doi.org/10.5194/bg-12-5291-2015

Wilson, D., Farrell, C. A., Fallon, D., Moser, G., Müller, C., and Renou-Wilson, F. (2016). Multiyear greenhouse gas balances at a rewetted temperate peatland. *Global Change Biology*, *22*(12), 4080–4095. https://doi.org/10.1111/gcb.13325

Wilson, D., Mackin, F., Tuovinen, P., Moser, G., and Renou-, C. F. F. (2022). *Carbon and climate implications of rewetting a raised bog in Ireland*. *July*, 1–17. https://doi.org/10.1111/gcb.16359

Wilson, D., and Müller, C. (2013). *Carbon emissions and removals from Irish peatlands : present trends and future mitigation measures*. *December 2014*, 37–41. https://doi.org/10.1080/00750778.2013.848542

Wilson, D., Müller, C., and Renou-Wilson, F. (2013). Carbon emissions and removals from irish peatlands: Present trends and future mitigation measures. In *Irish Geography* (Vol. 46, Issues 1–2, pp. 1–23). https://doi.org/10.1080/00750778.2013.848542

Wilson, F. R., Bolger, T., Bullock, C., Convery, F., Curry, J., Ward, S., Wilson, D., and Muller, C. (2011). *BOGLAND : Sustainable Management of Peatlands in Ireland* (Issue 75).

Windham-Myers, L., Bergamaschi, B., Anderson, F., Knox, S., Miller, R., and Fujii, R. (2018). Potential for negative emissions of greenhouse gases (CO2, CH4 and N2O) through coastal peatland re-establishment: Novel insights from high frequency flux data at meter and kilometer scales. *Environmental Research Letters*, *13*(4). https://doi.org/10.1088/1748-9326/aaae74

Wu, J., Roulet, N. T., Moore, T. R., Lafleur, P., and Humphreys, E. (2011). Dealing with microtopography of an ombrotrophic bog for simulating ecosystem-level CO2 exchanges. *Ecological Modelling*, *222*(4), 1038–1047. https://doi.org/10.1016/j.ecolmodel.2010.07.015

Xiao, J., Chevallier, F., Gomez, C., Guanter, L., Hicke, J. A., Huete, A. R., Ichii, K., Ni, W., Pang, Y., Rahman, A. F., Sun, G., Yuan, W., Zhang, L., and Zhang, X. (2019). Remote sensing of the terrestrial carbon cycle: A review of advances over 50 years. *Remote Sensing of Environment*, *233*(January), 111383. https://doi.org/10.1016/j.rse.2019.111383

Xiao, J., Davis, K. J., Urban, N. M., Keller, K., and Saliendra, N. Z. (2011). Upscaling carbon fluxes from towers to the regional scale: Influence of parameter variability and land cover representation on regional flux estimates. *Journal of Geophysical Research: Biogeosciences*, *116*(3), 1–15. https://doi.org/10.1029/2010JG001568

Yu, L., Wang, H., Wang, G., Song, W., Huang, Y., Li, S. G., Liang, N., Tang, Y., and He, J. S. (2013). A comparison of methane emission measurements using eddy covariance and manual and automated chamber-based techniques in Tibetan Plateau alpine wetland. *Environmental Pollution*, *181*, 81–90. https://doi.org/10.1016/j.envpol.2013.06.018

Yuan, W., Cai, W., Nguy-Robertson, A. L., Fang, H., Suyker, A. E., Chen, Y., Dong, W., Liu, S., and Zhang, H. (2015). Uncertainty in simulating gross primary production of cropland ecosystem from satellite-based models. *Agricultural and Forest Meteorology*, *207*, 48–57. https://doi.org/10.1016/j.agrformet.2015.03.016

Yuan, W., Liu, S., Zhou, G., Zhou, G., Tieszen, L. L., Baldocchi, D., Bernhofer, C., Gholz, H., Goldstein, A. H., Goulden, M. L., Hollinger, D. Y., Hu, Y., Law, B. E., Stoy, P. C., Vesala, T., and Wofsy, S. C. (2007). Deriving a light use efficiency model from eddy covariance flux data for predicting daily gross primary production across biomes. *Agricultural and Forest Meteorology*, *143*(3–4), 189–207. https://doi.org/10.1016/j.agrformet.2006.12.001

Zhang, C., Comas, X., and Brodylo, D. (2020). A Remote Sensing Technique to Upscale Methane Emission Flux in a Subtropical Peatland. *Journal of Geophysical Research: Biogeosciences*, *125*(10). https://doi.org/10.1029/2020JG006002

Zhang Caiyun, C. X., and David, B. (2020). A Remote Sensing Technique to Upscale Methane Emission Flux in a Subtropical Peatland Journal of Geophysical Research : Biogeosciences. *JGR Biogeosciences*, 1–13. https://doi.org/10.1029/2020JG006002

Zhang, J., Wang, X., and Ren, J. (2021). Simulation of gross primary productivity using multiple light use efficiency models. *Land*, *10*(3), 1–10. https://doi.org/10.3390/land10030329

Zhang, Y., Sachs, T., Li, C., and Boike, J. (2012). Upscaling methane fluxes from closed chambers to eddy covariance based on a permafrost biogeochemistry integrated model. *Global Change Biology*, *18*(4), 1428–1440. https://doi.org/10.1111/j.1365-2486.2011.02587.x

Zhang, Y., Song, C., Sun, G., Band, L. E., Noormets, A., and Zhang, Q. (2015). Understanding moisture stress on light use efficiency across terrestrial ecosystems based on global flux and remote-sensing data. *Journal of Geophysical Research: Biogeosciences*, *120*(10), 2053–2066. https://doi.org/10.1002/2015JG003023

Zhang Yao et al. (2017). A global moderate resolution dataset of gross primary production of vegetation for 2000–2016. *Nature Scientific Data*. https://doi.org/https://doi.org/10.1038/s41597-021-00854-6

Zheng, Y., Zhang, L., Xiao, J., Yuan, W., Yan, M., Li, T., and Zhang, Z. (2018). Sources of uncertainty in gross primary productivity simulated by light use efficiency models: Model structure, parameters, input data, and spatial resolution. *Agricultural and Forest Meteorology*, *263*(December 2017), 242–257. https://doi.org/10.1016/j.agrformet.2018.08.003